NEUROTOXIC MECHANISMS OF METHYLMERCURY:

CELLULAR AND BEHAVIOR CHANGES

A Dissertation

by

SAIRAM BELLUM

Submitted to the Office of Graduate Studies of
Texas A&M University
in partial fulfillment of the requirements for the degree of

DOCTOR OF PHILOSOPHY

December 2005

Major Subject: Toxicology

NEUROTOXIC MECHANISMS OF METHYLMERCURY: CELLULAR AND BEHAVIOR CHANGES

A Dissertation

by

SAIRAM BELLUM

Submitted to the Office of Graduate Studies of
Texas A&M University
in partial fulfillment of the requirements for the degree of

DOCTOR OF PHILOSOPHY

Approved by:

Chair of Committee,	Louise C. Abbott
Committee Members,	Timothy D. Phillips
	Kirby C. Donnelly
	Gheorghe Stoica
Chair of Toxicology Faculty,	Robert C. Burghardt

December 2005

Major Subject: Toxicology

ABSTRACT

Neurotoxic Mechanisms of Methylmercury: Cellular and Behavior Changes.

(December 2005)

Sairam Bellum,

B.V.Sc & A.H; M.V.Sc., Acharya NG Ranga Agricultural University

Chair of Advisory Committee: Dr. Louise C. Abbott

The organic or methylated form of mercury (Hg), consisting of one methyl group bound to each atom of Hg, (methylmercury; MeHg), accounts for most of the Hg to which humans are exposed. MeHg, by virtue of its lipophilicity is highly neurotoxic to both the developing and mature central nervous system (CNS). Historically, MeHg has been implicated in high morbidity and mortality rates over the last 40 years in Japan, Iraq, Pakistan and Guatemala. The most common symptom exhibited in these exposure episodes was cerebellar ataxia. Recent *in vitro* studies using cultured granule cells showed that MeHg alters intracellular calcium ion ($[Ca^{2+}]i$) homeostasis, potentiates reactive oxygen species (ROS) generation and loss of mitochondrial membrane potential leading to apoptotic death of cerebellar granule neurons. To better understand the neurotoxic mechanisms of MeHg on cerebellum, changes with respect to biochemical processes in cerebellar granule cells and associated behavior changes were investigated.

The aims of this dissertation were: (1) to assess mercury concentrations in mouse brain using different routes of administration and different tissue preparations, (2) to determine the behavior effects of *in vivo* MeHg exposure in young adult mice. (3) to

understand specific biochemical processes leading to granule cell death/dysfunction due to *in vivo* MeHg toxicity in mice, and (4) to determine the toxic effects of *in vivo* MeHg exposure on mice aged between 16-20 months.

The present results showed that repeated oral exposure to MeHg results in greater accumulation of Hg in brain tissue when compared to single oral or subcutaneous exposures at the same concentration of MeHg. Behavior analysis revealed that MeHg at the concentrations used in this study had profound effects on motor coordination and balance in young adult and aged mice. Investigation of biochemical processes in cerebellar granule cells of mice exposed to MeHg showed an increase in ROS generation, alteration of ($[Ca^{2+}]i$ (in young adult mice) and loss of MMP in young adult and aged mice. However, these changes did not lead to apoptotic cell death of granule cells at the concentrations of MeHg used and at the specific time point it was investigated in young adult mice.

ACKNOWLEDGEMENTS

I cordially offer my unboundful and deep sense of gratitude to my major advisor and Chair of the Advisory Committee Dr. Louise C. Abbott, for her immense interest, meticulous guidance, persistent encouragement and pragmatic suggestions during every phase of my graduate study. I humbly place on record my respect and gratitude to Drs. Stoica, Phillips and Donnelly for their valuable suggestions during my research work leading to the successful completion of my thesis work.

With great pleasure I express my profound sense of gratitude to Drs. Cannon, Landis and Russell for their valuable advice and guidance during the years of my graduate study as a teaching assistant in histology. I avail this opportunity to acknowledge the help and cooperation received from my colleagues Kerry Thuett, Tamy Frank-Cannon, Bhupinder Bawa and Sarah Wills. Special thanks to Raul Grajeda, René Ramon and Susan Hernandez for their technical support. My heartiest thanks are due to Dr. Sang-Soep Nahm for his valuable advice and guidance in my research work.

Lastly, no words are enough to express my profound gratitude, love and affection to my beloved wife, son, father, in-laws and specially my late mother and grandmother who have been a consistent source of inspiration and whose encouragement brings out my best in every one of my endeavors.

TABLE OF CONTENTS

CHAPTER Page

LIST OF FIGURES

FIGURE Page

FIGURE Page

LIST OF TABLES

CHAPTER I

INTRODUCTION

CEREBELLUM: DEVELOPMENT AND ANATOMICAL ORGANIZATION

The word cerebellum comes from Latin meaning "little brain". In mammals, cerebellum is located at the midbrain-hindbrain junction, dorsal to the brain stem and ventral to the occipital lobe. When compared to the total brain size, cerebellum is small and yet contains more neurons than are found in the rest of the brain (Lange, 1975). The cerebellum is a major association center for sensory input from various regions of the body such as the eyes, head and body, serving as a coordination center for body movements. The cerebellum plays an important role in controlling the rate, range and force of every movement (Ito, 1984a; Middleton and Strick, 1998; Izquierdo and Medina, 1998; Gilbert, 2001). In addition to the above-mentioned functions, there is a growing consensus of the cerebellum's involvement in a number of cognitive functions (Akshoomoff and Courchesne, 1992; Courchesne et al., 1994; Daniel et al., 1998; Ekerot and Kano, 1985; Fiez, 1996; Glickstein 1994; Ito, 2000; Leiner et al., 1991; Paulin, 1993; Siveri et al., 1994).

This dissertation follows the style of Journal of Neuroscience.

During central nervous system (CNS) development, the cerebellum is first noted at 5-6 weeks as rhombic lips in the rhombencephalic vesicle. These rhombic lips develop from the dorsolateral part of alar plate forming the cerebellar primordium (Larsen, 1997). The posterior part of the rhombencephalic vesicle gives rise to the precerebellar primordium. The primitive cerebellum and 4th ventricle are formed from the fusion of the cerebellar primordium and the precerebellar primordium (Larsen, 1997). Whereas in mice, the cerebellum appears between 10-12 days of gestation as a thickening anterior to the roof of fourth ventricle. The cells divide extensively and migrate by the 14th day of gestation forming a cerebellar plate (Miale and Sidman, 1961).

The cerebellar anlage consists of three zones: ventricular, mantle and marginal. In the ventricular zone, the neuroepithelial cells located in the posterior cerebellar primordium migrate above the marginal layer and form the external granule layer (Miale and Sidman, 1961). The external granule cells in turn proliferate and migrate down to form the internal granule cell layer. Also a few primordial cerebellar neuroepithelial cells contribute to the formation of stellate and basket cells found in the molecular layer. Purkinje, Golgi and unipolar brush cells arise from the neuroblasts of the cerebellar primordium (Miale and Sidman, 1961; Mugnaini and Floris, 1994). Purkinje cells are formed early in the cerebellar development but attain their characteristic size and single layered arrangement only ten days after birth. Unipolar brush cells also called as Lugaro cells have rounded cell bodies (9-12μm in diameter). The cell is composed of a single thin axon and a short dendrite that divides only at the tip, giving rise to tightly packed branchlets resembling a paintbrush (Mugnaini and Floris, 1994). Ventricular zone also

contributes to the formation of glial cell formation after neuroblasts complete initial migration (Miale and Sidman, 1961).

In rodents such as mice and rats, maturation of the cerebellum primarily takes place postnatally. Except for Golgi cells the rest of the neurons in the cerebellum mature postnatally. During embryonic development, between embryonic days (E) 10-12, the deep cerebellar neurons leave the ventricular zone (Uzman, 1960). Upward migration of the Purkinje cells at E 11-13 marks the beginning of cerebellar cortex formation. At E 15-17 the external granule cell layer is formed while Golgi cells start to leave the ventricular zone at E15 (Uzman, 1960). The majority of cerebellar cortical neurons complete migration by E20 and the rest of the development and fine-tuning of the cerebellar cytoarchitecture take place postnatally.

At birth (P0), the cerebellum consists of three layers viz., external germinal layer (EGL), a molecular layer and the Purkinje cell layer. At P7, a fourth layer viz., the internal granule cell layer (IGL) can be seen. Expansion of the molecular layer also is evident by this time (P7). Clear differentiation of stellate and basket cells can be made during this period. At P7 the Purkinje cell layer appears as a monocellular layer (Miale and Sidman, 1961). Starting at approximately P10, the Purkinje cells undergo extensive dendritic arborization and form synapses with parallel fibers of granule cells and climbing fibers from the inferior olive (Altman, 1972). This proliferation continues until P21. Due to extensive cell proliferation, the external granule cell layer also is thicker by P10. Granule cells begin to migrate inwards across the Purkinje cell layer starting at P11 and by P15 the majority of migration has taken place. These migrating granule cells

express a neural glycoprotein called astrotactin. Astrotactin acts a ligand and helps with inward migration of granule cells along the ascending Bergman glia (Hasel and Sutcliffe, 1990). Development of the cerebellum is complete in rodents by P21 (Fujita et al., 1966).

Cerebellar structure

The cerebellum is attached to the pons, the medulla and the midbrain by three paired cerebellar peduncles. The cerebellum is divided into a median portion called cerebellar vermis and two lateral lobules, the hemispheres. The paravermis is a region located between the vermis and each cerebellar hemisphere. Structurally, the cerebellum is divided into the cerebellar cortex (superficial grey mantle), the medullary substance (internal white matter) and deep cerebellar nuclei (the fastigial, the interpositus and, the dentate nucleus) (Parent, 1996). The cerebellum is divided into lobes and lobules by five main fissures viz., the primary, the posterior superior, the horizontal, the prepyramidal and the posterolateral or prenodular. The primary fissure divides the cerebellum into rostral and caudal lobes (Marani and Voogd, 1979). The cerebellum is thrown into numerous narrow folds called laminae or folia. Voogd and Glickstein (1998) conveniently divided the cerebellum into 10 lobules. When compared to humans and rats the mouse cerebellum has lobules I and Π and, lobules IV and V joined (Marani and Voogd, 1979) (Figure I-1A). Table I-1 summarizes different nomenclatures used in human and other mammalian cerebella.

Table I-1. Nomenclature of the cerebellar lobules

Vermis		Hemisphere	
Human	Other mammals	Human	Other mammals
Lingula	Lobule I	Vincingulum lingulae	Anterior lobule
Centralis	Lobule II & III	Ala lobulus centralis	Anterior lobule
Culmen	Lobule IV & V	Ant. quadrangulate lobule	Anterior lobule
Declive	Lobule VI	Post. quadrangulate lobule	Lobule simplex
Folium	Lobule VIIA	Sup. semilunar lobule	Ansiform lobule Crus I
Tuber	Lobule VIIB	Inferior semilunar and Gracile lobule	Ansiform lobule Crus II
Pyramis	Lobule VIII	Biventral lobule	Paramedian lobule
Uvula	Lobule IX	Tonsilla	Dorsal paraflocculus
Nodulus	Lobule X	Accessory paraflocculus	Ventral paraflocculus

Ant. = anterior, Post. = posterior, Sup. = superior, (Voogd and Glickstein, 1998).

Embryologically and functionally the cerebellum is divided into three parts, (a) the archicerebellum, (b) the paleocerebellum, and (c) the neocerebellum. The archicerebellum includes the nodulus, the paired flocculi and their connections (the flocculonodular lobe). The paleocerebellum represents the rostral lobe and the neocerebellum, the caudal lobe (Parent, 1996).

Histologically, the cerebellar cortex is composed of three well-defined layers containing five different types of neurons (Figure I-1B). The superficial layer is the molecular layer that contains stellate and basket neurons, granule cell axons, climbing fibers and Purkinje cell dendritic processes. Purkinje cells are aligned as a single layer of cell bodies between the molecular and granule cell layers. The characteristic feature of a

Purkinje cell is its monoplanar shape. It has a euchromatic nucleus with a prominent nucleolus and a fan shaped dendritic arbor (McCrea et al., 1976).

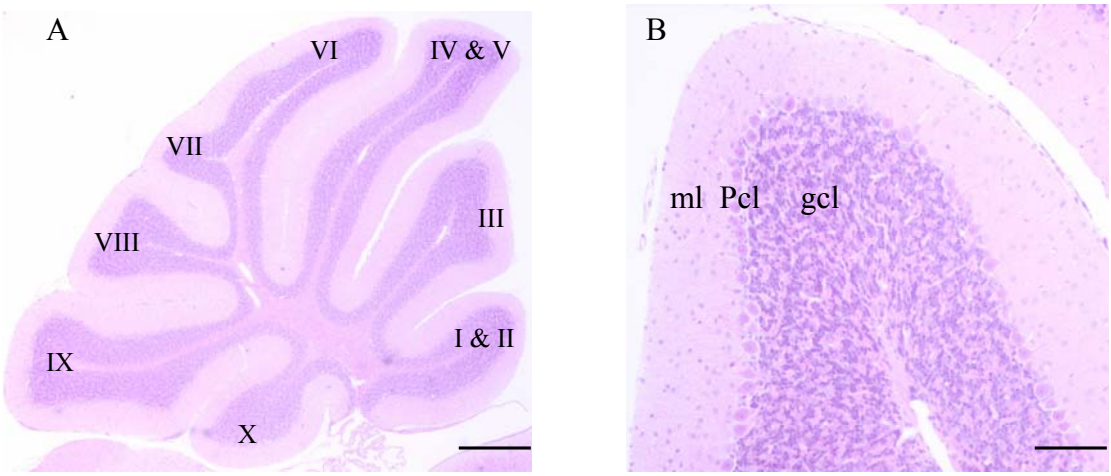

Figure I-1. Light microscopic appearance of an adult mouse cerebellum. (A) A sagittal view of a mouse cerebellum showing the cerebellar lobules I-X. (B) A high magnification view of a cerebellar lobule. Abbreviations; ml = molecular layer, Pcl = Purkinje cell layer, gcl = granule cell layer. Scale bar in A = 500 microns; B = 100 microns

The axons of Purkinje cells are myelinated and pass through the granule cell layer and white matter to make inhibitory synapses with neurons in the deep cerebellar nuclei (Altman and Bayer, 1997; Ito, 1984a). Purkinje cells are among the largest neurons of the brain measuring about 50-80μm in diameter. The granule cell layer is primarily composed of granule cells and Golgi cells. Granule cells are small neurons that measure approximately 5-8 μm in diameter. They are numerous and tightly packed (Ito, 1984c; Parent, 1996). The axons of granule cells are called parallel fibers. They synapse on

Purkinje cell dendrites and this type of synaptic contact is sometimes called a "cross-over" synapse (Gray, 1961; Hamori and Szentagothai, 1966). Golgi cells are found in the upper portion of the granule cell layer. Golgi cells measure approximately 6-11 μm in diameter. Their dendrites extend throughout all layers of the cerebellar cortex. The other less understood cells in terms of function in the granule cell layer are, Lugaro cells (Altman and Bayer, 1997). They are also known as unipolar brush cells and express calretinin (Abbott and Jacobowitz, 1995; Floris et al., 1994; Marini et al., 1997; Mugnaini and Floris, 1994; Rogers, 1989).

Intrinsic neuronal circuitry of the cerebellum

Figure I-2 summarizes cerebellar neuronal circuitry. The cerebellar cortex primarily receives all the afferent inputs from various tracts that enter the cerebellum via the caudal and middle cerebellar peduncles. Within the cerebellar cortex, the afferent fibers enter either as mossy fibers or climbing fibers after losing their myelin (Parent, 1996). Both mossy fibers and climbing fibers use glutamate as their major neurotransmitter and, thus, are excitatory to the only cerebellar cortical output system, the Purkinje cells (Oertel, 1993; Ottersen et al., 1984; Ottersen et al., 1992).

Mossy fibers arise from pontine, reticular, vestibular and external cuneate nuclei (Chan-Palay et al., 1977; Payne, 1983; Altman and Bayer, 1987). Mossy fibers upon entering the cerebellum via the caudal and middle cerebellar peduncles, synapse on the claw-like dendritic terminals of granule cells and form a complex synaptic structure called the glomerulus. Each glomerulus is formed by: (a) a mossy fiber, (b) a dendritic

terminal of a granule cell, (c) terminals of Golgi cell axons, and (d) proximal parts of Golgi cell dendrites. Before the mossy fiber enters the granule cell layer, it bifurcates repeatedly in the white matter and gives off collaterals to neurons in the deep cerebellar nuclei and to axons of unipolar brush cells.

Climbing fibers, whose name is derived from their characteristic pattern of synapse with Purkinje cells, form the second major category of input to the cerebellum (O'Leary et al., 1970). Silver staining established the origin of climbing fibers as the inferior olivary complex (Desclin, 1974). The inferior olive in turn receives inputs from the red nucleus, reticular nucleus, vestibular nucleus and rostral colliculi.

Diffuse monoaminergic and cholinergic afferent fibers form the last category of input to the cerebellum. Noradrenergic, serotonergic and dopaminergic fibers originate from the locus coeruleus, raphe nuclei and ventral mesencephalic tegmentum, respectively and extend from the white matter into all layers of the cerebellar cortex and the cholinergic afferents (Ghez and Thach, 2000; Parent, 1996).

Granule cells receive excitatory inputs from mossy fibers and in turn transmit excitatory stimuli to Purkinje cells, primarily via synapses on the tertiary dendrites (Palkovits et al., 1971). The parallel fibers of granule cells also synapse with stellate and basket cells located in the molecular layer (Eccles et al., 1967; Ito, 1984c). Stellate and basket cells receive excitatory input from granule cells and, in turn, exert inhibitory influence on Purkinje cells (Altman and Bayer, 1997; Martin, 1996). Golgi cells also are inhibitory interneurons in the cerebellar cortex. They receive inputs via parallel fibers of granule cells and collaterals from Purkinje cells and in turn inhibit the afferent input to

the cerebellar cortex at the mossy fiber-granule cell relay in the glomeruli (Altman and Bayer, 1997).

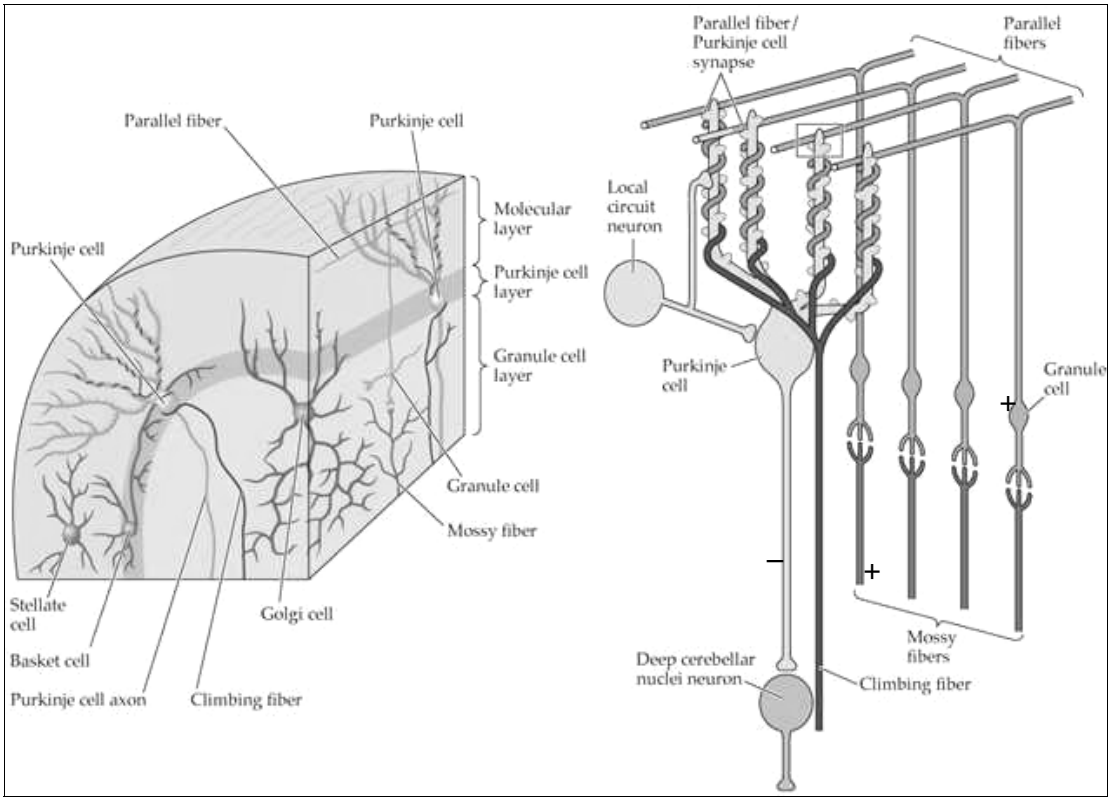

Figure I-2. Summary of cerebellar cortex organization and circuitry. A) Vertical section of a single folium in longitudinal and transverse planes showing the three-layer organization of cerebellar cortex containing five types of neurons. B) This figure shows the excitatory (+) and inhibitory (-) connection between various cell types involved in the basic neuronal circuitry of the cerebellum (modified from Ghez and Thach, 2000)

Climbing fibers from the inferior olive enter the contralateral cerebellum, branch, sending numerous collaterals to deep cerebellar nuclei, stellate, basket and Golgi cells and climb up the dendritic arborization of the Purkinje cell (Hamori and Szentagothai,

1966; O'Leary et al., 1971). Climbing fiber input is direct, all or none and excitatory to a single Purkinje cell (Eccles et al., 1964; Eccles et al., 1966; Larramendi and Victor, 1967). Purkinje cells are the sole output elements of the cerebellar cortex. They are influenced by three inhibitory interneurons (the stellate, basket and Golgi cells) and one excitatory neuron (the granule cells). Axons of Purkinje cells synapse on neurons in the deep cerebellar nuclei and vestibular nuclei and exert a powerful inhibition effect on them (Ito, 1984b; Walberg and Jansen, 1961). Table I-2 summarizes neurotransmitters associated with cerebellum.

ROLE OF CALCIUM IONS IN NEURONS

Calcium ions are important and ubiquitous intracellular signaling messengers in the nervous system (Berridge, 1998; Berridge et al., 2000; Carafoli, 2002; Limke et al., 2004). A large electrochemical gradient for calcium ions exists in neurons. At the resting stage most cells maintain a very low levels of intracellular calcium ions $[Ca^{2+}]_i$ (approximately 100nM) when compared to the extracellular calcium ions $[Ca^{2+}]_e$ (1-2mM) (Kass and Orrenius, 1999). When neurons are stimulated, $[Ca^{2+}]_i$ levels increase up to 10 times normal resting levels (Berridge, 1998). Within neurons, particularly at the active zones of the nerve terminals, $[Ca^{2+}]_i$ can rise transiently up to 100μM (Bennett et al., 2000; Llinas et al., 1995).

Table I-2. Presynaptic fibers, neurotransmitters and their postsynaptic targets in the cerebellum

Presynaptic fibers	Neurotransmitter	Postsynaptic targets
Mossy fibers	Glutamate, Acetylcholine	Granule cells
	Glutamate	Unipolar brush cells
Climbing fibers	Aspartate, CRF	Purkinje cells
	CRF	Deep cerebellar nuclei
Granule cells	Glutamate	Purkinje cells
Purkinje cells	GABA	Deep cerebellar nuclei
Golgi cells	GABA, Glycine	Granule cells
Basket cells	GABA	Purkinje cells
Stellate cells	GABA, Taurine	Purkinje cells
Deep cerebellar nuclei	GABA	Inferior olivary nuclei (ION)
	Aspartate, Glutamate	Other than ION

CRF = corticotrophin releasing factor, GABA = gamma amino butyric acid
(Altman and Bayer, 1997)

The rise in $[Ca^{2+}]_i$ can occur due to entry of $[Ca^{2+}]_e$ through various channels located in the plasma membrane and mobilization of calcium ions from intracellular stores. Two main intracellular calcium ion stores in neurons are the mitochondria and the smooth endoplasmic reticulum (SER). Mitochondria serve as low affinity, high-capacity calcium stores and the SER on the other hand serves as a high-affinity, low capacity calcium ion store (Somlyo et al., 1985). In neurons, the SER can take up calcium ions from the cytosol even at very low concentrations but mitochondria need at least 500nM of local extra mitochondrial calcium ions in order to take up calcium ions (Nicholls and Scott, 1980).

$[Ca^{2+}]_e$ enters into neurons via voltage-gated calcium ion channels (VGCC) or ligand-gated calcium ion channels (LGCC) (Berridge, 1998). Calcium ions enter into the cell via VGCC and triggers calcium induced calcium release (CICR) from the SER by

acting on their calcium ion sensors called ryanodine receptors (Berridge, 1998; Berridge et al., 2000). When a neurotransmitter binds to LGCC, calcium ions enter into the cell and stimulate the formation of inositol 1,4,5-triphosphate (IP_3), which in turn binds to its receptor IP_3R on the ER and induces CICR (Berridge, 1998; Berridge et al., 2000). Cerebellar granule cells express many types of VGCC and LGCC (Courtney et al., 1990; Pearson et al., 1995; Randall and Tsien, 1995).

VGCCs are complex membrane proteins composed of α1, α2, β, γ and δ subunits (Figure I-3). The α1 subunit forms the calcium-conducting pore, while the rest of the subunits modulates pore function during the process of calcium ion influx in excitable cells (Catterall, 2000; Ertel et al., 2000; Horn, 2000). VGCCs are further classified into high voltage activated channels that include L, N, P/Q and R-type channels and low voltage activated channels represented by T-type channels. This classification is based on their electrophysiological and pharmacological characteristics (Catterall, 2000).

MECHANISMS OF CALCIUM BUFFERING IN NEURONS

Neurons are equipped with a number of mechanisms for transporting calcium ions across their internal and external membranes. Although transient increase in $[Ca^{2+}]_i$ is necessary for neuronal signaling, uncontrolled increase or decrease in $[Ca^{2+}]_i$ could result in neuronal death. Because of the huge concentration gradient that exists across the plasma membrane of a neuron, calcium ion entry occurs rapidly without much expenditure of cellular energy. But restoration of physiological $[Ca^{2+}]_i$ following a transient increase is relatively slow and dependent on various calcium ion pumps and

sodium/calcium ion exchangers coupled to the plasma membrane (Carafoli, 2002). In a neuron, $[Ca^{2+}]_i$ regulation is maintained by a well developed calcium ion buffering system. This system includes the SER, mitochondria, the nucleus and cytosolic calcium-binding proteins (CaBP) (Carafoli, 2002).

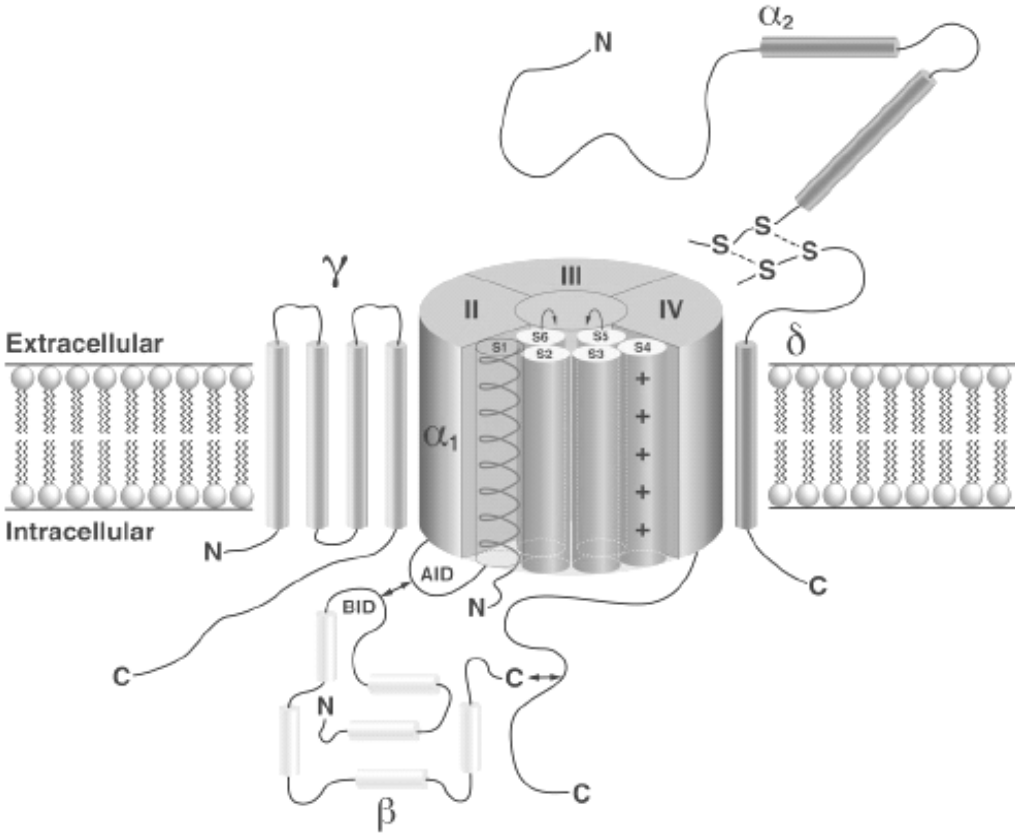

Figure I-3. Schematic representation of structure and assembly of the subunits of voltage-gated calcium channel (VDCC). The pore forming α1 subunit of VDCC consists of four homologous domains (I – IV). Each domain has six transmembrane repeats (S1 – S6) with S4 acting as a voltage sensor. The loop between S5 and S6 forms the lining of the pore (bent arrows in the pore). The β and γ subunits interact with the pore forming α1 subunit. The δ subunit is linked by disulfide bonds with the extracellular α2 subunit (adapted from Randall & Benham, 1999).

In the CNS, CaBPs act as intracellular calcium ion acceptors. They are commonly referred to as EF-hand proteins and include more than 1000 proteins. They are further grouped into 32 subfamilies based on their structure and functions (Slupsky and Skyes, 1999; Lewit-Bentley and Rety, 2000). CaBPs in the nervous system function as calcium ion sensors (calmodulin) or buffers. Calcium ion buffers consist of a group of three proteins viz., calretinin, calbindin and parvalbumin that are involved in immediate calcium ion buffering (Baimbridge et al., 1992). These proteins respond to sudden increases in $[Ca^{2+}]_i$ and buffer this excess calcium ion so that only 0.05-2.0% of calcium ions entering the cytosol remains free.

Calmodulin and annexins are the calcium ion sensing proteins that are expressed ubiquitously in the nervous system. The distribution pattern of CaBPs in the cerebellum is varied depending upon the specific cell type and so serve as excellent neuronal markers (Andressen et al., 1993). For example calbindin is highly expressed in the Purkinje, basket and stellate cells of the cerebellar cortex (Celio, 1990). Calretinin on the other hand is highly expressed by the cerebellar granule cells and their parallel fibers (Rogers, 1989).

Cellular organs like mitochondria, the ER and the nucleus further buffer the calcium entering the cytosol. As mentioned previously, the ER is a high-affinity, low capacity calcium ion store and therefore acts as a primary reservoir of calcium ions in the neurons (Meldolesi and Pozzan, 1998; Meldolesi, 2000). This helps the ER to sequester large amounts of calcium ions, which is vital because rapid intracellular calcium ion mobilization from intracellular depots is required for calcium ion signaling.

Calcium ions stored in the SER are used to amplify the signal when the amount of extracellular calcium ions entering the cytosol is not sufficient to generate a strong signal. In neurons cytosolic calcium ions are transported into the lumen of the SER via SERCA (sarcoplasmic-endoplasmic reticulum calcium ATPase) pumps located on the SER membrane (Meldolesi and Pozzan, 1998). Within the SER lumen another group of EF-hand CaBPs viz., calreticulin and calsequetrin further buffer calcium ions and regulate the release of free calcium ions upon stimulation (Meldolesi, 2000).

Mitochondria play a very important role in $[Ca^{2+}]_i$ signaling. There are at least two know transport systems available for calcium ion uptake into mitochondria. (1) The uniporter system transports unbound calcium ion down the calcium gradient between the cytosol and mitochondria (Gunter et al., 2000). The uniporters exhibit a high affinity for calcium ions but also bind to other cations with varying affinities. (2) Mitochondria also have a fast calcium ion uptake system (the rapid uptake mode or RaM), which allows calcium ion uptake from submicromolar, pulsed calcium ion transients and decodes the frequency as well as the amplitude of the signals (Gunter et al., 2000).

Mitochondria also operate ion exchangers that are coupled with sodium or hydrogen ions (Sparagna et al., 1995). Mitochondria also influence calcium ion signals through close interaction with SER by modulating the rate of delivery and the frequency of the calcium ion transients (Bernardi et al., 1998). As mentioned earlier, mitochondria serve as low affinity, high-capacity calcium ion stores and so mitochondria require much higher $[Ca^{2+}]_i$ to take up calcium ions. Mitochondrial calcium ion uptake takes place in

close proximity with the SER and so serves as a second line for calcium ion buffering in conjunction with the SER (Gunter et al., 2000; Meldolesi, 2000).

Finally the nucleus is also associated with calcium ion signaling. But calcium ion mediated signaling in the nucleus is used for regulating gene transcription rather than passive calcium ion buffering. Nuclear calcium ion trafficking occurs in close conjunction with the SER because the outer nuclear membrane is closely associated with the SER membrane. Calcium ion sequestered in the SER is transported to the nucleoplasm via ryanodine receptors and IP_3R and taken back into the SER through calcium-ATPases (Santella and Bolsover, 1999).

MITOCHONDRIAL ROLE IN CELL LIFE AND DEATH

Mitochondria play a central role in many aspects of a cell's life and death. Besides their role in $[Ca^{2+}]_i$ regulation and signaling discussed previously, mitochondria carry out the tasks of ATP production, glucose homeostasis and oxygen sensing (Duchen and Biscoe, 1992; Rowe et al., 1996). Mitochondria are thought to have originated from free-living α proteobacteria and entered the precursor of eukaryotic cells (Smeitink et al., 2001). This process not only resulted in a more efficient way of metabolizing food (by using oxygen) but also led to evolution of the present oxidative phosphorylation system. Oxidative phosphorylation is the process by which organic nutrients are broken down to produce energy in the form of ATP (Smeitink et al., 2001).

Mitochondria are bound by two membrane systems: the outer and inner membranes. They occasionally come together to form junctional complexes or contact sites. The

space between the two membranes or intermembrane space, houses several proteins which are thought to play important roles in cell physiology, mitochondrial bioenergetics and also in cell death. The functional significance of the outer membrane is less well understood but it is known to be selectively permeable to ions and small molecules. It is also speculated that the outer membrane could play a significant role in modulating calcium uptake by a uniporter in association with the voltage dependent anionic channel (VDAC). The inner membrane is thrown into folds called cristae, which are the sites for several membrane bound enzyme systems (Duchen, 2004). Recent electron microscopic studies reveal the fact that mitochondrial cristae are not staggered into neat folds but are a complex array of tubules that divide and fuse continuously (Duguez et al., 2002; Perkins et al., 2001; Renken et al., 2002).

The enzymatic components of mitochondria include the citric acid cycle or tricarboxylic acid (TCA) cycle and respiratory (electron transport) chain. The enzyme systems involved in TCA cycle breakdown acetyl coenzyme A, a product of protein, fatty acid and pyruvic acid metabolism. These substrates get broken down to generate carbon dioxide and in the process reduce NAD^+ to NADH and FAD^+ to $FADH_2$. Both NADH and $FADH_2$ serve as substrates in the process of electron transport across a series of enzyme systems attached to the inner mitochondrial membrane (Figure I-4). These enzyme systems are identified as complex I (NADH dehydrogenase), II (succinate dehydrogenase), III (ubiquinol cytochrome C reductase) and IV (cytochrome C oxidase). Electrons are transferred from NADH and $FADH_2$ to complex I and complex II; both of them in turn shuttle electrons to complex III. Electrons from complex III require the

assistance of a small protein molecule (cytochrome C) attached to the outer surface of the inner mitochondrial membrane to shuttle electrons to complex IV. During the process of electron transport, the substrates viz., NADH and $FADH_2$ get reduced and generate protons at complexes I, III and IV.

The protons are pumped into the intermembrane space, which help in establishing an electrochemical proton gradient or proton motive force. This proton motive force has two components to it: (a) a pH gradient, because protons are acidic and (b) ionic gradient, because protons are charged. The ionic gradient represents the mitochondrial membrane potential and is usually 150 -180 mV negative relatively to the cytosol. This membrane potential drives the major bioenergetic functions of mitochondria, which include ATP synthesis, and accumulation of calcium ions. It provides a force that drives the inward movement of protons into the matrix via a fifth complex called ATP synthase. The energy stored in these protons is utilized in ATP synthesis from ADP and inorganic phosphate. Protons also neutralize the electrons that are eventually accepted by oxygen to form water (Duchen, 2004).

Mitochondria are the major site of reactive oxygen species (ROS) production within the cell. Normal physiological activity of the electron transport chain in mitochondria results in the production of semi-quinones that are a potential source of ROS (Papa and Skulachev, 1997). Oxidative stress occurs due to excess ROS in mitochondria. Within the mitochondria ROS mainly target the protein components of the membranes and polyunsaturated fatty acids. ROS targets cysteine residues or sulfhydryl groups of the membranes, resulting in cross-linking and formation of protein aggregates.

Hydroxyl radicals are known to initiate lipid peroxidation and generate peroxyl-radical and alkoxyl-radical intermediates. Mitochondrial DNA is probably the preferred target of ROS owing to its close proximity to the respiratory chain and absence of mitochondrial DNA-protecting mechanisms (Shiji et al., 1995).

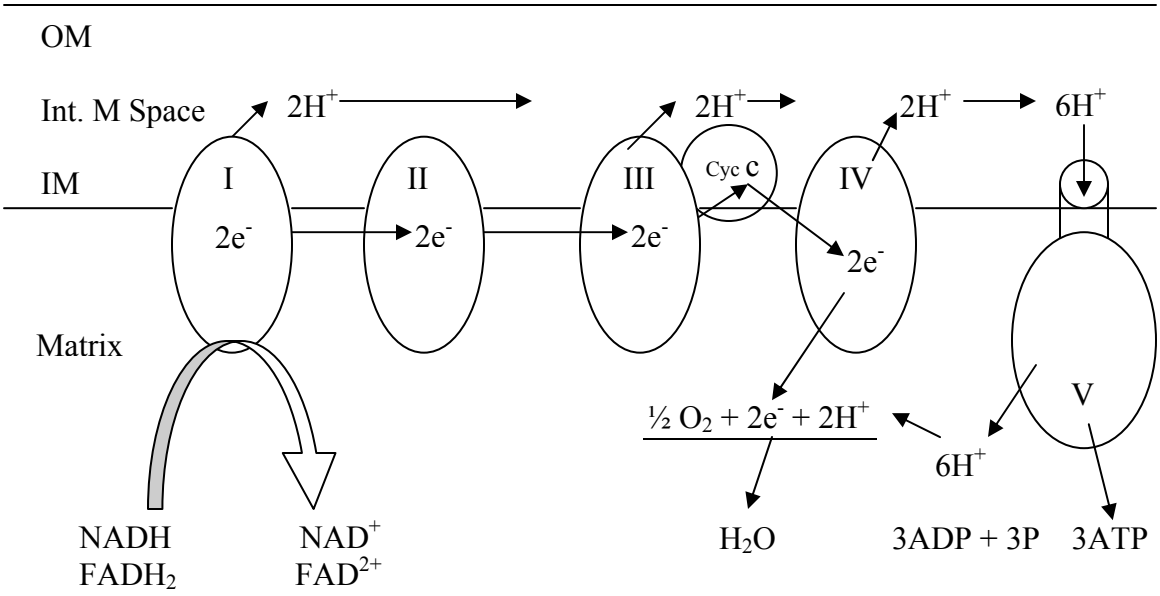

Figure I-4. Schematic representation of electron transport chain in mitochondria. Substrates of oxidative phosphorylation (NADH and $FADH_2$) are reduced during the process of electron transport across the inner membrane by a series of complexes I – IV. Protons are pumped into the intermembrane space, which not only contribute to the membrane potential but also help in the synthesis of ATP and neutralize electrons, which are then accepted by oxygen to form water. Abbreviation; OM = outer membrane, Int. M Space = intermembrane space, IM = inner membrane, Cyc C = cytochrome C

Severe damage to mitochondria can lead to cell death because mitochondria are the main sources of cells energy (ATP). Once ATP levels drop, energy dependent processes in the cell like maintaining calcium ion homeostasis, ion gradients, secretion of transmitters etc., will be disrupted. Disruption of ionic gradients will result in inability of the cell to maintain osmolarity. Eventually the cells will swell and die due to necrosis. In the brain this is especially important because neurons are totally dependent on mitochondrial oxidative phosphorylation for normal functioning. On the other hand, there is growing evidence that mitochondria by way of release of mitochondrial specific proteins into the cytosol, participate in an organized cell death process called apoptosis or programmed cell death.

Apoptosis is achieved through the mitochondrial permeability transition pore (MTP) or megachannel, which is a large maximal conductance pore with an estimated pore diameter of approximately 2 nm (Crompton and Costi, 1990) (Figure I-5). These pores are concentrated on the contact sites between inner and outer mitochondrial membranes. Hunter and Harworth first characterized these pores in the 1970s (Zoratti and Szabo, 1995; Ichas and Mazat, 1998). The opening of this megachannel is believed to increase the inner membrane permeability to solutes of molecular mass less than 1.5 kDa (Bernardi et al., 1999; Petronilli et al., 1994).

Opening of this megachannel can be triggered by various conditions (Zoratti and Szabo, 1995). However, an increase in mitochondrial calcium ion concentration coupled with a decrease in the ATP/ADP ratio as well as a state of oxidative stress is most likely to be a key event (Ichas and Mazat, 1998; Petronilli et al., 1994). The MTP appears to

have two different open confirmation states, one that allows low conductance and another that allows high-conductance. Under the low conductance state the MTP is involved in normal regulation of intracellular calcium ion homeostasis influenced through changes in the mitochondrial matrix pH (Davidson and Halestrap, 1990; Ichas et al, 1994). Under the high-conductance state opening of MTP results in irreversible changes in the membrane potential, eventually rupturing the outer mitochondrial membrane and causing release of proapoptotic factors into the cytosol (Zamzami et al., 1996; Scarlett and Murphy, 1997).

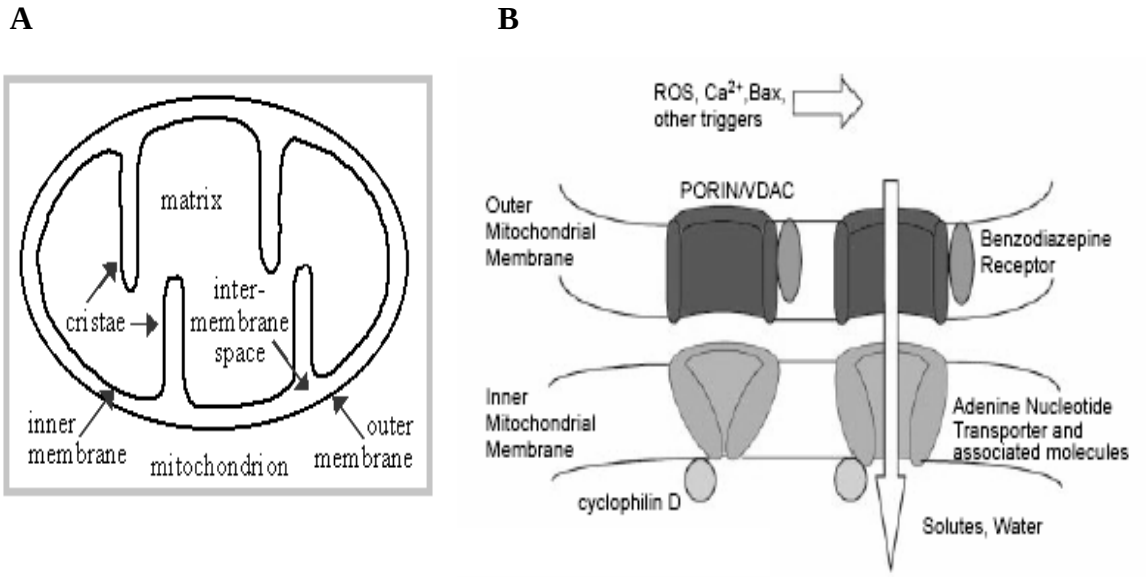

Figure I-5. Mitochondria and mitochondrial permeability transition pore (MTP). A) Schematic representation of a mitochondrion showing outer membrane, inner membrane folded to form cristae and matrix. B) Represents the formation of MTP in response to excessive ROS production or alteration of calcium homeostasis or proapoptotic proteins like Bax, resulting accumulation of excessive amounts of water and solutes in the mitochondria (adapted from Green and Reed, 1998).

APOPTOSIS (OR) PROGRAMMED CELL DEATH

Cell death is a fundamental biological process occurring during normal developmental and pathological processes. Cell death has been classified as being one of two distinct types viz., apoptotic or necrotic, which differ morphologically and biochemically (Gerschenson and Rotello, 1992; Kerr, 1971; Kerr et al., 1972). Cells dying as a result of acute injury typically swell, burst and spill their contents into their immediate surroundings. Rapid depletion of ATP and severe alteration of mitochondrial ultrastructure occurs resulting in initiation of an inflammatory response. This process of cell death is referred to as necrosis. By, contrast, a cell that undergoes apoptosis, dies without damaging its neighbors. The cell loses contact with the immediate viable cells, shrinks and condenses. The cytoskeleton scaffolding collapses, the nuclear envelope dissembles, and the nuclear DNA breaks up into fragments accompanied by maintenance of ATP levels (Kroemer, 1997; Mattson, 2000). The cell surface is altered such that it is swiftly recognized as a dying cell and is rapidly phagocytosed, by macrophages, before any leakage of the dying cells contents occurs. This not only avoids the damaging consequences of cell necrosis but also allows the organic components of the dead cell to be recycled by the cell that ingests it (Savill et al., 1993). Therefore, apoptosis can be defined as a type of cell death that is controlled by the dying cell itself (Hengartner, 2000; Reed, 2000). Recent findings based on the morphology of excitotoxic neuronal cell death suggest a possibility of an apoptosis-necrosis continuum (Portera-Cailliau et al., 1997a, b). Summary of differences between apoptosis and necrosis is given in Table I-3.

Cell death by apoptosis has a fundamental role during nervous system development and degeneration. During the normal development of the nervous system, neurons are initially over produced. This process is essential for establishing neuronal network or synaptic integration. The excess neurons are subsequently eliminated by apoptosis (Oppenheim, 1991; Sastry and Rao, 2000). Apoptosis in these neurons might be occurring due to competition for trophic factors (such as nerve growth factor) derived from target tissues and the Schwann cells that myelinate their processes in the peripheral nervous system (Snider, 1994; Oppenheim, 1991). Apoptosis in the nervous system has advantages over necrotic cell death because the latter process results in spread of inflammatory processes to the adjacent tissue. However, apoptosis on a large scale in the CNS can result in various neurodegenerative disorders like Alzheimer's disease or Parkinson's disease (Savitz and Rosenbaum, 1998).

Apoptosis is a process characterized by a complicated cascade of events that occur following many intracellular or extracellular insults (Hengartner, 2000; Raff, 1998; Reed, 2000; Savitz and Rosenbaum, 1998). The initial insult results in activation of pro-apoptotic genes that subsequently activate a family of proteases called "caspases". Caspases execute the final phase of apoptosis by cleaving key protein components of the cell so that cellular processes are disabled and the cell is phagocytosed (Cryns and Yuan, 1998; Thornberry and Lazebnik, 1998). Neurons are also susceptible to a variety of internal and external insults. Notable internal insults include NGF withdrawal, glutamate excitotoxicity, calcium ion imbalance, and oxidative stress. External insults include

neurotoxicants like methylmercury, DNA damaging agents and irradiation (Sastry and Rao, 2000).

Table I-3. Comparision between apoptosis and necrosis

Apoptosis	**Necrosis**
Also called "Active degeneration" Occurs in single cells	Also called "Passive atrophy" Occurs in groups of cells
No depletion of energy or ATP	Early depletion of energy or ATP
No initial major changes	Loss of cellular homeostasis
Cell adhesion lost at early stage	Cell adhesion lost at late stage
Altered membrane permeability - not an early event Cells shrink and fragment	Altered membrane permeability - early event Cells swell and rupture
Nucleus undergoes condensation - karyorrhexis & DNA fragmentation Cellular organelles generally intact	Nucleus undergoes karyolisis and - DNA undergoes diffuse degradation Mitochondria and other organelles damaged
Activation of macromolecular synthesis	Lowered macromolecular synthesis
Dense chromatin condensation seen	Chromatin seen as loose aggregates
De novo gene expression seen	De novo gene expression absent

(Sastry and Rao, 2000; Savitz and Rosenbaum, 1998)

In neurons, the plasma membrane, the ER, nucleus and mitochondria all can detect apoptotic signals. The plasma membrane has receptors for several neurotrophic factors and based on their presence or absence, pro- or anti-apoptotic signals are generated. For example: Apoptosis inducing factor-1 (Apaf-1) is known to trigger apoptosis by activating a caspase cascade. But the anti-apoptotic protein, bcl-2, whose activation

depends upon the binding of NGF to NGF receptor, inhibits its activation. In the absence of this signal bcl-2 fails to inhibit Apaf-1 activation, which eventually leads to activation of downstream caspases, and promotes apoptosis (Zou et al., 1997).

Nakagawa et al., (2000) reported that an ER-dependent apoptotic pathway is activated due to disruption of intracellular calcium ion homeostasis. This pathway activates caspase-12 to induce apoptosis. The nucleus, on the other hand, responds to DNA damage by activating a tumor suppressor gene, p53. Various cell cycle checkpoint proteins that sense DNA damage also activate p53, which in turn activates proteins responsible for apoptosis initiation.

There has been increasing evidence in the recent past that mitochondria participate in a critical effector stage of apoptosis. Mitochondrial membranes contain both pro- and anti-apoptotic proteins, collectively called the bcl-2 family (Adams and Cory, 1998). Localization of bcl-2 on the outer mitochondrial membrane facing the cytosol further supports the role of mitochondria in apoptosis (Lithgow et al., 1994). Members of the bcl-2 family protooncogene family have homologous domains (BH-1, BH-2 and BH-3) which function in interactions between the members. Of these, bcl-2, bcl-x_L and mcl-1 are anti-apoptotic, where as bax, bad, bak, bik and bcl-x_S are pro-apoptotic. The complex interactions of these proteins determine whether a cell lives or dies. For example, bcl-2 forms a heterodimer with bax to exert its anti-apoptotic function (Merry and Korsmeyer, 1997). Bcl-2 proteins regulate the pore forming subunit of the MTP and there by alter mitochondrial homeostasis. When the permeability transition pore opens, membrane potential is lost and in the process small proteins that are mitochondria-specific like

cytochrome C, apoptosis inducing factor (AIF) and/or Smac/Diablo are released into the cytosol (Adams and Cory, 1998). These proteins in turn can act alone or activate caspases and trigger apoptosis.

Cytochrome C release from the mitochondria has been shown to be a key event in the regulation of apoptosis (Kluck et al., 1997; Liu et al., 1996; Yang et al., 1997). In the cytosol, cytochrome C in presence of ATP and Apaf-1 binds to and activates caspase 9, which in turn cleaves and activates caspase 3. Caspase 3 further activates a down stream caspase cascade to induce apoptosis in a dying cell (Li et al., 1997; Liu et al., 1996).

Caspases are aspartic acid-specific cysteine proteases, which become activated in most forms of apoptosis. In cells, caspases are found in the nucleus, cytoplasm and the mitochondrial intermembrane space. Caspases can also be translocated to plasma membrane receptors via adaptor proteins (Boldin et al., 1996; Muzio et al., 1996; Thornberry et al., 1992). In most tissues caspases are expressed in an inactive form, called a proenzyme, that has an amino-terminal prodomain, a large subunit domain (~20kDa) and a small subunit domain (~10 kDa). The procaspase is proteolytically cleaved upon activation to remove the prodomain and release the large and small subunits. Active caspase enzyme has two active sites and is formed when two large and two small subunits assemble together (Rotonda et al., 1996)

At present, 14 caspases have been identified in the mouse (Kidd et al., 2000). Of these, 12 have been identified in humans. Phylogenetically caspases can be classified in to two sub groups, one with involvement in apoptosis (caspases –2, -3, -6, -7, -8, -9, -10 and –12), and the other called IL-1β-converting enzyme (ICE)-like caspases (caspases –

1, -4, -5, -11, -13 and –14). Caspases involved in apoptosis are further divided into initiator (8, 9, 10, 12) and effector (2, 3, 6, 7) caspases based on their proteolytic function. Initiator caspases process each other and the effector caspases. The effector caspases are mainly responsible for further activation of their down stream caspase effectors and proteolysis of a variety of cellular proteins resulting in cellular disassembly. ICE-like caspases have no known apoptotic function but are thought to be involved in pro-cytokine activation (Kidd et al, 2000; Thornberry et al., 1992).

Mitochondria are also known to play an important role in determining the type of cell death (apoptotic or necrotic). Availability of ATP is essential in order to execute apoptosis. The level of available ATP determines whether cell death follows an apoptotic pathway or a necrosis pathway (Magistretti et al., 1999).

The other pathway of apoptosis is *via* membrane bound death receptors such as tumor necrosis receptor superfamily (TNF-R1, Fas or DR 3-6). These receptors bind to their corresponding ligands resulting in receptor mediated recruitment of adaptor proteins (TRADD, FADD) (Ashkenazi and Dixit, 1998). This results in recruitment and activation of procaspases like caspase 8 and 2. The complex formed by the receptor, ligand and procaspase 8 or 2 is called as death inducing signaling complex (DISC). DISC activates caspase 8, which subsequently activates downstream caspases to induce apoptosis (Cohen, 1997).

AGING

Aging is a well known yet less understood phenomenon of human biology. Aging is a process marked by progressive decline in the efficiency of physiological processes with a tendency for reduced rate of recovery by organs and tissues following any insult. Over the years, many theories have been proposed regarding the process of aging. Among them one theory (free radical-mitochondrial) has remained the most promising. Denman Harman in 1956 proposed this theory in which he implicated free radical reactions as a cause for aging associated with environment, disease and natural aging processes. This theory gained further momentum after the role of mitochondria as both a source of ROS and a prime target of oxidative stress in aging tissues was recognized. According to this theory, oxidative damage to mitochondria due to intrinsic metabolic processes and/or environmental insults, results in triggering a cascade of events characterized by disruption of electron transport and generation of ROS in the inner mitochondrial membrane. This will eventually lead to depletion of ATP and promote tissue aging (Linnane et al., 1992; Samson and Nelson, 2000).

A number of observational and experimental studies both *in vivo* and *in vitro* have been done to support the free radical-mitochondrial theory. It was observed that in many tissues, ROS production, oxidative damage and mitochondrial dysfunction would increase as a function of advancing age. It was observed that the longevity of many vertebrate and invertebrate species is inversely proportional to oxygen consumption and basal metabolic rate and directly proportional to the antioxidant defense mechanisms (Barja, 2002; Golden et al., 2002). Mitochondrial DNA (mtDNA) is particularly

vulnerable to oxidative stress resulting in increased mutations in mtDNA and subsequent downstream effects (Linnane et al., 1992).

METHYLMERCURY AS A NEUROTOXICANT

Mercury (Hg) is one of the most ubiquitous and hazardous environmental contaminants found in ocean and freshwater fish, shellfish and in plants. The organic or methylated form of Hg, consisting of one methyl group bound to each atom of Hg, (methylmercury; MeHg), accounts for most of the Hg to which humans are exposed. Methylmercury (MeHg) is well known for its neurotoxic effects on both the developing and mature central nervous system (CNS).

Natural sources of mercury

Gas release from the earth's crust is a major source of environmental metallic Hg. Mercury vapor evaporates from the earth's crust, sea surfaces and volcanoes, marking the beginning of global cycling of mercury (Fitzgerald and Clarkson, 1991). Mercury vapor is a very stable gas with approximate residence time of about 1 year in the atmosphere. Therefore, mercury can be globally distributed even to remote regions of the planet from point sources. Mercury vapor in the upper atmosphere is oxidized to water-soluble ionic mercury by an unknown process. This form of mercury is then returned to the earth's surface in the form of rainwater (Clarkson, 2002) (Figure I-6).

The other natural source of mercury exposure is from consumption of fish and other seafood from Hg-polluted water. The inorganic form of Hg found in aquatic

environments is methylated to primarily monoMeHg and to a lesser extent diMeHg by microbial action (methanogenic bacteria) or nonenzymatic reactions. This is the first step in bioaccumulation process in the aquatic food chain. MeHg moves up the food chain from plankton to small fish and finally to top fish predators such as sharks and other fish eating marine mammals (Chang, 1991; Clarkson, 2002).

Other sources of mercury

Metallic Hg pollution is produced from smelters, combustion of fossil fuel, refining of gold and from mining operations. Hg is used in large quantities in the chloralkali industry during the production of chlorine and caustic soda through the electrolysis of brine (NaCl solution). It is also used in the electrical industry in the production of control instruments such as thermometers and barometers, fluorescent tubes, and alkaline batteries, and in dentistry for amalgam fillings. Occupational exposure can occur to workers in all these settings.

Chemical and physical properties

Hg has an atomic weight of 200.6, an atomic number of 80, a melting point of – 38.9°C, a boiling point of 356.6°C and a density of 13.6 (Chang, 1997). It is perhaps the only metal that is in a liquid state at room temperature. Its vapor is much more hazardous than the liquid form. It exists in three oxidation states. In the zero oxidation state (Hg°) Hg exists in metallic form or as vapor. Hg^{+} and Hg^{++} (mercurous and mercuric states) are the two higher oxidation states. Mercuric Hg can form a number of

stable organic Hg compounds by attaching to one or two carbon atoms. Methyl Hg is the most important form from the point of view of human exposure (Massaro et al., 1996).

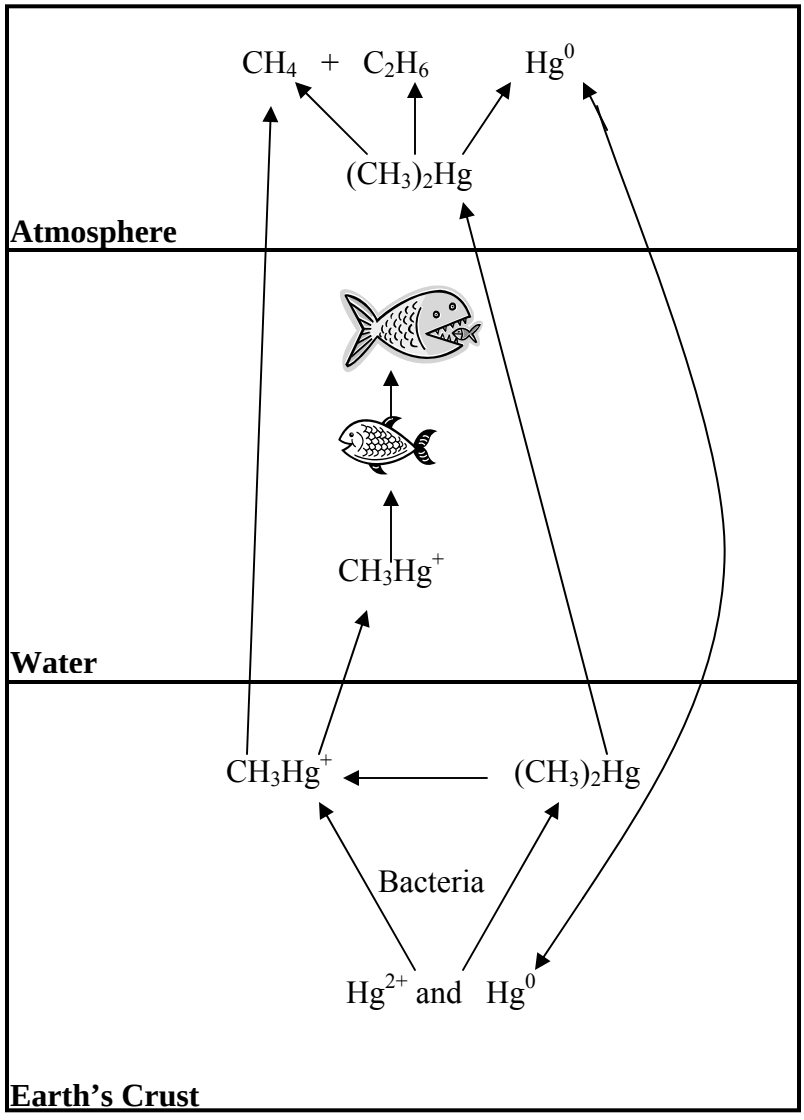

Figure I-6. Schematic representation of biological cycling of mercury. Inorganic and elemental forms of mercury are converted to organic/methylated form of mercury in earths crust. Methylmercury moves up the aquatic food chain and gets bioaccumulated. Methylmercury also gets evaporated into the atmosphere where it breaks down to elemental form and returns to earth's crust in the rainwater.

Disposition of methylmercury in the body

About, 95% of MeHg ingested orally is absorbed in the gastrointestinal tract (Aberg et al., 1969). Within 30 hours it is completely distributed to all tissues. 5% of the absorbed MeHg is found in the blood compartment, with more than 90% attached to hemoglobin in red blood cells (Kershaw et al., 1980). About 10% of the absorbed MeHg is found in brain where it is slowly demethylated to inorganic mercury. *In vivo* studies in rodents suggest that MeHg is transported as MeHg-L-Cysteine complex across the blood brain barrier via a leucine preferring amino acid transporter (Aschner et al., 1991; Kerper et al, 1992). The other possible mechanism of MeHg transport is by forming a MeHg-glutathione complex (Fujiyama et al., 1994). MeHg crosses the placental barrier and accumulates in the fetal blood at slightly higher levels than in maternal blood. Fetal brain mercury levels were found to 5-7 times higher than the maternal blood (Cernichiari et al., 1995).

MeHg is metabolized at the rate of 1% of the body burden per day mainly by the intestinal microflora and to some extent by the phagocytes. Although the precise mechanism is not known, Hg as MeHg during exposure is converted to inorganic Hg and retained in the central nervous system for a long time, probably in an inert form such as insoluble mercury selenide (Clarkson, 2002). Major routes of excretion from the human body are via the bile and feces. About 1% of the body burden is excreted daily. While 90% of ingested mercury is excreted in feces the remaining 10% is excreted in urine as mercuric Hg. The biological half-life of Hg in the whole human body is 70-80 days.

Biomarkers of exposure

Two important biomarkers of exposure for MeHg are blood and hair. Nail clippings have also been used to assess Hg exposure (MacIntosh et al., 1997). Adult blood Hg concentration is routinely used as a biomarker of MeHg exposure and to calculate dose-response relationships in adult neurotoxicity (Hecker et al., 1974; Mahaffey and Mergler, 1998). Similarly, fetal cord-blood or maternal-blood levels of Hg were being used to assess exposure to the developing fetus (Fujita and Takabatake, 1977; Kuhnert et al., 1981; Kuntz et al., 1982; Grandjean et al., 1992; Girard and Dumont, 1995; Oskarsson et al., 1996). The present detection limits for total Hg in blood is in the range of 0.1-0.3 ppb (Grandjean et al., 1992; Girard and Dumont, 1995; Mahaffey and Mergler, 1998; Oskarsson et al., 1996). Mean blood level of Hg in populations with limited or no fish consumption was reported to be ~2ppb (Brune et al., 1991). On the other hand the mean cord-blood level of Hg in a high fish eating population located on the Faroe Islands was found to be ~24 ppb (Grandjean et al., 1992). These examples suggest measuring blood Hg levels is a good biomarker of MeHg exposure.

Although blood Hg levels serve as good biomarkers of exposure, it is an invasive method of sample collection. On the other hand hair sampling is a noninvasive technique that can be done without medical supervision. Detection limits for assessing hair Hg levels are in the range of 0.01-0.04 ppm (Gaggi et al., 1996; Lopez-Artiguez et al., 1994; Stern et al., 2001) using standard cold-vapor analytical techniques. Using this technique hair Hg levels obtained from little or no fish consuming population were 0.2-0.8 ppm

(Grandjean et al., 1992; Smith et al., 1997). In the fish consuming population of the Seychelles and Faroe Islands Hg levels in hair were found to be 6.8 and 4.8 ppm, respectively (Cernichiari et al., 1995; Grandjean et al., 1992). Finally, measurement of Hg in the brain also serves as a good biomarker of exposure as brain is the ultimate target of MeHg toxicity.

Historical perspective of methylmercury

Historically, MeHg exposures have been connected with high morbidity and mortality rates over the last 40 years in Japan, Iraq, Pakistan and Guatemala (Bakir et al, 1973; Rikuzo et al, 1996). In Japan, in May 1956, the first official case of MeHg poisoning was discovered in Minamata city, situated in the southwest region of Japan's Kyushu Island. At the time of outbreak nearly 200,000 people lived in the surrounding areas. At the time of the disease outbreak the cause was not known and so it was named "Minamata disease" after the place where it was first discovered.

During the same period, residents of the Minamata Bay area began to notice strange phenomena like the birds falling while in flight, fish rotating continuously and floating with their belly pointing towards the surface. But the most shocking incidences were noticed in cats. Cats showed signs of excessive salivation, convulsions, violent rotation movements, and abnormal gait leading to death. Many cats appeared frenzied and jumped into the sea to their death. Cats played an important role in identifying the etiology of the disease (Harada, 1995).

The cause of the disease was identified as MeHg by a visiting Scottish physician based on the neurological signs and symptoms noticed in affected individuals. Finally, the source of this epidemic was traced to a factory manufacturing acetaldehyde, where inorganic Hg compounds were used as catalysts. Inorganic Hg was converted into MeHg during the synthesis process and was let into the Minamata Bay. MeHg later bioaccumulated in fish to lethal levels and triggered the epidemic (Clarkson, 2002). In 1960, Hg levels of 2010 ppm in wet weight were detected from the sludge near the drainage canal of this factory. The marine fauna of the Minamata Bay exhibited high levels of Hg concentration (crabs-35.7 ppm; oysters-5.61 ppm, *Hormomya* nutabilis (fish)-11.4 to 39.0 ppm). Patients who died from MeHg poisoning also exhibited high levels of Hg in their internal organs (liver-22.0 to 70.5 ppm; brain-2.6 to 24.8 ppm; kidneys-21.2 to 140.0 ppm) (Harada, 1995). A similar outbreak occurred in Niigata, Japan and by 1970, 47 cases of Hg poisoning were registered along with 6 deaths.

A second episode of MeHg poisoning was reported in Iraq in 1972 when seed grain treated with a MeHg-containing fungicide, originally intended for planting was ground into flour and consumed as bread. This episode of MeHg poisoning was most catastrophic in terms of morbidity and mortality. Of the 6530 cases reported throughout the country, 459 deaths were attributed to MeHg poisoning. Hg treated grain was distributed to farmers in September 1971 and cases of poisoning began to surface and increased by early January 1972. Mean MeHg content of the wheat grain samples were around 7.9 ppm with one sample showing 30.6 ppm. The mean MeHg content of the flour samples tested was 9.1 ppm (Amin-Zaki et al, 1974; Bakir et al., 1973).

Other significant cases of MeHg poisoning were reported in Guatemala and Pakistan during the 1960s. In Guatemala, poisoning cases were originally thought to be viral encephalitis, where 45 people were affected and 20 died. Later, the causative agent was identified as methylmercury dicyandiamide containing fungicide that was used to treat wheat before distribution to the farmers. A similar outbreak was reported in Pakistan in 1969 (Bakir et al, 1973).

Clinical signs and pathological findings

The CNS is the major target site of MeHg toxicity. Toxic effects of MeHg differ in the developing brain when compared to the adult/mature brain in terms of both mechanism of action and outcome (ATSDR, 1999; U.S EPA, 2001). A latency period exists in adults between exposure to MeHg and onset of symptoms. This period can extend from weeks to several months depending upon the dose and length of exposure. The case of fatal poisoning of a chemistry professor due to dimethylmercury goes down in history as an example of latent effects of organic mercury. Following a single exposure to liquid dimethylmercury, the first signs of poisoning appeared after 4 months. Within few weeks symptoms of severe MeHg poisoning became clear (Nierenberg et al., 1998).

In the case of acute adult exposure in the Minamata Bay episode, symptoms like concentric constriction of visual fields, sensory disturbances, ataxia, dysarthria, auditory disturbances and tremors were observed (Harada, 1995). Pathological changes included massive loss of neurons in the cerebral and cerebellar cortex. Within the cerebral cortex,

significant changes were observed in the visual, motor, sensory and auditory cortices. In the cerebellum, granule cell atrophy was remarkable while Purkinje cells were spared (Takeuchi et al., 1962). In the peripheral nervous system, characteristic findings included damage and demyelination of dorsal root or sensory nerve fibers (Takeuchi et al., 1962).

Children exposed prenatally to acute, high doses of MeHg exhibited congenital cerebral palsy, mental retardation, primitive reflexes, cerebellar ataxia, disturbances in physical development and nutrition, dysarthria, deformity of the limbs, hyperkinesias, hypersalivation, and strabismus (Harada, 1977). Although mothers of children born with congenital Minamata disease appeared asymptomatic, a detailed examination revealed that they suffered from mild symptoms of MeHg poisoning. Symptoms such as sensory disturbances, focal cramps, mild ataxia, auditory disturbances, pain in the limbs, constriction of visual fields, dysarthria and tremors were observed (Harada, 1995). Hair samples of mothers when analyzed 5-8 years later revealed 1.82-191 ppm of Hg while their children exhibited a range of 5.25-110 ppm. In another incidence in Niigata, Hg content in the hair of a mother who gave birth to a prenatally exposed child was 293 ppm. Only mild symptoms like sensory disturbances were observed in the mothers (Harada, 1995). Pathological findings in children exposed prenatally to MeHg included generalized atrophy and hypoplasia of cortex, abnormal cytoarchitecture, hypoplasia of corpus callosum and dysmyelination of pyramidal tract (Matsumoto and Takeuchi, 1965).

Chronic Minamata disease patients were categorized into one of the three group's viz., 1) gradually progressive, 2) delayed onset and 3) escalating or progressive with

aging. These patients exhibited sensory disturbances described as “glove and stocking”. They experienced difficulty in putting on gloves and stocking due to generalized weakness of the extremities. Constriction of visual fields and auditory disturbances were relatively high while ataxia was not as severe when compared to acute and subacute patients (Harada, 1995). Autopsies of more than 100 patients with chronic Minamata disease who lived in heavily contaminated areas, revealed higher concentrations of both total Hg and MeHg when compared to the controls (Takeuchi et al., 1979). Pathological findings included lesions in cerebral and cerebellar cortices and changes in peripheral nerve fibers (Takeuchi et al., 1979).

In the Iraq MeHg exposure episode, predominant symptoms closely resembled those of Minamata disease. The first symptoms observed were numbness of extremities and perioral area. In some cases symptoms did not appear until sometime after consumption of contaminated bread was stopped while in others appearance of symptoms coincided with cessation of consumption of contaminated bread. The mean latency periods for onset of clinical signs ranged from 16-38 days, with a few cases extending to 60 days. Severity of symptoms depended upon the level of exposure. People exposed to contaminated bread for a short time exhibited only numbness or paresthesia. Long term exposure to contaminated bread resulted in symptoms like ataxia, constriction of visual fields, slurred speech and hearing difficulties. Medical treatment could not rescue severely poisoned patients (Bakir et al., 1973). In prenatally exposed infants, symptoms like gross impairment of motor and mental development with cerebral

palsy, deafness and blindness were observed. Mothers of the prenatally exposed infants also exhibited symptoms of MeHg poisoning (Amin-Zaki et al., 1974; Bakir et al, 1973).

Biochemical mechanisms of methylmercury neurotoxicity

After reaching the target cells, MeHg becomes associated with various intracellular organelles like mitochondria, ER, Golgi complexes, lysosomes and the nuclear envelope. In the peripheral nervous system, MeHg is primarily localized in the myelin sheath and mitochondria of the nerve fibers (Chang, 1977). Clinical cases from the Iraq episode suggest a possible role of MeHg toxicity in increased incidence of neuromuscular weakness (Rustam et al., 1975). In experiments on frog muscle-nerve preparations, it was found that acute MeHg exposure did not have any direct affect on muscle contraction. However, nerve-evoked responses were blocked in a time dependent manner due to acute MeHg exposure (Juang, 1976). Such a response could be due to a decrease in nerve-evoked release of acetylcholine (ACh) by altering its spontaneous quantal release, much of which depends upon the extent of $[Ca^{2+}]_i$ disruption. In these experiments MeHg was directly applied to muscle-nerve preparations. Somjen et al., (1973) reported similar findings in rats exposed to acute or subchronic doses of MeHg. In these experiments gastrocnemius muscle contraction measured *in situ* was diminished in MeHg treated rats when compared with controls. These results indicate that MeHg affects muscle contractility by impairing conduction of nerve action potentials or by disrupting synaptic transmission or both. These changes can be seen following direct application and systemic administration.

MeHg is known to bind both muscarinic and nicotinic cholinergic receptors (Shamoo et al, 1976; Coccini et al 2000). MeHg was found to inhibit binding of ACh to nicotinic receptors in the *Torpedo* electroplax (Shamoo et al., 1976). Muscarinic receptors might be the most likely targets for MeHg induced neurotoxicity because mammalian brain consists more of muscarnic than nicotinic receptors. A typical muscarinic receptor consists of a pair of extracellular cysteine/thiol residues that form a disulfide bond between the two extracellular loops of the receptor (Zeng et al., 1999). Agents that modify these thiol groups can alter muscarinic receptor activity, as they are very critical in agonist and antagonist binding (Hedlund and Bartfai, 1979). MeHg as such is known to bind to thiol groups with high affinity and so it is not surprising to see it inhibiting agonist binding to muscarinic receptors. By preventing the agonist binding to the receptor MeHg is disrupting neurotransmission post synaptically (Castoldi et al., 1996).

Rats exposed to MeHg exhibited a significant increase in the density of muscarinic receptors in the cerebellum and hippocampus with no affect on receptor affinity. This increase was observed 2 weeks after MeHg treatment was stopped indicating a delayed up-regulation effect on the receptor density in these regions of the brain (Coccini et al., 2000). This effect was found to be region specific as no such changes were observed in cerebral cortex. Granule cells were found to express a higher density of muscarinic receptors than any other cell type in the cerebellum (Neustadt et al., 1988). Two regions of the brain viz., cerebellum and hippocampus, are of particular importance with respect

to muscarinic receptors and MeHg toxicity because both these brain regions tend to show up-regulation in muscarinic receptors and accumulate MeHg (Coccini et al., 2000).

MeHg is also known to play a key role in induction of apoptosis by interfering with cell cycle progression at the G2-M phase through microtubular disruption (Miura et al, 1999). Several *in vitro* experiments using cultured cells demonstrated that MeHg binds to tubulin dimer SH-groups and depolymerizes cytoplasmic microtubules and/or inhibits tubulin polymerization (Miura et al., 1978, 1984; Imura et al., 1980; Sager et al., 1983; Vogel et al., 1985, 1989). This result in mitotic arrest of the cultured cells exposed to MeHg (Miura et al, 1978, Sager, 1988). Rodier et al (1984) and Sager et al (1984) demonstrated the same phenomenon in developing rat brain. In all these studies the effect of MeHg on microtubule disruption was compared with the effects of colchicine, a mitotic inhibitor known to cause G2-M phase arrest of cell cycle before triggering apoptosis.

Disruption of protein synthesis is considered to be an early indication and primary mechanism of MeHg toxicity in the nervous system (Yoshino et al., 1966; Verity et al., 1977). However, a direct relationship between MeHg exposure and inhibition of protein synthesis has not been established. Cerebral and cerebellar slices of rats exposed *in vivo* to MeHg showed decreased incorporation of [^{14}C] leucine in both latent and neurotoxic phases. Interestingly, this effect occurred even before the neurological symptoms appeared (Yoshino et al., 1966; Verity et al., 1977). Verity et al (1975) demonstrated a similar effect of MeHg in an *in vitro* study using brain slices and synaptosomes. Effect of MeHg on protein synthesis and phosphorylation differed from study to study. While

some studies showed no change (Kawamata et al., 1987), others showed a decrease (Kuznetsov et al., 1987) or increase (Sarafian and Verity, 1990) in protein synthesis.

MeHg has been shown in a number of studies to alter intracellular calcium ion homeostasis (Atchison and Hare, 1994; Denny and Atchison, 1996). Increases in $[Ca^{2+}]_i$ was considered a key event in MeHg induced neurotransmitter release (Atchison, 1986). The source of these calcium ions is considered to be primarily from mitochondria, with minimal or no contribution from the smooth endoplasmic reticulum (Gasso et al., 2000; Levesque and Atchison, 1988). MeHg was shown to elevate $[Ca^{2+}]_i$ in a number of cell types including cultured rat cerebellar granule neurons (Shenker et al., 1992, 1993; Denny et al., 1993; Marty and Atchison, 1997; Mundy and Freudenrich, 2000). *In vitro* studies using cultured granule cells and *in vivo* studies using rats demonstrated that MeHg induced $[Ca^{2+}]_i$ elevations were not as a result of direct excitotoxic insult because inhibition of excitatory amino acid receptor-activated channels did not prevent MeHg induced elevations in $[Ca^{2+}]_i$ (Castoldi et al., 2000; Marty and Atchison, 1997; Marty and Atchison, 1998).

In contrast, when voltage-gated calcium channels (VDCC) were blocked with known calcium ion channel blockers like nifedipine, the time of onset of MeHg mediated increase in $[Ca^{2+}]_i$ was delayed both in NG108-15 neuroblastoma (Hare and Atchison, 1995b) and primary cerebellar granule cell cultures (Marty and Atchison, 1997). The response of granule cells to MeHg induced elevation of $[Ca^{2+}]_i$ was found to be approximately 10 times that of NG108-15 neuroblastoma cells (Hare and Atchison, 1995a).

Experiments using a ratiometric fluorescent dye, Fura 2AM, indicated that cells in presence of extracellular calcium ions, when exposed to acute, submicromolar concentrations of MeHg, preceded by a brief depolarization with 40 mM potassium ions, exhibited multiphasic alterations in Fura 2 fluorescence. The first phase of increase in $[Ca^{2+}]_i$ was both temporally and kinetically distinct from the second phase. The first phase was a result of release of calcium ions from intracellular stores like mitochondria and smooth endoplasmic reticulum (Bearrs et al., 2001; Limke et al., 2003). The second phase was thought to occur as a result of influx of extracellular calcium ions into the cell through L, N and/or Q-type VDCCs (Marty and Atchison, 1997). Thus, MeHg induced neurotoxicity was attributed to a calcium dependent component, as toxic effects including cell death were prevented by inhibiting alterations in $[Ca^{2+}]_i$ homeostasis.

MeHg is also implicated in disrupting several functions of mitochondria, such as electron transport or respiration and oxidative phosphorylation. Levesque and Atchison (1991) showed that mitochondria isolated from rat forebrain when exposed to MeHg resulted in the release of mitochondrial-associated calcium ions, and at the same time prevented uptake of calcium ions by the mitochondria. Decrease in mitochondrial respiration was thought to occur as a result of MeHg induced inhibition of the citric acid cycle or tricarboxylic acid (TCA) cycle. Decreases in rate of respiration were observed both *in vitro* using synaptosomes from rats (Verity et al., 1975) and guinea pig brain slices (Fox et al., 1975) and *in vivo* in rats exposed to MeHg (Yoshino et al., 1966).

More recently, MeHg was shown to open the mitochondrial permeability transition pore (MTP) leading to apoptotic cell death (Limke and Atchison, 2002; Limke et al.,

2003, 2004). This could result in dissipation of mitochondrial membrane potential (MMP), which eventually could result in efflux of mitochondrial calcium ions and inhibition of mitochondrial calcium ion uptake (Komulainen and Bondy, 1987; Hare et al., 1993; Denny et al., 1993). Opening of MTP and depletion of MMP could occur due to excessive accumulation of calcium ions within the mitochondrial lumen or production of reactive oxygen species (ROS) and depletion of ATP (Bernardi et al., 1998). All of these processes either independently or in combination have been implicated in MeHg toxicity (InSug et al., 1997; Shenker et al., 2000; Limke and Atchison, 2002). Opening of the MTP results in the escape of molecules < 1.5 kDa including proapoptotic cytochrome C across the inner mitochondrial membrane (He et al., 2000; Pastorino et al., 1999; Petronilli et al., 2001). In cultured granule cells Limke and Atchison (2002) demonstrated a delay in MeHg induced elevation of $[Ca^{2+}]_i$, loss of MMP and cell death by inhibiting MTP using cyclosporine A.

Reactive oxygen species such as hydroxyl radicals, hydrogen peroxide and superoxide anion are believed to initiate peroxidative cell damage. MeHg is also widely implicated as a cause for elevation in ROS levels. When human monocytes (Insug et al., 1997), T cells (Shenker et al., 1998) and neurons from mice and rats (Ali et al., 1992; Yee and Choi, 1994) were exposed to MeHg, increases in ROS were observed. All aerobic cells generate ROS not only as by products of metabolism but also in response to various stimuli (Fridovich, 1978). *In vivo* as well as cell culture studies using antioxidants like vitamin E, probucol and propylgallate reduced generation of ROS after prior treatment with MeHg (Usuki et al., 2001; Gasso et al., 2001). This certainly

indicates a role of ROS in cell damage in response to MeHg toxicity. Another interesting phenomenon observed was the localization of ROS in brain regions that are specifically sensitive to the effects of MeHg, including the cerebellum (LeBel et al., 1990, 1992). However, MeHg induced oxidative stress may not result in cell death. Sarafian and Verity (1991) demonstrated in rat cerebellar granule cells that MeHg induced ROS levels and lipid peroxidation were prevented by vitamin E pretreatment but could not protect them against cell death. Taken together, these studies provide convincing evidence that MeHg induced ROS production is not the determining factor for its neurotoxic abilities.

A number of studies have demonstrated a prominent role for astrocytes in mediating MeHg induced neurotoxicity (Gatti et al., 2004; Shanker and Aschner, 2003; Shanker et al., 2004). Although MeHg was shown to cause neuronal cell death in many *in vivo* and *in vitro* studies (Davis et al., 1994; Sarafian et al., 1994), it predominantly accumulates within astrocytes (Charleston et al., 1996, Davis et al., 1994). Astrocytes are known to play a vital role in providing glutathione (GSH) precursors to neurons. In addition, astrocytes also play important role in neuronal migration, release of neurotrophic factors, glutamate uptake and metabolism (Allen et al., 2002).

Both neurons and astrocytes are known to possess at least three temperature dependent transport systems (sodium independent, X_C; Sodium dependent, X_{AG}; γ-glutamyltranspeptidase, GGT) for cysteine, a GSH precursor (Allen et al., 2001). Inhibition of all three-transport systems decreased cysteine transport in both astrocytes and neurons. In astrocytes treated with MeHg cysteine uptake was inhibited exclusively

due to its action on the X_{AG}- transporter system (Allen et al., 2001). Taken together, MeHg causes overproduction of ROS and also decreases astrocytic GSH levels as a result of inhibition of cysteine transport. Thus, one can conclude that MeHg ultimately can lead to decreased neuronal GSH levels and increase glutamate toxicity (Allen et al., 2002).

OBJECTIVES OF THE DISSERTATION

The main objective of this dissertation was to determine the underlying mechanisms of MeHg induced neurotoxicity in young adult and aged population-using mice at postnatal (P) day 29 and between 16-20 months of age as a model. Two exposure levels were tested (1.0 mg/kg and 5.0 mg/kg body weight). The long-term goal of this research is to understand the effects of MeHg on fully developed central nervous system (CNS) and compare those results to developing CNS. This will enable us to understand the critical factors involved in MeHg toxicity across the human life span.

The four specific objectives of this dissertation are as follows:

I. To assess the mercury concentrations in mouse brain using different routes of administration and different tissue preparations.

II. To determine the behavior effects of *in vivo* MeHg exposure in young adult mice.

III. To understand specific biochemical processes leading to granule cell death/dysfunction due to *in vivo* MeHg toxicity in mice.

IV. To determine the toxic effects of *in vivo* MeHg exposure on mice aged between 16-20 months.

Mercury concentration in mouse brain tissue was determined by combustion / trapping / atomic absorption method using Milestone Direct Mercury Analyzer 80 (DMA 80). Assessment of mercury concentration in brain tissue provided useful information on brain mercury levels obtained by different routes of exposure and different dosing regimen. Based on the results obtained in this specific objective, divided oral dosing protocol was used to accomplish other specific objectives.

In the second objective, behavior analysis was performed to determine the extent of cerebellar dysfunction as a result of *in vivo* MeHg exposure. Identifying behavior deficits provided valuable insights for further investigations related to subcellular effects of MeHg toxicity.

In the third objective, biochemical processes leading to granule cell dysfunction/death was assessed. Fluorescent confocal microscopy, electron microscopy, histochemistry and immunohistochemistry were carried out to investigate alteration in cellular function in young adult mice exposed to MeHg.

In the last objective, toxic effects of *in vivo* MeHg exposure was determined in mice aged between 16 and 20 months using confocal microscopy and behavior tests.

CHAPTER II

ASSESSMENT OF MERCURY CONCENTRATIONS IN MOUSE BRAIN USING DIFFERENT ROUTES OF EXPOSURE AND DIFFERENT TISSUE PREPARATIONS*

SUMMARY

The objective of this study was to determine the best method for preparing brain tissue for mercury analysis from mice exposed to methylmercury either through subcutaneous (sc) injection or through ingestion. C57BL/6J mice at postnatal day 29 were exposed to 0.0 or 5.0 mg/kg methylmercuric chloride (MMC) given sc or through food containing MMC. Eighteen mice received vehicle (sodium bicarbonate; sc) and 18 additional mice received 5.0 mg/kg MMC (sc). Whole brain tissue was prepared using one of four tissue preparation methods: rapid freezing, saline perfusion, 4% paraformaldehyde perfusion fixation, and 4% paraformaldehyde immersion fixation. Brains from vehicle-treated mice exhibited minimal levels of mercury (0.0007-0.0018 ppm) in all preparation methods. Mercury content in rapidly frozen control brains differed statistically from immersion fixed control brain tissue. There was no significant difference in mercury content from mice given 5.0 mg/kg MMC (sc) in all preparation methods (0.2660-0.3650 ppm). Additional mice were divided into groups of six mice

* Reprinted with permission from "Assessment of mercury concentrations in mouse brain using different routes of exposure and different tissue preparations" by Sairam Bellum, Kerry A. Thuett and Louise C. Abbott, 2002. Toxicology Mechanisms and Methods, In press. Copyright 2005 by Taylor and Francis.

each: single oral dose of 5.0 mg/kg MMC; total oral dose of 5.0 mg/kg MMC divided into five doses; and vehicle only. Forebrain (0.3243 ppm) and hindbrain (0.1908 ppm) mercury content in MMC treated mice given multiple doses was 10 times higher than in brain tissue from mice given a single 5.0 mg/kg dose. Brain mercury content following administration of 5.0 mg/kg MMC *via* the oral route (0.5354 ppm) differed statistically from the sc route (0.3430 ppm). In conclusion, different tissue preparation methods do not significantly affect brain mercury content, but route of administration and dosing regimen can influence total brain mercury content.

INTRODUCTION

Mercury (Hg) is a ubiquitous contaminant found in ocean and freshwater fish, shellfish and in plants (Shenker et al, 1998; Sanfeliu et al, 2001; Risher et al, 2002; Siciliano et al, 2003; Eisler, 2004). The organic form consisting of one methyl group bound to each atom of mercury, (methylmercury; MeHg), accounts for most of the mercury to which humans are exposed (Rice, 1995). Inorganic mercury that is a byproduct of numerous industrial processes is converted to MeHg *via* bacterial metabolism.

In 1997, the U.S. Environmental Protection Agency (EPA) recommended a reference dose of no more than 0.1 μg/kg body weight/day for MeHg exposure in the human population (Clarkson, 2002), which translates into limiting consumption of food sources with MeHg contamination including freshwater fish and ocean fish such as tuna (Rice, 1995; Limke and Atchison, 2002). The persistent contamination of our

environment with mercury indicates that mercury will remain bioavailable as MeHg for decades, affecting current as well as future generations (Grandjean and Weihe, 1998).

MeHg is primarily a potent neurotoxicant known to cause neuronal degeneration (Bakir et al, 1973; Nielsen, 1992; Rikuzo and Mitsuhiro, 1996). In both humans and rodents, neocortical and cerebellar granule neurons in particular are very sensitive to MeHg toxicity (Yuan and Atchison, 1999; Limke and Atchison, 2002). Therefore, brain mercury concentration appears to be an important biomarker of MeHg exposure. Studies involving chronic, low dose exposure to MeHg have been carried out to assess mercury distribution within the central nervous system (Newland and Reile, 1999). Although chronic, low dose exposure in experimental animal models simulates the most common form of human exposure (Newland and Reile, 1999), acute and/or short-term exposures also occur in humans. Therefore, it is of interest to assess mercury accumulation in brain tissue subsequent to more short-term exposures.

Most *in vivo* experimental exposures to MeHg have been carried out using MeHg added to drinking water because it is a convenient method of administration and because up to 95% of ingested MeHg can be absorbed from the gastrointestinal tract (Newland and Reile, 1999). MeHg also can be administered by oral gavage or subcutaneous injection (Norseth and Clarkson, 1970; Rowland et al, 1980; O'Kusky, 1983; Aschner and Clarkson, 1988; Yasutake and Hirayama, 1988; Leyson and Morgan, 1991). However, these last two administration methods are typically associated with additional stress experienced by the treated animals or increased potential accidental exposure of laboratory personnel to MeHg. We have developed an easy, reliable, relatively safer and

relatively stress free method to administer MeHg to lab animals through addition of MeHg to their food. We have compared this method of MeHg administration to subcutaneous injection of MeHg. In addition, we also have examined different techniques for processing brain tissue before measuring mercury content. It is clear that the method of processing tissues prior to mercury content analysis may effect the mercury concentrations that are observed. We investigated whether the amount of total mercury measured in brain tissue varied with different methods of tissue preparation and determined the best method to prepare brain tissue samples for mercury analysis using direct mercury analysis. We determined whether the concentration of mercury observed in the forebrain was different from hindbrain following acute exposure, since mercury concentrations in different parts of the brain are likely to be related to different clinical signs exhibited by exposed animals and/or humans. We also determined whether the dosing regimen affected the observed concentration of mercury in brain tissue. We chose mice as our experimental model to perform these studies because there is some evidence to suggest that mice might be a slightly better model for MeHg toxicity than the rat, especially when comparing *in vivo* data to human subjects (Lewandowski et al, 2003). Information obtained from this investigation will contribute to better understanding of various factors such as route of exposure, method of tissue processing and distribution of mercury in brain tissue following *in vivo* exposure.

MATERIALS AND METHODS

Animals

Adult C57BL/6J: +/+ (wild type) male and female mice, originally obtained from The Jackson Laboratory (Bar Harbor, MA, USA), were bred to produce wild type offspring. All mice were housed at the Laboratory Animal Research and Resource building, Texas A&M University, in a constant temperature (21-22°C) and constant humidity (45-50%) room with a 12-hour light-dark cycle. All procedures were carried out in accordance with the National Institutes of Health Guide for the Care and Use of Laboratory Animals (National Institutes of Health Publication No. 85-23, revised 1996). A total of 54 mice were used for these experiments, which was the minimum number of animals needed to complete this study. The mice were weaned at 29 days of age and housed individually for the duration of experimentation. Equal numbers of male and female mice (± 1 male or female per group) were used in each set of test and control individuals.

Chemicals

Sodium bicarbonate (8.4%) was obtained from Abbott Laboratories (Chicago, IL, USA). Methylmercuric chloride (MMC; 95% purity) was purchased from Alfa Aesar (Ward Hill, MA, USA). MMC was initially dissolved in sterile, deionized water and further diluted with sodium bicarbonate for subcutaneous injection or sterile deionized water for addition to food. All MMC solutions were stored at 4ºC until used.

Treatment

Thirty-six mice were used to determine the optimal method to prepare brain tissue samples to measure mercury content. Mice were randomly divided into two treatment groups with eighteen mice in each group. Eighteen control mice received a subcutaneous injection of vehicle (8.4% sodium bicarbonate; 0.1 ml/10 gm body weight). Eighteen experimental mice received a subcutaneous injection of MMC in vehicle at a dose of 5.0 mg/kg. An additional eighteen mice were divided into three treatment groups of six mice each. Six mice received a single oral dose of 5.0 mg/kg MMC in 2.0 g of moistened rodent chow; another six mice received 1.0 mg/kg MMC orally in 2.0 g of moistened rodent chow given every day for five consecutive days to achieve a total dose of 5.0 mg/kg. Six control mice received only vehicle (0.1 ml sterile deionized water) in 2.0 g of moistened rodent chow. Mice received moistened rodent chow during the dark phase of the light : dark cycle without access to dry rodent chow during the dark phase to ensure that the mice ate all the moistened rodent chow. The mice had access to dry rodent chow *ad libitum* during the light phase of the light : dark cycle. Mice always had access to water. No mice lost weight during the feeding protocol. All mice were anesthetized and the brains collected 8 to 11 days after the last dose of MMC or vehicle.

Tissue collection and processing

We utilized four common techniques of tissue processing in this study: 1) rapid freezing of unfixed brain tissue; 2) saline perfusion followed by freezing; 3) immersion

fixation followed by freezing and 4) perfusion fixation followed by cryoprotection and freezing to determine the best way to prepare brain tissue samples for mercury analysis. All tissues were rapidly frozen using powdered dry ice. To obtain non-perfused brain tissue, mice were anesthetized with isoflurane (Abbott Laboratories, Chicago, IL, USA) and killed *via* decapitation. To obtain fixed tissue mice were deeply anesthetized with xylazine (Vedco, St. Joseph, MO, USA) and ketamine (Vedco, St. Joseph, MO, USA; 0.5 mg xylazine plus 3.0 mg ketamine per 20 gm body weight, given intraperitoneally) and then perfused. All tissue samples were stored in plastic tubes to avoid contact with metal surfaces, which could have potentially contaminated the tissue samples.

Rapid freezing: Brains were quickly removed from the anesthetized mice, cut mid-sagittally and each half weighed. One half was frozen stored at –70°C until submitted for analysis. The other half was immersion fixed.

Immersion fixation: After weighing, the second half was placed in 50 ml of 4% paraformaldehyde in 0.1M-phosphate buffer (pH 7.2-7.4) at 4°C for 48 h; transferred to 50 ml of 20% sucrose in 0.1M-phosphate buffer (pH 7.4) for cryoprotection for 24-48 h at 4°C. The cryoprotected brain halves were rapidly frozen and stored at -70°C until they were submitted for analysis.

Saline perfusion: Mice were anesthetized for perfusion and perfused transcardially with Tyrode's saline (50 ml; pH 7.2-7.4). The brains were removed from the skulls and cut mid-sagittally. Each half was weighed, and immediately frozen with powdered dry ice and kept frozen at -70°C until they were submitted for analysis.

Perfusion fixation: Mice were anesthetized for perfusion, perfused transcardially with Tyrode's saline (50 ml; pH 7.2-7.4) followed by cold 4% paraformaldehyde (200 ml) in 0.1M phosphate buffer (pH 7.2-7.4). The bodies were stored for 4 h at 4°C, then the brains removed, cut midsagittally and each half weighed and stored in 4% paraformaldehyde at 4°C for 48 h. The brain halves were transferred to 20% sucrose in 0.1M phosphate buffer (pH 7.4) for 24-48 h at 4°C for cryoprotection, and then the brain halves were frozen and kept at -70°C until they were submitted for analysis.

Mercury analysis

All samples were analyzed in the Trace Element Research Laboratory at Texas A&M University, using a Milestone Direct Mercury Analyzer 80 (DMA 80) equipped with an autosampler and dual cell detector. After thawing, samples were homogenized to insure that a representative sample was taken for analysis. Each sample was subdivided as necessary, placed into precombusted nickel boats, weighed to the nearest 0.0001 gm on a Sartorius BP221S analytical balance and loaded into the DMA 80's autosampler tray. The samples were analyzed for mercury by combustion / trapping / atomic absorption using the method of Salvata and Pirola (1994). Calibration was accomplished using a calibration blank and a series of seven aliquots of certified reference standards spanning the range of 1– 750 ng mercury. The calibration line was verified using an independent CRM standard (NRCC DOLT-2) and a blank that was analyzed following calibration. Each batch of brain tissue samples analyzed included a method blank, a certified reference material, a duplicate sample, and a spiked sample.

Statistical analysis

Data were analyzed using General Linear Model (GLM)-Univariate Analysis of Variance at $\alpha = 0.05$, using SPSS Version 11.0 for Windows. Significant differences among treatment and control groups were interpreted by Tukey's HSD post hoc test.

RESULTS

In the vehicle-treated (control) brain tissue from mice that received MMC *via* subcutaneous injection, very low levels of mercury (in ppm) were detected in all four different tissue preparation methods (Figure II-1). However, the GLM-Univariate Analysis of Variance indicated that a significant difference existed in the data set, even though all of the observed concentrations were very low. The Tukey's HSD post hoc test revealed a significant difference in the mercury concentration of brain tissue prepared by immersion fixation when compared to rapid freezing of unfixed, unperfused brain tissue. Samples of brain tissue that were exposed to perfusion fixation and saline perfusion were not statistically different from rapid freezing or immersion fixation.

In mice that received 5.0 mg/kg MMC *via* subcutaneous injection the brain tissue samples revealed no significant difference between the tissue preparation methods with regards to the observed mercury concentrations (Figure II-2). There was a trend towards a lower concentration of mercury (in ppm) in the perfusion fixed brain tissue when compared to the other forms of tissue preparation, but this trend was not statistically significant. The range of concentrations of mercury observed in vehicle treated brain tissue (0.0007-0.0018 ppm; see Figure II-1) was approximately 0.5% of the range of

concentrations of mercury observed in MMC-treated brain tissue (0.2660-0.3650 ppm; see Figure II-2).

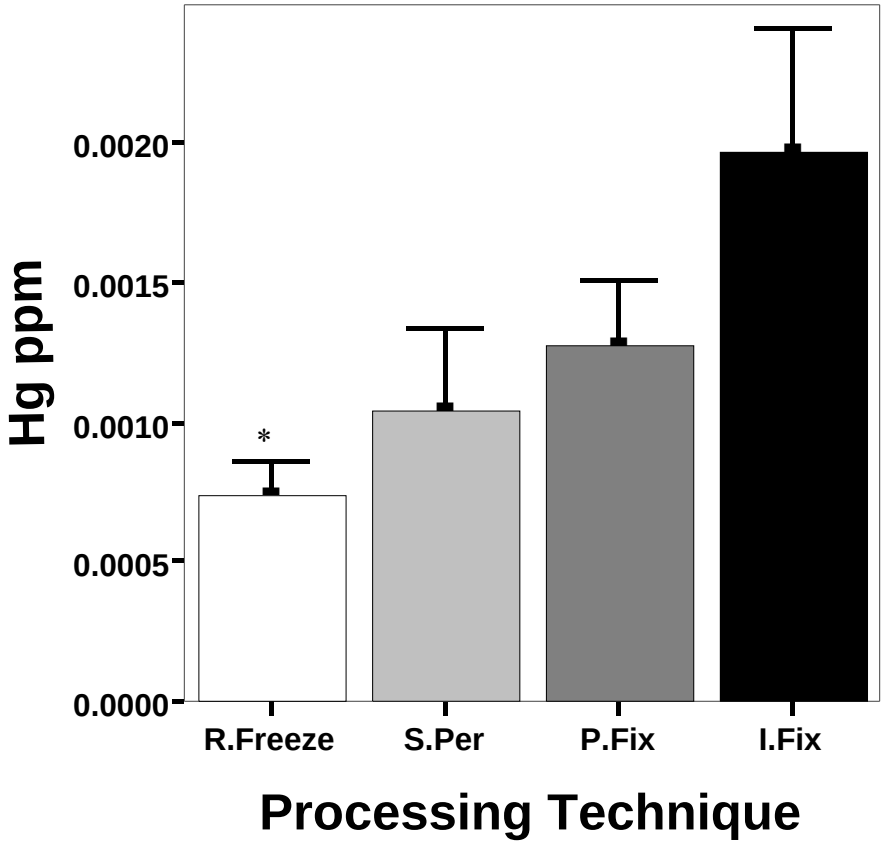

Figure II-1. Effect of processing technique on mercury content of control/vehicle-treated mouse brains. Mercury content (in ppm) in control/vehicle-treated (0.1ml/10gm sodium bicarbonate, given subcutaneously) mice brains following (R.Freeze) rapid freezing (0.0007), (S.Per) saline perfusion (0.0010), (P.Fix) perfusion fixation (0.0013) and (I.Fix) immersion fixation (0.0020). GLM-Univariate Analysis of Variance indicated a significant difference (P=0.044) between the tissue preparation methods and the Tukey's HSD post hoc test indicated a significant difference between rapid freezing (*) and immersion fixation.

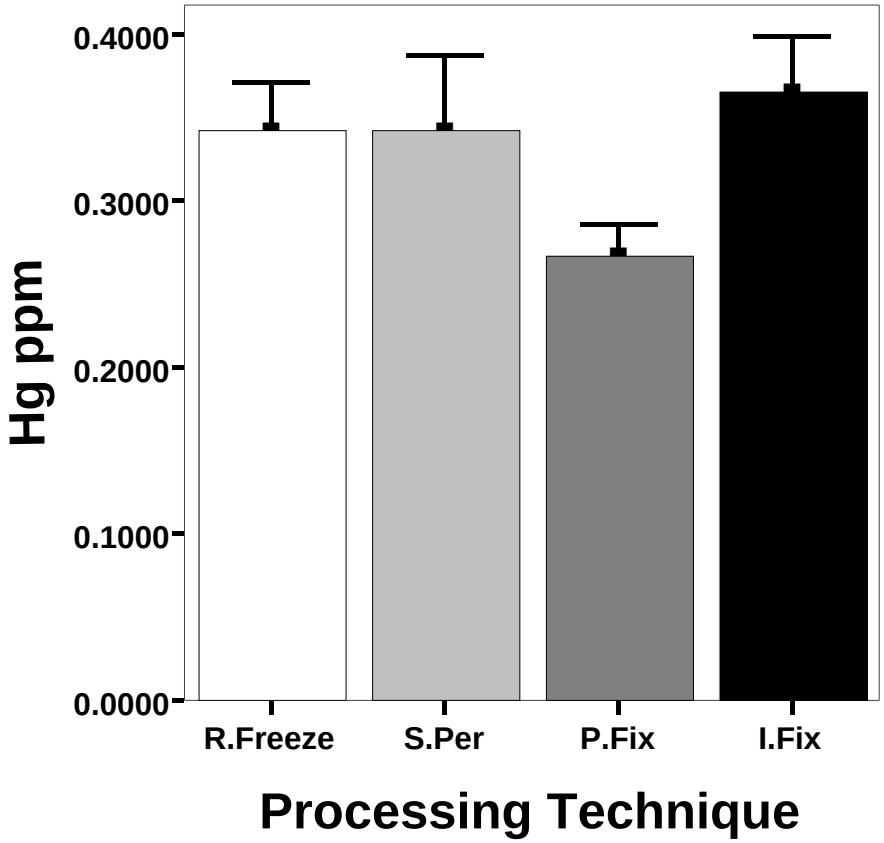

Figure II-2. Effect of processing technique on mercury content of 5.0 mg/kg MMC treated mouse brains. Mercury (in ppm) content in brain tissue from mice given a total dose of 5.0 mg/kg MMC (subcutaneously) following (R.Freeze) rapid freezing (0.3430), (S.Per) saline perfusion (0.3430), (P.Fix) perfusion fixation (0.2660) and (I.Fix) immersion fixation (0.3650). GLM-Univariate Analysis of Variance indicated no significant difference (P = 0.193) between the tissue preparation methods.

To compare mercury content between forebrain and hindbrain, before freezing, the forebrain was separated from the hindbrain by cutting the brain coronally immediately caudal to the inferior colliculi, then the brain tissue was stored frozen. At the time of analysis the specific tissues were thawed and analyzed as described in methods. In addition, in this experiment mice were exposed to 5.0 mg/kg MMC via moistened rodent chow either as a single dose or as doses divided over five consecutive days to achieve a total dose of 5.0 mg/kg body weight. Brain tissue from MMC-exposed mice was then compared with vehicle-treated mouse brain tissue. In the vehicle-only exposed mice a very low amount of mercury (in ppm) was detected in both the forebrain and hindbrain tissue, which was comparable to whole brain tissue levels observed from mice exposed only to subcutaneously injected vehicle (see Figure II-1). GLM-Univariate Analysis of Variance indicated no significant difference between forebrain and hindbrain with respect to levels of mercury from mice fed vehicle only in their food (Figure II-3). However, in mice fed a total of 5.0 mg/kg MMC divided over five consecutive days, the average mercury concentration was 0.3243 ppm in the forebrain and 0.1908 ppm in the hindbrain (Figure II-4). Average forebrain mercury content was approximately twice that of the hindbrain, and this difference was statistically significant.

In mice that ingested a single dose of 5.0 mg/kg MMC in their food, an approximately 10 fold reduction in mercury content was observed in both forebrain and hindbrain when compared to the average mercury content from forebrains and hindbrains from mice that received MMC in five divided doses yet they still achieved a total dose of MMC of 5.0 mg/kg (Figure II-4).

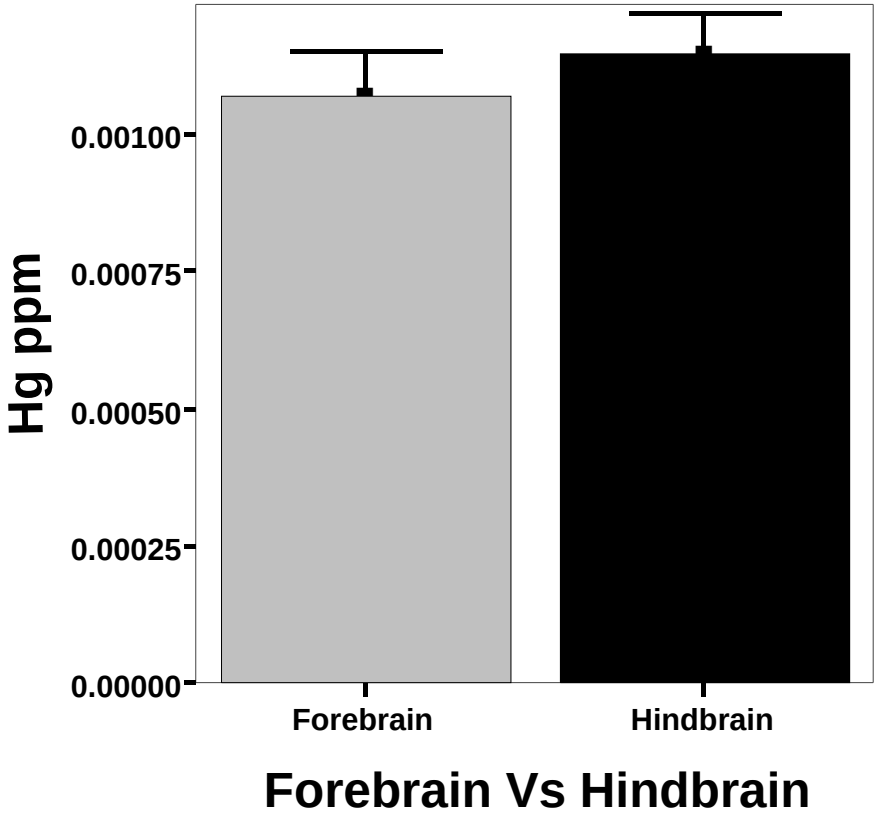

Figure II-3. Mercury content (in ppm) in forebrain and hindbrain from control (vehicle-treated) mice. A very low concentration of mercury was observed in either brain region. GLM-Univariate Analysis of Variance indicated no significant difference (0.497) in mercury content between forebrain (FBr; 0.0011) and hindbrain (HBr; 0.0012) in control mice.

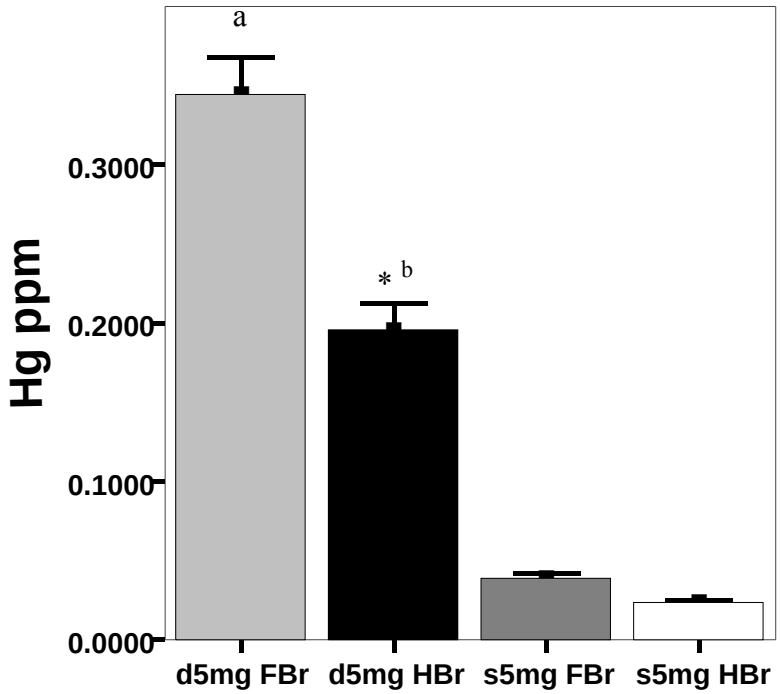

Figure II-4. Effect of dosing regimen on brain mercury content. Graph showing comparison of mercury content (in ppm) between forebrain (FBr) and hindbrain (HBr) from mice given, orally, either a divided dose (d) or a single total dose (s) totaling 5.0 mg/kg MMC. GLM-Univariate Analysis of Variance indicated a significant difference ($P<0.001$). A Tukey's HSD, post hoc test indicated a significant difference between the dosing patterns (single versus multiple doses) between forebrain (a) and hindbrain (b) and between forebrain and hindbrain of mice that received the five divided doses of 5.0 mg/kg MMC (*).

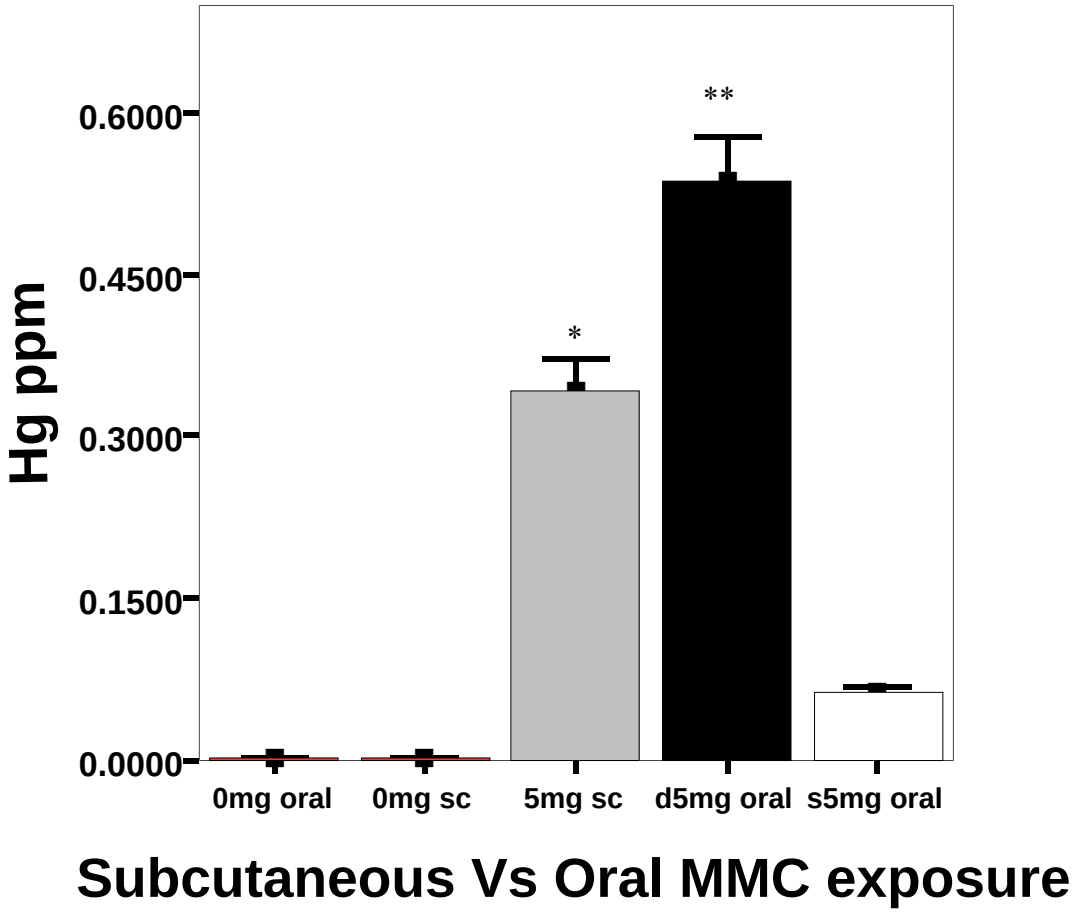

Figure II-5. Effects of route of exposure and dosing regimen on brain mercury content. Graph comparing mercury content (in ppm) in control and 5.0 mg/kg MMC treated mice following a single subcutaneous (sc) injection, oral dose divided into five doses (d), totaling 5.0 mg/kg and a single total oral dose (s) totaling 5.0 mg/kg. GLM-Univariate Analysis of Variance indicated a significant difference ($P<0.001$). A Tukey's HSD, post hoc test indicated a significant difference between the dosing pattern (**) and route of administration (*).

Finally, we compared whole brain mercury content in mice exposed to 5.0 mg/kg MMC orally as both single and five divided doses to the whole brain mercury content from mice exposed via a single subcutaneous injection (Figure II-5). The whole brain mercury content from mice given a single 5.0 mg/kg dose of MMC subcutaneously was significantly higher than the mercury content from brain tissue from mice given a single 5.0 mg/kg oral dose of MMC, but the concentration was significantly lower than the average concentration of mercury in brain tissue from mice that were given a total dose of 5.0 mg/kg MMC divided into five doses.

DISCUSSION

The present study assessed tissue concentrations of mercury in mouse brain tissue using oral and subcutaneous routes of methylmercury administration, different methods of tissue preparation, and different dosing regimens. After each brain was removed, it was subjected to one of four tissue preparation procedures described in the Materials and Methods section. Although very low concentrations of mercury were recovered from vehicle-treated (control) mouse brain tissue, it is interesting to note that brain tissue prepared by immersion fixation differed statistically from unfixed, unperfused brain tissue prepared by rapid freezing. Brain tissue perfused with saline and 4% paraformaldehyde and submerged in 4% paraformaldehyde and 20% sucrose for 24-48h both had higher concentrations of mercury when compared to unfixed and unperfused brain tissue. This suggests that the water used to make up these solutions may have contributed to the observed increased mercury content. Brain tissue prepared by saline

perfusion (0.0010 ppm) and perfusion fixation (0.0013 ppm) had higher concentrations of mercury when compared to rapid freezing (0.0007 ppm) and fell in between rapid freezing and immersion fixation. This is convincing evidence that the longer the tissue was exposed to solutions made out of water, more mercury could be recovered from the brain tissue (Figure II-1) when compared to unfixed and unperfused brain tissue. In a report by Kosta et al (1975), non-exposed control human subjects showed average mercury levels of 0.0042 ppm (range of 0.001-0.007) in brain tissue from five cases. Thus, the range of mercury levels observed in non-exposed mouse brain tissue in this study is very similar to the range reported by Kosta et al (1975), for control human brain tissue.

Brain tissue prepared by the four different tissue preparation methods following a single subcutaneous injection of 5.0 mg/kg MMC did not differ statistically with respect to the mercury concentrations obtained from the different tissue preparation methods (Figure II-2). In addition when we compared mercury concentrations between brain tissue obtained from female mice (0.3364 ppm; n=14) to those obtained from male mice (0.3198 ppm; n=10) no statistical differences were observed. However, female mice showed a tendency to accumulate more mercury in brain tissue than did male mice.

The average mercury concentration observed in saline perfused MMC exposed brains (0.0734 μg) when expressed as percentage of the total cumulative dose (66.6 μg) in this study was less than 0.5% of the total dose. Average brain mercury concentrations observed in two other studies where rats were either dosed via the common carotid artery with 0.5 mM MMC or intravenously with 10.0 mg/kg MMC also were observed

to be less than 0.5% of the total dose (Aschner and Clarkson, 1988; Norseth and Clarkson, 1970). In this study the mean mercury concentration observed in terms of percent of the total dose following preparation of brain tissue using rapid freezing or saline perfusion followed by rapid freezing was 0.12% and 0.11% respectively. Yasutake and Hirayama (1986) reported in a study that strain differences exist within mice with respect to urinary elimination of mercury and brain mercury levels. Specifically, male C57BL mice exposed to a single oral dose of 5.0 mg/kg MMC showed excretion rates 3.9-4.7 times higher than males of other strains. In a subsequent study Yasutake and Hirayama (1988) reported sex differences within the C57BL strain of mice with respect to urinary mercury elimination and brain mercury levels. Male C57BL mice showed a higher rate of urinary mercury excretion and 50% lower brain mercury concentrations when compared to female C57BL mice. In the 1988 study, mice were dosed with 5.0 mg/kg methylmercury daily until they died due to toxicity. Male mice survived for 45 days while female mice succumbed by day 21. Similar differences were also observed between male and female rats with respect to brain mercury concentrations (Hirayama and Yasutake, 1986). In a chronic gestational exposure study where female rats were exposed to either 0.5 or 6 ppm MMC in drinking water, when examined at birth, brain mercury concentrations in female pups were 10-15% higher than in the male pups in the low dose group. However, in the high dose group, newborn male pups had slightly higher brain mercury concentrations when compared to the newborn female pups (Newland and Reile, 1999).

Control mice given sterile deionized water in the moistened rodent chow in this study showed very low levels of mercury in both the forebrain and hindbrain and the concentrations observed in the two different brain regions did not differ statistically (Figure II-3). In a study using male Wistar rats, mercury was non detectable in the cerebellum of unexposed control rats using a Varian Techtron Model 100 atomic absorption spectrophotometer (Leyson and Morgan, 1991). The source of mercury observed in the control mice in this study could be from water or food. It is also possible that the method of mercury analysis used in this study was able to detect the presence of mercury in brain tissue at lower concentrations than was possible in earlier studies.

It was interesting to note that the concentration of mercury observed in the treated mice was approximately twice as high in the forebrain when compared to the hindbrain in both single 5.0 mg/kg dose and divided 5.0 mg/kg dose groups (Figure II-4). It also was interesting to note that the concentration of mercury in the divided oral 5.0 mg/kg dose group was approximately 10 times higher than that of the single 5.0 mg/kg dose group. The hindbrain (cerebellum along with the brainstem) was observed to have a concentration of 0.1908 ppm (5.0 mg/kg as divided dose) and 0.0231 ppm (5.0 mg/kg single dose), respectively. Leyson and Morgan (1991) reported a concentration of 25 ppm mercury in the cerebellum at day 14 following administration of 10.0 mg/kg MMC for five days via gastric gavage in rats. Thus, the mercury concentrations obtained in this study from hindbrains of mice given 5.0 mg/kg MMC over five doses is approximately one tenth the amount detected in rat cerebellum from animals given a total dose of 50.0 mg/kg over five doses. Since the pattern and route of dosing in this

study was the same as used in the Leyson and Morgan (1991) study, this suggests that comparable amounts of mercury were sequestered in brain tissue in both studies when the differences in final total doses are considered.

Finally, it was noted that brain mercury concentrations in both forebrains and hindbrains of mice dosed with a single 5.0 mg/kg MMC was approximately one tenth the amount observed in the divided dose group that received the same total dose of 5.0 mg/kg MMC, indicating that the dosing regimen used to administer MMC can significantly affect brain mercury concentration.

Distribution of mercury was examined in nine different brain regions from dogs administered methylmercury thioacetamide intravenously with either 30.0 mg/kg and sacrificed on day 19 or 60.0 mg/kg and sacrificed on day 6, showed a range of mercury levels in various brain tissues ranging from 4.8 ppm to 38.7 ppm (Yoshino et al, 1966). Dogs given the lower dose of 30 mg/kg exhibited an average brain tissue mercury concentration of 8.28 ppm, while dogs given the higher dose of 60 mg/kg exhibited an average mercury concentration of 23.38 ppm (Yoshino et al, 1966). This range of brain tissue mercury concentrations is larger than expected based on the results of this study. This disparity could be explained by differences in how "efficiently" mercury is sequestered into brain tissue in dogs versus mice.

Finally brain mercury concentrations were found to be significantly different when different routes of exposure were used (Figure II-5). Mercury concentration in brain tissue obtained following five divided oral doses was higher than the concentration of mercury obtained after a single dose of methylmercury that was given as a subcutaneous

route of exposure. However, it is interesting to note that brain mercury concentrations were higher in mice given a single subcutaneous injection when compared to mice that received a single oral dose of methylmercury. This is the first study that differentiates the effect of route of exposure and dose regimen on brain mercury concentrations using one final total dose of 5.0 mg/kg.

In summary, there were no differences in brain mercury content obtained from four different tissue preparation methods used in this study. There were significant differences in the distribution of mercury within the brain tissue (forebrain vs. hindbrain). Dosing regimen (single vs. divided total dose of 5.0 mg/kg) also had a significant impact on the observed brain mercury content. Finally we found that route of exposure has a significant effect on mercury accumulation in brain tissue. These observations suggest that different tissue preparations can be used to prepare brain tissue for analysis, and the tissue can still be analyzed for mercury content. However, different regions of the brain can accumulate mercury to different degrees and the route of exposure needs to be an important consideration in experimental planning.

CHAPTER III

NEUROBEHAVIORAL CHANGES IN YOUNG ADULT MICE TREATED WITH METHYLMERCURY

SUMMARY

Male and female C57BL/6J mice at postnatal (P) day 34 were exposed orally to five divided doses totaling 1.0 or 5.0 mg/kg of methylmercuric chloride (MMC) or sterile deionized water in moistened rodent chow. After a five-day waiting period, experimental mice were subjected to a standard battery of behavior testing for balance and motor coordination. Latency to falling on the accelerating rota-rod was significantly decreased in 5.0 mg/kg MMC exposed mice when compared to control mice. In the open field, horizontal exploration with respect to total distance traveled during the first 5 minutes on the first test day was significantly reduced in 1.0 mg/kg MMC exposed mice when compared to control mice. Rearing activity was not affected by MMC treatment. In the foot print analysis, angle of foot placement measured in 1.0 mg/kg MMC treated mice was significantly greater compared to control mice. Base stance and stride length were unaffected by MMC treatment. On the vertical pole test, 10 mice from each treatment group fell off the pole, while none of the control mice fell. These results indicate that short term, low to moderate doses of MMC in young adult mice can be detrimental to motor coordination and balance.

INTRODUCTION

Mercury (Hg) is one of the most ubiquitous and hazardous environmental contaminants found in ocean and freshwater fish, shellfish and plants (Eisler, 2004; Risher et al., 2002; Sanfeliu and Sebastia, 2001; Shenker et al, 1998; Siciliano et al., 2003). The organic or methylated form of Hg, consisting of one methyl group bound to each atom of Hg, (methylmercury; MeHg), accounts for most of the Hg to which humans are exposed (Rice, 1995). Hg as MeHg gets rapidly absorbed from the gastrointestinal tract and is readily transported into the fetal and adult brain. MeHg is sequestered within the brain and gradually gets converted into inorganic Hg. MeHg is primarily a potent neurotoxicant known to cause neuronal degeneration (Bakir et al., 1973; Nielsen, 1992; Rikuzo and Mitsuhiro, 1996). In both humans and rodents, neocortical and cerebellar granule neurons, in particular, are very sensitive to MeHg exposure (Limke and Atchison, 2002; Yuan and Atchison, 1999).

One of the most severe intoxications ever reported in humans was from eating contaminated fish and shellfish from the Minamata Bay in Japan in the 1950s. Children exposed prenatally to chronic high doses of MeHg suffered from mental retardation, disturbances in physical growth, cerebellar ataxia, under developed or “primitive” reflexes, limb deformities and dysarthria (Harada, 1995). Adults exposed to chronic high doses of MeHg commonly exhibited peripheral neuropathy, dysarthria, tremors, cerebellar ataxia, concentric constriction of visual fields, and auditory impairment (Clarkson, 2002). Autopsies of two affected infants revealed diffuse and extensive cortical damage, with marked abnormalities in cortical cytoarchitecture (Matsumoto and

Takeuchi, 1965). Autopsies of affected adults revealed extensive damage of the cerebellum and cortical sulci (Matsumoto and Takeuchi, 1965).

In the early 1970s a second significant episode of MeHg poisoning occurred in Iraq. Numerous individuals consumed homemade bread prepared from seed grain treated with a MeHg containing fungicide. In this case, the affected individuals experienced acute high dose exposure. Iraqi children exposed to MeHg prenatally exhibited symptoms comparable to the residents of Minamata Bay (Amin-Zaki et al., 1974).

In 1997, the U.S. Environmental Protection Agency (EPA) recommended a reference dose of no more than 0.1 μg/kg body weight/day for MeHg exposure in the human population (Clarkson, 2002). This translates into limiting consumption of food sources with MeHg contamination including freshwater fish and ocean fish such as tuna (Limke and Atchison, 2002; Rice, 1996). The persistent contamination of our environment with mercury indicates that mercury will remain bioavailable as MeHg for decades, affecting current as well as future generations (Grandjean and Weihe, 1998).

Studies using rodents as animal models have proven to be very helpful in simulating the neurobehavioral effects of MeHg exposure (Spyker and Smithberg, 1972; Spyker et al., 1972). However, most of the neurological affects tested in rodents followed developmental exposure to MeHg (Goulet et al., 2003; Kakita et al., 2000; Kim et al., 2000; Newland and Rasmussen, 2000; Newland et al., 2004; Rasmussen and Newland, 2001; Rossi et al., 1997; Sakamoto et al., 2002; Salvaterra et al., 1973; Su and Okita, 1976). Motor deficits were the most salient neurobehavioral effects observed after developmental exposure to MeHg (Rice, 1996). A careful review of the literature

indicates that most of the early studies using rodents examined the developmental neurobehavioral changes following a single or a few treatments (Baraldi et al., 2002; Dore et al., 2001; Inouye et al., 1985; Kim et al., 2000; Lown et al., 1977; Pereira et al., 1999; Salvaterra et al., 1973; Su and Okita, 1976; Vicente et al., 2004; Watanabe et al., 1999; Yin et al., 1997). Several studies in the recent past have reported behavior defects following chronic exposure to MeHg during prenatal and early postnatal development (Goulet et al., 2003; Kakita et al., 2000; Newland and Rasmussen, 2000; Newland et al., 2004; Rasmussen and Newland, 2001; Rossi et al., 1997; Sakamoto et al., 2002). Most of the developmental studies reported deficits in motor coordination and equilibrium on the rota-rod and/or changes in horizontal and vertical exploration in the open field (Dore et al., 2001; Elsner et al., 1988; Inouye et al., 1985; Kim et al., 2000; Rossi et al., 1997; Spyker and Smithberg, 1972). Sakamoto et al., (1993) demonstrated apparent deficits in rota-rod performance in rats exposed to a total dose of 71.4 mg/kg starting from postnatal day (P) 35 and a dose dependent inhibition in rota-rod performance in rats at P14 exposed to total dose of 26 mg/kg given over a period of 10 days. However, little is known about the behavioral effects of MeHg exposure on young adults at environmentally relevant exposure levels, especially because they could be potentially exposed to MeHg through the environment or by consumption of fish contaminated with MeHg.

In the present study, male and female C57BL/6J mice at postnatal day (P) 34 were exposed to MeHg via food using a total dose of either 1.0 mg/kg or 5.0 mg/kg body weight. They were compared with age matched control (given vehicle only) mice using a

standard battery of behavior tests for motor coordination, equilibrium and open field activity.

MATERIALS AND METHODS

Animals

Adult C57BL/6J wild type (+/+) male and female mice, originally obtained from The Jackson Laboratory (Bar Harbor, MA, USA), were bred to produce wild type offspring. A total of 43 male and 34 female mice were used in this study. Mice were further divided into three treatment groups as follows: control (22), 1.0 mg/kg MMC (26) and 5.0 mg/kg MMC (29). All mice were housed at the Laboratory Animal Research and Resource building, Texas A&M University, in a constant temperature (21-22°C) and humidity (45-50%) room with a 12-hour light-dark cycle. The mice were weaned at 29 days of age and housed individually for the duration of training, dosing and behavior testing. All procedures were carried out in accordance with the National Institutes of Health Guide for the Care and Use of Laboratory Animals (National Institutes of Health Publication No. 85-23, revised 1996).

Chemicals and dosing

Methylmercuric chloride (MMC; 95% purity) was obtained from Alfa Aesar (Ward Hill, MA, USA). MMC was initially dissolved in sterile deionized water and further diluted with sterile deionized water for addition to food. All MMC solutions were stored at 4ºC until used. Mice at postnatal day (P) 29 were divided into three treatment groups

and trained to eat moistened rodent chow for five days as described earlier by Bellum et al., (in press). Starting at P34, one group of mice received 0.2 mg/kg and a second group of mice received 1.0 mg/kg MMC orally in 2.0 g moistened rodent chow given daily for five consecutive days to achieve a total dose of 1.0 mg/kg or 5.0 mg/kg body weight, respectively. The control mice received only vehicle (0.1 ml sterile deionized water) in 2.0 g moistened rodent chow for five consecutive days. The mice were given moistened rodent chow with MMC or vehicle only during the dark phase of light:dark cycle and had access to dry rodent chow *ad libitum* only during the light phase of the light:dark cycle. All mice had access to water 24 hours every day.

Rota-rod

Quantitative measurement of motor coordination in control, 1.0 mg/kg and 5.0 mg/kg MeHg treated mice was performed using an accelerating rota-rod, model 7650 (UGO Basile, Comerio, VA, Italy). The rota-rod consisted of a rod (diameter = 3 cm; length = 30 cm) partitioned off with round plates in order to accommodate up to five mice simultaneously and to prevent escape from the sides. The rod was made of plastic, covered with smooth plastic tubing and suspended at a height of 16 cm above five plastic levers attached to timers that stop as soon as the mice land on the surface of the lever. The mice were placed on top of the rod that rotated at 3 rpm at 0 min and accelerated to 26 rpm at 3 min. Mice were placed with their backs facing the experimenter and oriented perpendicular to the long axis of the rod, such that the mice had to make a forward walking movement to avoid falling from the rod. Starting at P44, the latency time to

were measured for three consecutive days (days 6, 7 and 8 after the last dose of MMC), with each mouse experiencing four trials per day with an intertrial interval of 10 minutes. The first three trials on each day were considered training and data recorded from the fourth trial of each day were analyzed.

Initially in our experiments using the accelerating rota-rod we observed that the mice clung to the rod and passively rotated with the rod for one or more rotations before they gained back their balance and began walking on the rod again. This behavior was observed in all three-treatment groups. To circumvent this situation we covered the surface of the rod with smooth plastic tubing that increased the diameter of the rod and prevented the mice from passively rotating with the rod.

Activity in the open-field

Horizontal and vertical exploration were analyzed in control, 1.0 mg/kg and 5.0 mg/kg MeHg treated mice by measuring total distance traveled and rearing activity in the open field using Versa Max System activity chambers (Accuscan Instruments, Inc Columbus, OH). Each activity chamber was equipped with photocell beams that use x-, y- and z- coordinates to detect and digitally record horizontal and vertical movements. The chamber (42 X 42 cm) was made of plexiglas and the walls were 30 cm in height. Each chamber was further divided into four equal compartments of (21 X 21 cm). Only two compartments (second of top row and first of bottom row) were selected for testing in order to prevent overlap of the beam pathways. The mice were always placed in one

specific corner of the chamber at the beginning of each trial and activity levels were recorded for 30 minutes per day, on days 9 and 10 after the last dose of MMC.

Foot print analysis

Changes in motor coordination and balance were assessed using foot print analysis. A plastic-lined walkway walled off at one end that was, 100 cm long, 6 cm wide, and 15 cm tall was used. The hind paws of each mouse were dipped in non-toxic glass paint and the mouse was allowed to walk on a strip of paper placed on the floor of the walkway. Stride length (in mm), angle of foot placement (in degrees) and distance between the two hind feet (base stance, in mm) were measured for five consecutive strides and averaged for each mouse.

Vertical pole test

The vertical pole test also is used to assess changes in coordination and balance. Control and MMC treated mice were placed on a 60 cm long, 2.5 cm diameter plastic rod with tape wound around it to provide adequate grip. The rod was held horizontally at a height of 50 cm above the surface of the counter that was padded with a soft cushion to prevent injuries to the mice when falling. Mice were placed approximately midway on the rod facing the end that was lifted up. Keeping one end of the rod stationary the other end was lifted to a 45 degree angle in 10 seconds. An additional 5 seconds was taken to shift the rod from 45 degrees to 90 degrees. Whether mice stayed on or fell off the rod during the 15 second testing period was recorded.

Statistical analysis

General Linear Model (GLM)-repeated measure analysis at $\alpha = 0.05$, using SPSS version 11.0 for Windows was performed on the rota-rod data. GLM-Multivariate Analysis of Variance was used to analyze open field and foot print data. Analysis included treatment, gender and interaction effects (3-way ANOVA). Significant differences among treatment and control groups were interpreted by Tukey's honest significant difference (HSD) post hoc test at $\alpha = 0.05$. A Chi-Square test was used to analyze the vertical pole test data.

RESULTS

Rota-rod performance

On the fourth trial of all three days, GLM - repeated measure analysis indicated a significant treatment effect ($P = 0.031$) (Figure III-1). No significant differences were observed between males and females ($P = 0.145$), and the interaction between treatment and sex ($P = 0.553$) was not significant. On the fourth trial of the third day, GLM – Univariate Analysis of Variance and the Tukey's HSD post hoc test indicated the latency to falling exhibited by 5.0 mg/kg MMC exposed mice was significantly lower when compared to age matched control mice ($P = 0.001$). However, 1.0 mg/kg MMC treated mice were not significantly different from control mice or 5.0 mg/kg MMC treated mice (Figure III-1). GLM - Multivariate Analysis of Variance and the Tukey's HSD post hoc test indicated a significant increase in latency to falling in control mice on day 3 when compared to day 1. Latency to falling on day 2 for control mice was not significantly

different from day 1 or day 3 ($P < 0.05$). There was no significant increase in latency to falling in 1.0 mg/kg MMC exposed mice when data from all three days were compared ($P = 0.335$). The 5.0 mg/kg MMC exposed mice exhibited a significant increase in latency to falling on day 2 when compared to day 1 ($P = 0.033$). The latency to falling observed on day 3 for the 5.0 mg/kg MMC exposed mice was not significantly different from day 1 or day 2.

Activity in the open field

Analysis of the total distance traveled and rearing activity during a 30-minute session of both days 1 and 2 did not reveal any significant differences (data not shown). We then focused on the first 5 minutes of the first day in order to assess exploratory behavior in a novel environment. Generally for preliminary assessment of motor activity or to evaluate gross abnormalities in locomotion, 5 minutes of test session in an open field is sufficient (Crawley, 1999). Figures III-2 and 3 present spontaneous locomotion and rearing activity in the open field during the first 5 minutes of recording on day 1 for all control and MMC treated mice. GLM - Multivariate Analysis of Variance indicated a significant difference in total distance traveled ($P = 0.015$) (Figure III-2). There were no significant differences between males and females ($P = 0.153$). The interaction between MMC exposure and sex was not significant ($P = 0.239$). Vertical exploration (i.e., rearing activity) (Figure III-3) was not affected by MMC treatment ($P = 0.517$). Males and females did not differ in the number of rearing motions made during the 5-minute

session (P = 0.269), and no interaction effects were observed (P = 0.224).

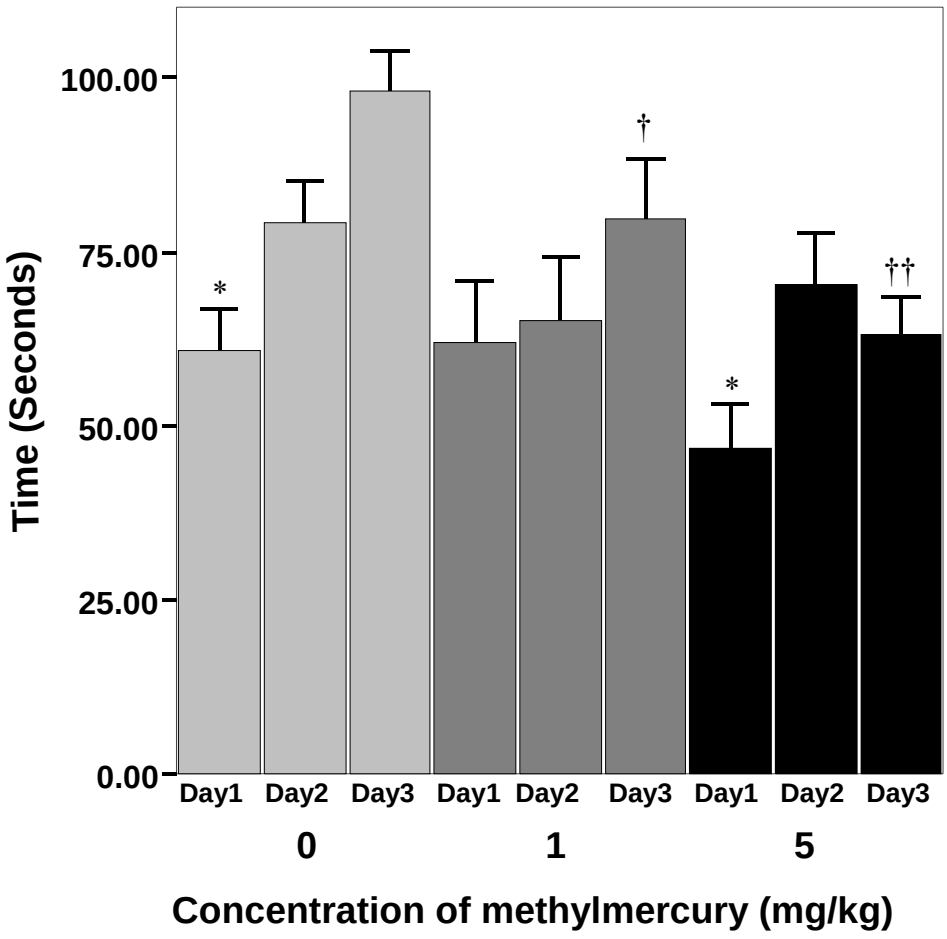

Figure III-1. Effects of MMC administration on cerebellar motor coordination tested using accelerating rota-rod. GLM-repeated measure analysis indicated a significant treatment effect (P = 0.031) on the relative time spent on the rota-rod by 0 mg/kg, 1.0 mg/kg and 5.0 mg/kg MMC treated mice on trial 4 of days 1, 2 and 3. GLM - Multivariate Analysis of Variance and Tukey's HSD post hoc test indicated a significant difference in performance on rota-rod for on days 1 and 3 in control mice (P<0.001) (*) and for trial 4 on days 1 and 2 for 5.0 mg/kg MMC treated mice on day 1 and 2, (P= 0.033) (*). GLM -Univariate Analysis of Variance and Tukey's HSD post hoc test indicated a significant (P=0.001) difference between 0 mg/kg and 5.0 mg/kg MMC treated mice (††). 1.0 mg/kg MMC exposed mice were not significantly different from 0 mg/kg or 5.0 mg/kg MMC mice (†).

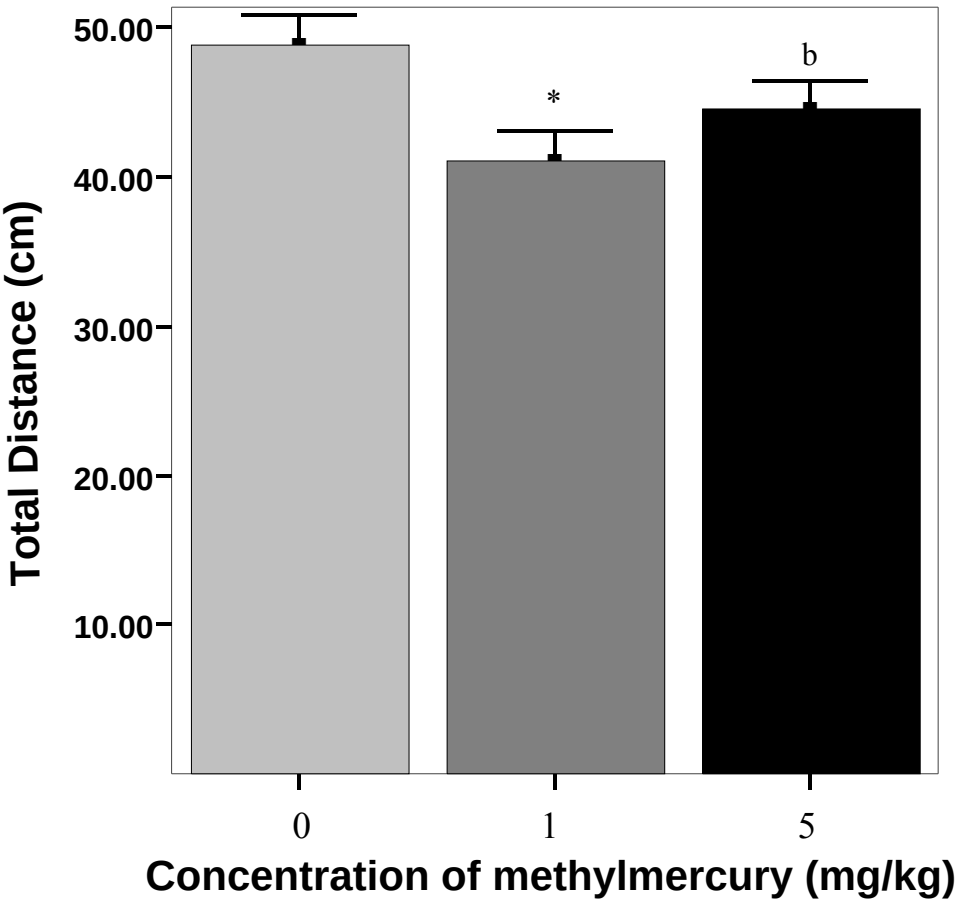

Figure III-2 Effect of MMC administration on horizontal activity level tested in an open field chamber. GLM-Multivariate Analysis of Variance and Tukey's HSD post hoc test indicated a significant difference in spontaneous locomotion between 0 mg/kg and 1.0 mg/kg MMC treated mice (P = 0.015; *). 5.0 mg/kg MeHg treated mice were not significantly different from 0 mg/kg or 1.0 mg/kg MMC treated mice (b).

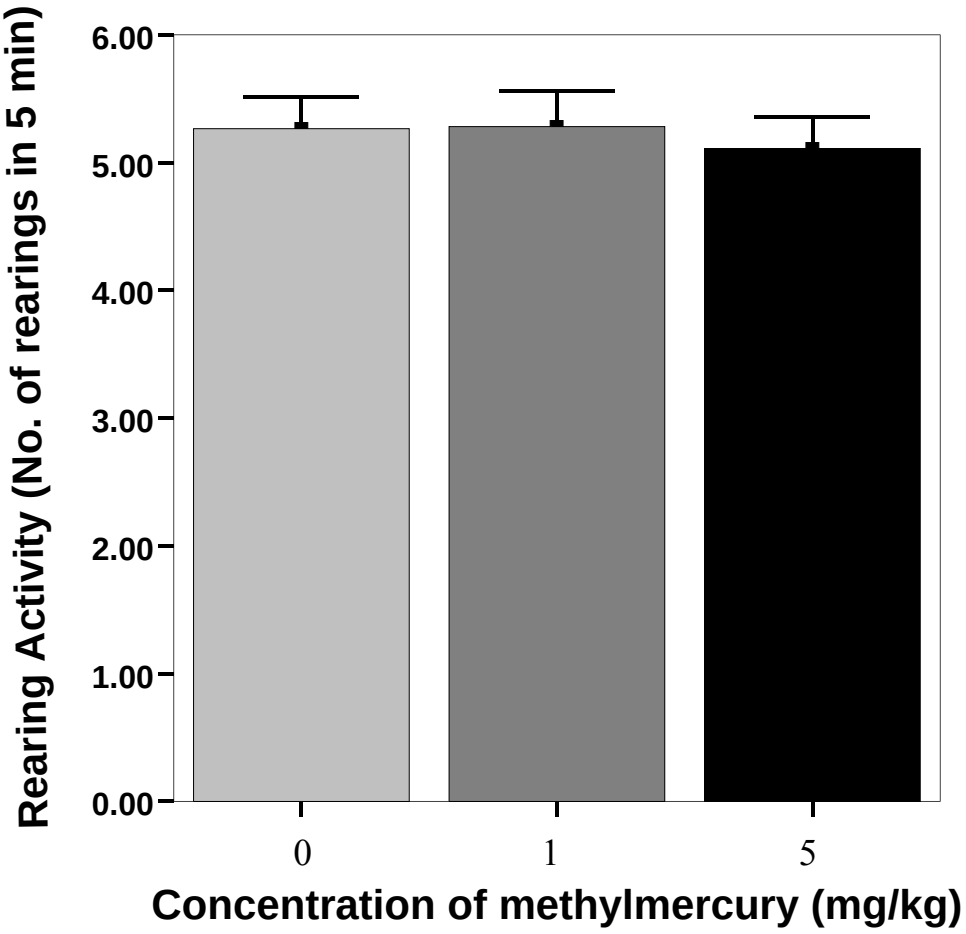

Figure III-3. Effect of MMC administration on vertical activity level tested in an open field chamber. GLM-Multivariate Analysis of Variance and Tukey's HSD post hoc test indicated no significant difference in rearing activity between 0 mg/kg, 1.0 mg/kg and 5.0 mg/kg MMC treated mice (P = 0.517).

Foot print analysis

Average angle of foot placement (Figure III-4) was highly significantly different in 1.0 mg/kg MMC treated mice when compared to control mice (P = 0.003). The Tukey's HSD post hoc test indicated that 5.0 mg/kg MMC treated mice were not significantly different from control or 1.0 mg/kg MMC treated mice. There was no gender effect (P = 0.087) or interaction effect between MMC treatment and gender (P = 0.130). The stride length (P = 0.123) (Figure III-5) and base stance (i.e., distance between two hind paws) (P = 0.532) did not differ between control and MMC exposed mice (Figure III-6).

Vertical pole test

A Chi-Square test indicated that there was a significant difference between control and MeHg treated mice at $\alpha = 0.05$. The Chi-Square calculated value at degrees of freedom (DF) 4 was 14.34. The Chi square table value at DF 4 was 9.488 (Table III-1). No significant differences were observed when the Chi-Square test was performed with males and females separated within a treatment group (Chi-Square calculated value = 13.82; Chi-Square table value = 18.31 at $\alpha = 0.05$ and DF 10). Significant differences were observed when the Chi-Square test was performed between control and 1.0 mg/kg MeHg treated mice (Chi-Square calculated value = 10.73; Chi-Square table value = 5.991 at $\alpha = 0.05$ and DF 2) and control and 5.0 mg/kg MeHg treated mice (Chi-Square calculated value = 10.38; Chi-Square table value = 5.991 at $\alpha = 0.05$ and DF 2).

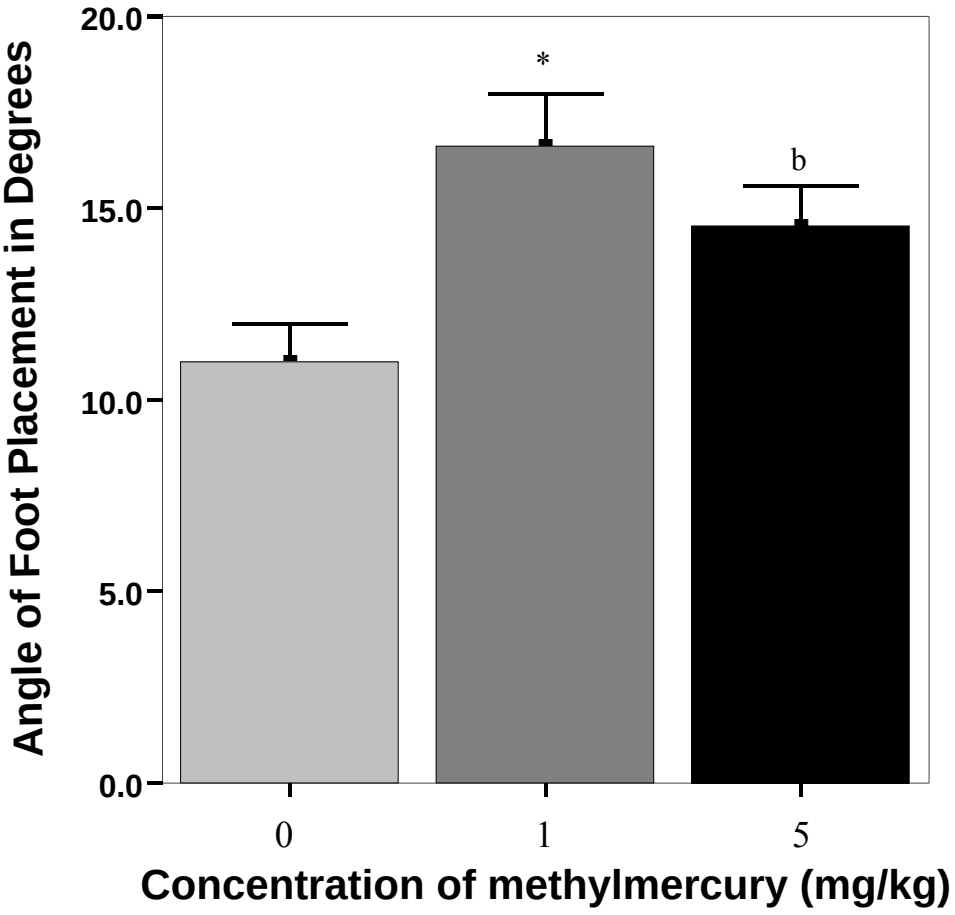

Figure III-4. Graph showing the average angle of hind foot placement from foot print analysis. GLM-Univariate Analysis of Variance and Tukey's HSD post hoc test indicated a significant (P=0.003) difference between 0 mg/kg and 1.0 mg/kg MMC treated mice (*). The post hoc test indicated no significant difference in the performance of 5.0 mg/kg MMC treated mice with 0 mg/kg or 1.0 mg/kg MeHg treated mice (b).

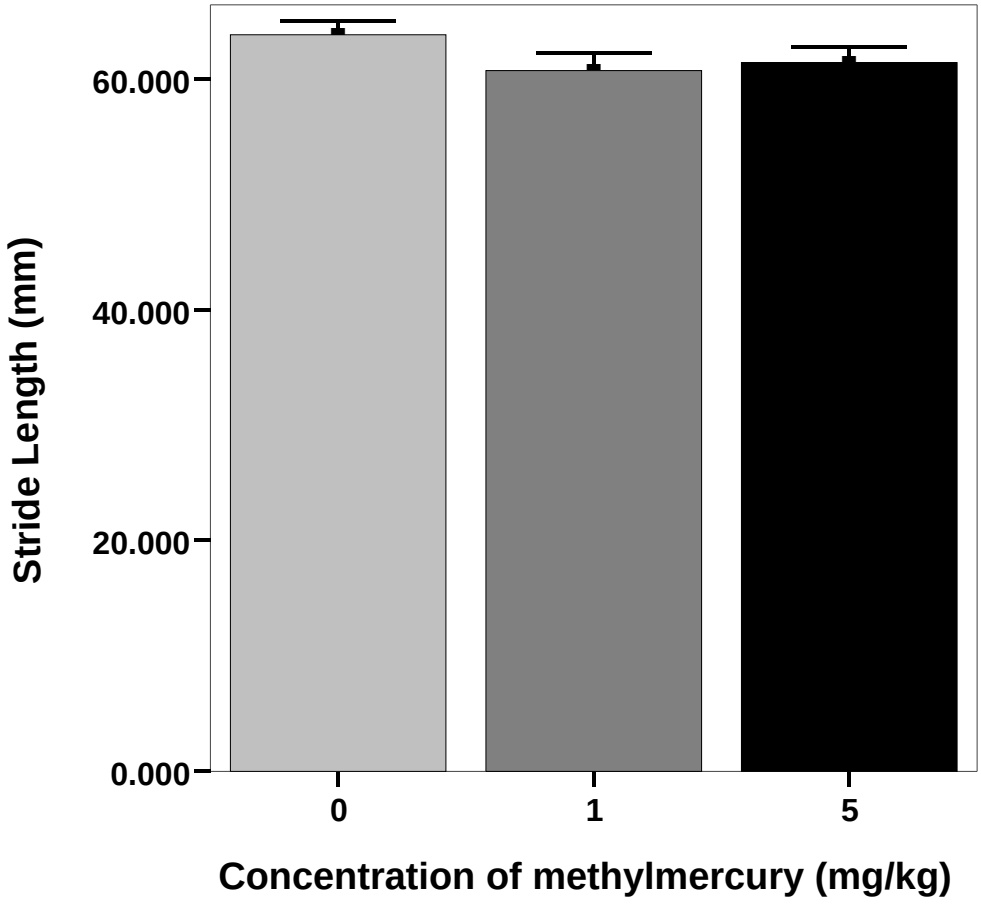

Figure III-5. Graph revealing the average stride length from foot print analysis. GLM-Multivariate Analysis of Variance indicated no significant difference in stride length (P = 0.123) between 0 mg/kg, 1.0 mg/kg and 5.0 mg/kg MMC treated mice or between males and females (P = 0.193).

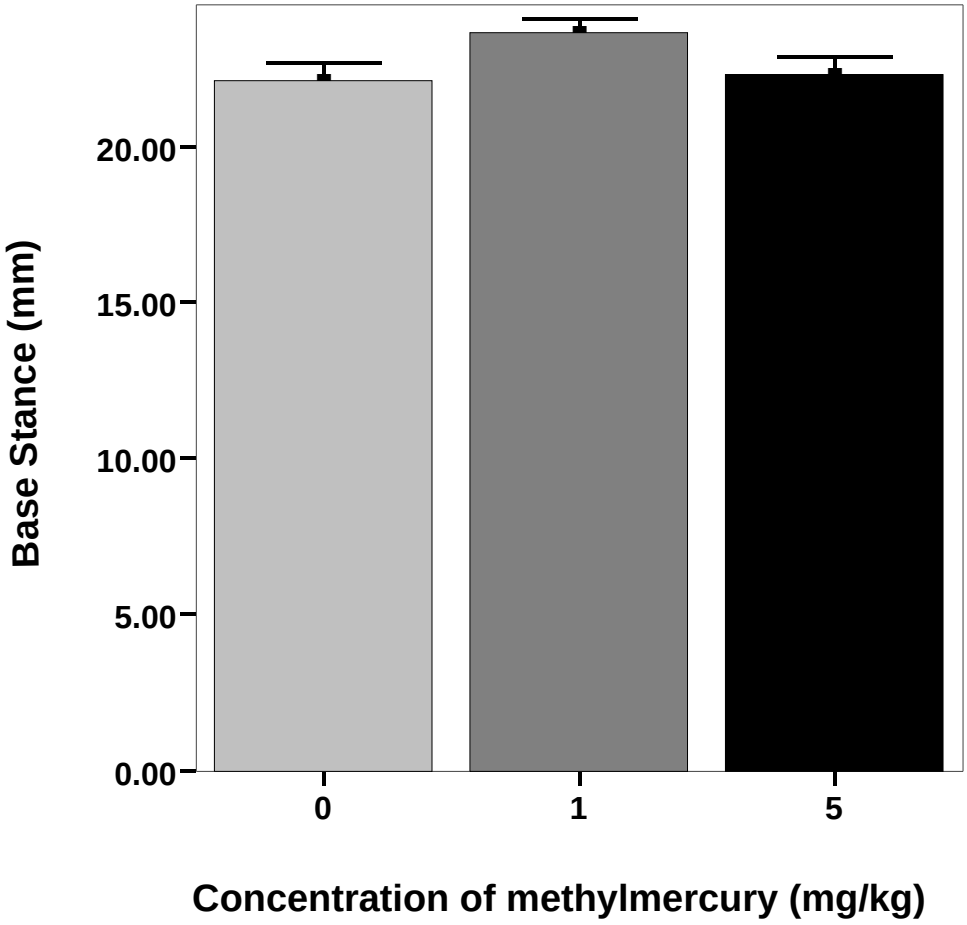

Figure III-6. Graph revealing the average base stance from foot print analysis. GLM-Multivariate Analysis of Variance indicated no significant difference in base stance (P = 0.532) between 0 mg/kg, 1.0 mg/kg and 5.0 mg/kg MMC treated mice or between males and females (P = 0.75).

Table III-1. Relative frequency of falling exhibited by 0 mg/kg, 1.0 mg/kg and 5.0 mg/kg MMC treated mice subjected to the vertical pole test. A Chi-Square test indicated a significant difference in the frequency of falling between the 0 mg/kg and both groups of MMC treated mice at $\alpha = 0.05$ (Chi-Square calculated value = 14.34; Chi-Square table value at DF 4 = 9.488). Significant differences were observed when Chi-Square tests were performed between 0 mg/kg and 1 mg/kg (Chi-Square calculated value = 10.73; Chi-Square table value = 5.991) and 0 mg/kg and 5.0 mg/kg (Chi-Square calculated value = 10.38; Chi-Square table value at DF 2 = 5.991) MMC treated mice.

Treatment MeHg (mg/kg)	Body wt. (gm)	Did not fall	Fell at/or before 45°	Fell between 45° and 90°	Total number of mice in each group
0	15.3	21	0	0	21
1.0	15.8	15	2	8	25
5.0	16.4	17	0	10	27

DISCUSSION

In the present study, we monitored behavior changes in young adult mice exposed to one of two different doses of MeHg and compared these changes with age matched control mice. The accelerating rota-rod is used widely in biomedical research as a means to test balance and motor coordination (Goulet et al., 2003; Rustay et al., 2003; Sakamoto et al., 2002). When we examined the results from the fourth trial on the third day we observed a significant decrease in latency to falling in the 5.0 mg/kg MMC exposed mice when compared to age matched control mice (FigureIII-1). In a study where Wistar rats were exposed to a moderate dose of MMC (5 ppm/day) throughout gestation and lactation periods, Sakamoto et al (2002) observed a significant difference on rota-rod performance between control and MMC exposed rats at 5 weeks of age. In

another study using rats, Sakamoto et al., (1993) demonstrated a dose dependent decrease in latency to falling with a total oral dose of 26.0 and 71.4 mg/kg MMC. But the concentrations of MMC used in this study were 5 –14 times higher than the 5.0 mg/kg MMC treated mice in our study. In contrast to our results, Goulet et al (2003) found no differences in latency to falling in 6-week-old mice that were chronically exposed to 4, 6 or 8 ppm MMC *via* drinking water during prenatal and early postnatal periods. Mice in their experiments were subjected to a constant speed of 20 rpm, whereas in our experiments mice were subjected to acceleration from 3 to 26 rpm over three minutes.

Motor learning is a complex phenomenon controlled by mutual assistance and coordination of various brain areas such as the cerebellum, basal ganglia and the motor, pre-frontal and parietal cortices (Rustay et al., 2003). In human studies, activation of the frontal and parietal cortices, the association areas of basal ganglia and the cerebellum was seen during early motor learning (Rustay et al., 2003). Mice in our experiments were tested on the accelerating rota-rod for three consecutive days, experiencing four trials on each day. Results of our experiments showed a substantial learning effect in control mice as demonstrated by an increase in performance from day 1 to day 3 (Figure III-1). While the mice treated with 1.0 mg/kg MMC showed a slight trend toward increased latency to falling when days 2 and 3 were compared, no significant differences between trials from days 1 to 3 were actually observed. In contrast, the mice treated with 5.0 mg/kg MMC showed significant improvement between days 1 and 2, but they showed no improvement between days 2 and 3 of testing on the rota-rod. In fact, the 5.0

mg/kg treated mice showed a tendency towards worse performance on day 3 compared to day 2 (Figure III-1). When the fourth trial on the third day is compared for all three groups, the 5.0 mg/kg treated mice demonstrated a significantly shorter latency to falling than the control mice.

Activity (horizontal and vertical exploration) and emotionality are two traits that have been tested in the open field for nearly forty years (Kulkarni, 1977). Mice when exposed to a novel environment try to explore during the first few minutes in order to get acquainted with the new atmosphere and/or try to find ways to escape (Crawley, 1999). The two major locomotor patterns are horizontal and vertical exploration. Mice that show deficits in motor movements might become restricted in terms of one or both of the exploratory movements and therefore might show reduced activity. However, because behavior involves complex interactions of many different areas of the brain, the specific brain regions that might be involved in producing altered behavior in the open field test can be hard to identify. Also the specific neurobehavioral importance of the different individual activities is still poorly understood. In our experiments, open field behavior testing during the first 5 minutes revealed a decrease in horizontal exploration in MeHg exposed mice (Figure III-2). The decrease was statistically significant for 1.0 mg/kg MMC treated mice. 5.0 mg/kg MMC exposed mice showed a trend towards decreased horizontal exploration when compared to controls, but the difference compared to control mice was not statistically significant. The data are consistent with other rodent studies reported in the literature that examined horizontal exploration after exposure to methylmercury (Dore et al., 2001; Goulet et al., 2003; Kim et al., 2000; Lown et al.,

1977; Pereira et al., 1999; Su and Okita, 1976). However, it is important to note that in our experiments, mice were exposed to acute doses of MMC between P34-38. Most of the behavior studies cited in the literature were performed on mice exposed to MMC during gestation and early postnatal periods. On the other hand, consistent with some studies (Dore et al., 2001; Goulet et al., 2003; Rossi et al., 1997) and contrary to others (Baraldi et al., 2002; Kim et al., 2000; Lown et al., 1977; Morganti et al., 1976; Salvaterra et al., 1973), we did not see any significant difference in rearing activity between the control mice and mice exposed to either dose of MMC (Figure III-3).

Three parameters were analyzed using the foot print test. Of the three parameters, angle of foot placement was found to be statistically significant in 1.0 mg/kg MMC treated mice when compared to the controls (Figure III-4). A statistically significant difference was not observed between 5.0 mg/kg MMC treated mice and controls with respect to angle of foot placement. However, a tendency towards increase in the mean angle of foot placement was observed in 5.0 mg/kg MMC exposed mice when compared to control mice. Stride length (Figure III-5) and base stance (Figure III-6) between the two hind paws did not differ statistically between MMC treated mice and controls. However there seems to be a tendency towards reduction in mean stride length and increase in base stance in MMC exposed mice. Foot print analysis is used extensively to assess gait abnormalities especially in spinal cord injury (Hammers et al., 2001) and with animal models of Huntington's disease and Parkinson's disease (Carter et al., 1999; Fernagut et al., 2002). Fernagut et al (2003) used foot print analysis to test hypokinesia due to alteration in the nigrostriatal system caused by knocking out the dopamine

transporter gene and found a significant difference in the stride length between dopamine transporter knockout mice and wild type mice.

The vertical pole test was performed with slight modification from the conventional method described in the literature (Fernagut et al., 2003; Kurosaki et al., 2003; Matsuura et al., 1997). This test is extensively used to assess motor deficits in animal models of movement disorders like Parkinson's disease (Arai et al., 1990; Ohno et al., 1994). We modified this test in order to assess motor coordination and balance deficits as a result of MMC toxicity. Mice without any motor deficits, when placed on the pole in a horizontal position facing towards the end that will be lifted (keeping the other end stationary), should be able to hold on and move up the pole as it is raised from a horizontal to a vertical position and maintain balance. In our experiments, 10 mice out of 25 mice treated with 1.0 mg/kg MMC and 10 mice out of 27 mice treated with 5.0 mg/kg MMC were not able to maintain balance and fell off the pole before the pole reached 90 degrees. No control mice fell off the pole during the 15 second testing period when the pole was lifted from 0 degrees to 90 degrees (Table III-1). Most of the control mice moved up the pole while the MMC treated mice remained in one place or tried to move down the pole as it was being raised.

There appear to be significant effects of acute MMC exposure on young adult mice as demonstrated by significant behavior changes observed in our experiments. These concentrations of MeHg used in this study are environmentally relevant exposure levels. The major source of MeHg exposure in the US population is from the consumption of fish. Within this population, exposure levels vary based on the individual characteristics

of fish consumption and the amount and types of fish consumed in different regions of the country. Mercury concentrations in commercial fish and seafood in the US span from 0.01-1.0 ppm (U.S.EPA, 1997). An estimated average MeHg intake for 25-50% of the US population is 1.4-3.5 μg/day and for 5-10% of the US population is 9.1-15.6 μg/day (U.S. EPA, 1997). In our study, total amount of mercury administered over a period of 5 days in the 1.0 mg/kg and 5.0 mg/kg MMC treated mice calculated using their average body weight (Table III-1) is 15.8 and 82.0 μg respectively. Based on the U.S. EPA estimation, the average intake of MeHg in the above mentioned population groups for 5 days would be between 7.0-17.5 and 45.5-78.0 μg /day respectively. The exposure levels of 1.0 mg/kg and 5.0 mg/kg MMC in our study is towards the upper limit of the estimated exposure levels of MeHg as per the U.S. EPA (1997).

Of the four behavioral tasks used in this study, we found a significant difference in rota-rod performance, suggesting alteration in motor coordination and balance in MMC exposed mice. In the open field there was a significant reduction in horizontal exploration during the first 5 minutes after exposure to a novel environment. Although the precise behavioral significance of activity in the open field is not known, one can conclude that it measures the complex interaction between the cerebellum, motor cortex and limbic system that work together in mediating locomotion and exploration. We also found significant differences in the angle of foot placement and the vertical pole test, which are commonly used to assess motor deficits in various movement disorders. An interesting observation in our study was the performance of low dose (1.0 mg/kg) MMC exposed mice. On both open field and foot print analysis, the high dose (5.0 mg/kg)

MMC exposed mice performed better than the low dose group when compared to control mice. These observations suggest that MMC at very low doses may be disturbing the normal neuronal function but at high doses MMC is lethal to these neurons. The surviving neurons in the high dose group of mice may be compensating for the dead neurons so their behavior is only slightly altered when compared to the low dose group where the neurons are not dead yet, but compromised and outwardly manifested as more severe behavior deficits.

In conclusion, our findings in this study suggest that these tests can be used as effective tools to measure subtle motor deficits that result from exposure to moderate to low doses of neurotoxicants. We found that MMC is not only a potent neurotoxic agent when exposure occurs prenatally, but also can be dangerous when individuals are exposed during early adulthood. It would be interesting in future experiments to see if there is any affect of such exposures in aged populations, as we know that fish forms a major source of protein in the aging population, and fish is a major source of MeHg.

CHAPTER IV

CHANGES IN BIOCHEMICAL PROCESSES IN CEREBELLAR GRANULE CELLS OF MICE EXPOSED TO METHYLMERCURY

SUMMARY

At postnatal (P) day 34, male and female C57BL/6J mice were exposed orally to five divided doses totaling 1.0 or 5.0 mg/kg of methylmercuric chloride (MMC) or sterile deionized water in moistened rodent chow. After eleven days cerebellar granule cells were acutely isolated to measure reactive oxygen species (ROS) levels and mitochondrial membrane potential (MMP) using CM-H2DCFA and TMRM dyes respectively. For visualizing intracellular calcium ion distribution using transmission electron microscopy (TEM), mice were perfused eleven days after last dose of MMC by oxalate-pyroantimonate method. Histochemistry (Fluoro-Jade dye) and immuno histochemistry (activated caspase 3) was performed on frozen serial cerebellar sections to label granule cell death and activation of caspase 3 respectively. MMC treated mice granule cells showed elevated ROS levels and decreased in MMP when compared to control mice granule cells. Electron photomicrographs of MMC treated granule cells showed altered intracellular calcium ion homeostasis ($[Ca^{2+}]i$) when compared to control mice granule cells. However, in spite of these subcellular changes, the concentrations of MMC used in our study did not produce significant programmed cell death / apoptosis at the time point examined as evidenced by Fluoro-Jade and activated caspase 3 immunostaining.

INTRODUCTION

Mercury is a ubiquitous chemical found in our environment as a result of natural events (volcanic eruptions) and anthropogenic sources (burning of charcoal etc.,). An organic form of mercury (methylmercury, MeHg) is highly neurotoxic by virtue of its lipophilicity. Based on two epidemics of MeHg poisoning (Minamata Bay, Japan and Iraq), ingestion of contaminated food can be considered as the primary route of exposure (Takeuchi et al., 1962; Bakir et al., 1973). In both of these episodes the primary signs of neurological dysfunction were cerebellar ataxia, generalized weakness of extremities and sensory disturbances.

All aerobic life forms depend upon oxygen for survival. Generation of ROS through the electron transport chain (ETC) attached to inner membrane of mitochondria is a part of normal life. Excessive ROS formation can result from inefficient functioning of ETC. Yoshino et al., (1966) reported that mitochondria are the earliest sites of mercury accumulation in the brain following administration of MeHg. O'Kusky (1983) reported changes in mitochondrial morphology in the developing rat brain. Several *in vitro* studies using cultured granule cells and brain slices demonstrated excessive ROS formation due to MeHg treatment (Gasso et al., 2000; Yee and Choi, 1996).

MeHg has been associated with altered intracellular calcium ion homeostasis ($[Ca^{2+}]i$) in a number of cells including cultured rat cerebellar granule cells (Shenker et al., 1992, 1993; Denny et al., 1993; Marty and Atchison, 1997; Mundy and Freudenrich, 2000). Recent *in vitro* studies using cultured cerebellar granule cells from rats demonstrated that MeHg causes the opening of MTP leading to apoptotic cell death

(Limke and Atchison, 2002; Limke et al., 2003). Opening of MTP is associated with release of mitochondrial factors like cytochrome C, which in turn activates caspase 3 (InSug et al., 1997; Limke and Atchison, 2002; Wigdal et al., 2002). Nagashima et al., (1996) demonstrated the process of apoptosis in cerebellar granule cells of rats exposed to a total oral dose of 40 mg/kg MMC divided into 10 equal doses given on alternate days over a period of 20 days.

Most the studies demonstrated activation of the mitochondrial pathway of apoptosis either in cultured granule cells or exposing rodents to high concentrations of MeHg. The objective of this investigation is to determine whether short term low dose *in vivo* exposure of rodents to MeHg through contaminated food (the most common route of exposure) will lead to subcellular events like elevation of ROS, alteration in $[Ca^{2+}]i$ and loss of MMP. Whether these changes will lead to apoptosis of granule cells at such low exposure levels will provide valuable insights with respect to *in vivo* toxicity studies.

In the present study we exposed male and female C57BL/6J mice at postnatal (P) day 34 age to MeHg via food using a total dose of 1.0 mg/kg and 5.0 mg/kg body weight and compared with age matched control (given vehicle only) mice for subcellular changes (ROS production, alteration in $[Ca^{2+}]i$ homeostasis and loss of MMP). In addition, we performed Fluoro-Jade staining on serial frozen sagittal sections of cerebellum to label dying neurons. Additional frozen sections were immunolabelled with anti-activated caspase 3 antibody to determine caspase 3 activation.

MATERIALS AND METHODS

Animals

Adult C57BL/6J wild type (+/+) male and female mice, originally obtained from The Jackson Laboratory (Bar Harbor, MA, USA), were bred to produce wild type offspring. A total of 43 male and 35 female mice were used in this study. Mice were further divided into three treatment groups as follows: control (23), 1.0 mg/kg MMC (26) and 5.0 mg/kg MMC (29). All mice were housed at the Laboratory Animal Research and Resource building, Texas A&M University, in a constant temperature (21-22°C) and humidity (45-50%) room with a 12-hour light-dark cycle. The mice were weaned at 29 days of age and housed individually for the duration of training, dosing and behavior testing. All procedures were carried out in accordance with the National Institutes of Health Guide for the Care and Use of Laboratory Animals (National Institutes of Health Publication No. 85-23, revised 1996).

Chemicals and dosing

Methylmercuric chloride (MMC; 95% purity) was obtained from Alfa Aesar (Ward Hill, MA, USA). MMC was initially dissolved in sterile deionized water and further diluted with sterile deionized water for addition to food. All MMC solutions were stored at 4ºC until used. Mice at postnatal day (P) 29 were divided into three treatment groups and dosed with MMC as described in chapter III. Fluorescent dyes (TMRM and CM-H_2DCFDA) were obtained from Molecular Probes (Eugene, OR).

Acute isolation of cerebellar granule cells

Cerebellar granule cells were acutely isolated as described in Current Protocols in Toxicology (Oberdoerster, 2001). At P50, mice were anesthetized using isofluorane and killed by decapitation. The brain was removed from the cranium and the cerebellum separated from the rest of the brain. The meninges were removed and the cerebellum was chopped in 6-8 pieces and transferred to a chilled 50ml falcon tube containing minimum essential medium with Earle's salts (MEM; Life Technologies inc., Rockville, MD) on ice. Cerebellar granule cells were isolated using dissociation medium containing MEM and 1.5U/ml protease (Sigma, St. Louis, MO).

Measurement of cell viability

Aliquots of dissociated cells were stained with Trypan blue dye to check their viability. Trypan blue dye selectively stains dead cells. A clean coverslip was placed over the counting area of a hemocytometer and 10 μL of cell suspension containing 0.08% Trypan blue dye was transferred into the groove on the edge of the hemocytometer. The solution containing cells was drawn under the coverslip by capillary action. Cells were counted in four 1-mm^2 squares using a inverted compound microscope at 100X magnification. The cell number was determined by multiplying with dilution factor (x 10,000). Based on this dye exclusion method we observed that cell viability was 90% or greater (Figure IV-1).

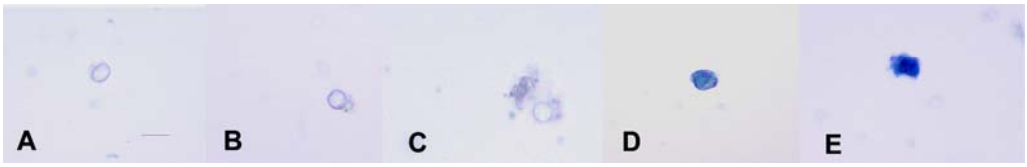

Figure IV-1. Photomicrograph showing Trypan blue staining of acutely isolated cerebellar granule cells. A, B and C represent viable granule cells that have excluded Trypan blue. D and E represent dead cells that have taken up Trypan blue. Scale bar in 1A = 15 microns

Reactive oxygen species (ROS)

Cerebellar granule cells were acutely dissociated as described above, plated onto chambered slides (VWR International Inc) and incubated in 95% O_2 and 5% CO_2 at 37°C for 25 minutes. The cells were loaded with an indicator dye, Chloromethyl-dihydrodichlorofluorescein diacetate (CM-H_2DCFDA) (Molecular Probes Inc., Eugene, OR) at a concentration of 500 nmol and incubated in 95% O_2 and 5% CO_2 at 37°C for 8 minutes. CM-H_2DCFDA is a redox- sensitive dye used to determine ROS levels. It is membrane permeable and gets trapped in cells by binding of the chloromethyl group to cellular thiols. Subsequently the dye becomes fluorescent when oxidized by hydrogen peroxide and/or downstream free radical products of hydrogen peroxide. Sequential time course fluorescent image capturing was performed for 22.5 minutes using a 90 second interval with a 20X objective on an Olympus 1X-70 microscope and a Hamamatsu ORCA-ER cooled charge-coupled device camera at excitation and emission of 490 nm and 520 nm respectively. Image capturing and reactive oxygen species levels were analyzed using Simple PCI Version 5.0.0.1503 Compix Inc. and Imaging (Cranberry Township, PA).

Intracellular calcium distribution

Control and MMP treated mice at P50 were anesthetized with xylazine and ketamine and, perfused with 20 ml of 90mM potassium oxalate (Sigma, St. Louis, MO) followed by 20 ml of 3% glutaraldehyde (EMS, Fort Washington, PA, USA) containing 90 mM potassium oxalate (Silklos et al., 2000). Mouse bodies were wrapped in aluminum foil and stored at 4ºC for 2 hours. The brain was removed from the cranial vault and the cerebellum was separated and sliced into 1 mm thick sagittal sections and further fixed in the same oxalate containing fixative for 24 hours at 4ºC. Cerebellar sections were rinsed in 7.5% sucrose containing 90mM potassium oxalate and further fixed in a solution containing 2% potassium pyroantimonate (Sigma, St. Louis, MO), 1% osmic acid (EMS, Fort Washington, PA, USA) and 0.01N acetic acid for 2 hours at 4ºC. Cerebellar sections were briefly rinsed in distilled water and dehydrated in a graded series of ethanol followed by acetone. The sections were than transferred to acetone: araldite mixture for 4 hours at room temperature. Sections were transferred to fresh araldite (EMS, Fort Washington, PA, USA) and stored at 4ºC overnight. The next day the sections were quickly brought to room temperature and infiltrated (twice) with fresh araldite for 2 hours at 40ºC. Cerebellar sections were then embedded into beam capsules and kept at 60ºC for 3 days (Rhyu et al., 1999). Cerebellar slices were cut at 100 Aº and viewed under Zeiss 10C electron microscope.

Mitochondrial membrane potential (MMP)

MMP was evaluated by using confocal fluorescence microscopy. Acutely dissociated cerebellar granule cells plated onto cover slips were incubated at 37°C for 25 minutes in MEM. Cells were loaded with an indicator dye TMRM at 150nmol and further incubated in 95% O_2 and 5% CO_2 at 37°C for 15 minutes. TMRM is a lipophilic cation that accumulates in the mitochondria in proportion to the mitochondrial membrane potential. Fluorescent images were acquired using a 40X oil objective on an Olympus 1X-70 microscope and a Hamamatsu ORCA-ER cooled charge-coupled device camera at excitation and emission of 555nm and 600nm respectively. Image capturing and membrane potential analysis were carried out using Simple PCI Version 5.0.0.1503 Compix Inc. and Imaging System (Cranberry Township PA).

Activated caspase 3 immunohistochemistry

Control and MMC treated mice at P50 were anesthetized with ketamine/xylazine (intra peritoneally) and perfused transcardially with Tyrode's saline (50 ml) followed by 4% paraformaldehyde (300 ml). Brains were removed from the cranium and cryoprotected with 20% sucrose in 0.1 M phosphate-buffered saline (PBS). 20µm sagittal sections were cut using a cryostat and mounted on gelatin coated slides. Sections were permeabilized using 0.3% Triton X-100 for an hour followed by a 5 minute incubation in 3.0% hydrogen peroxide in 0.1M PBS to quench endogenous peroxidases. The sections were then blocked in 5% normal goat serum and incubated overnight at 4ºC in anti-activated caspase3 antibody (R&D Systems, Minneapolis, MN, USA) at a

1:50,000 dilution. Sections were incubated for 2 hours in biotinylated goat anti-rabbit, secondary antibody at 1:400 dilution (Vector Laboratories, Burlingame, CA, USA) followed by peroxidase labeled streptavidin at 1:5000 dilution (Kirkegaard and Perry Laboratories, Gaithersburg, MD, USA). Signal was detected with 0.024% 3,3-diaminobenzidine in 0.006% hydrogen peroxide and 0.05 M Tris-HCl buffer (pH 7.6). The reaction was stopped after achieving optimal signal by transferring the sections to 0.05 M Tris-HCl buffer. The slides were transferred briefly to 0.1 M PBS and dehydrated in graded series of ethanol followed by two changes of xylene and coverslipped with DPX mounting media.

Fluoro-Jade staining procedure

At P50, mice were anesthetized with isofluorane and brains were removed from the cranium, frozen with powdered dry ice and stored at -70ºC. 20 µm thick serial sagittal sections were made on a cryostat and stored at -70ºC until they were stained with Fluoro-Jade (Histo-chem Inc., Jefferson, AR, USA). The fixed frozen sections were thawed and dried thoroughly at 45ºC for 20 minutes in an oven. The slides were stained with Fluoro-Jade using the protocol described by Schmued et al (1997) with a few modifications. Briefly, slides were immersed in 100% ethanol for 3 minutes followed by 1-minute washes in 70% ethanol then deionized water. Brain sections were transferred to a 0.06% potassium permanganate solution for 15 minutes on a rotating platform. Slides were then washed in deionized water for 1 minute and incubated in 0.001% Fluoro-Jade in deionized water with 0.1% acetic acid for 30 minutes on a rotating platform. After

staining with Fluoro-Jade, slides were rinsed with three 1-minute changes of deionized water, dried thoroughly with a hot-air gun, immersed in xylene and coverslipped using DPX mounting media (EMS, Fort Washington, PA, USA). Sections were examined under epifluorescence microscope using FITC filter. Fluorescent images were acquired using a Zeiss Axioplot 2 research microscope (Carl Zeiss, Inc., Thornwood, NY, USA) equipped with a three-chip Hamamatsu video camera.

Statistical analysis

MMP, Fluoro-Jade and activated caspase 3 data was analyzed using General Linear Model (GLM) - Univariate Analysis of Variance at $\alpha = 0.05$, using SPSS version 11.0 for Windows. ROS data was analyzed using GLM - repeated measure analysis. Significant differences among treatment and control groups were interpreted using the Tukey's honest significant difference (HSD) post hoc test.

RESULTS

Reactive oxygen species

Figure IV-2A shows representative photomicrographs of cerebellar granule cells from control, 1.0 mg/kg and 5.0 mg/kg MMC-treated mice. We examined the ROS levels in three treatment groups based on analysis of the intensity of fluorescence of CM-H_2DCFDA dye (Figure IV-2B). GLM-Multivariate Analysis of Variance (three-way ANOVA) indicated an overall significant difference between control and MMC-treated mice ($P<0.001$). The GLM-Repeated measure test also indicated a significant treatment effect (P 0.012). No significant difference was observed with respect to gender ($P = 0.239$), and interaction between treatment and gender ($P = 0.624$). GLM-Multivariate Analysis of Variance and the Tukey's HSD post hoc test indicated a significant difference ($P < 0.05$) starting with the fourth measurement (*) between control and 5.0 mg/kg MMC exposed mice granule cells. Significant differences were observed between all three-treatment groups on the sixteenth measurement (**).

Intracellular calcium distribution

Figure IV-3 shows representative electron photomicrographs of cerebellar granule cells from control, 1.0 mg/kg and 5.0 mg/kg MMC treated mice. A qualitative analysis of the electron micrographs revealed alteration in intracellular calcium ion homeostasis in both the MMC exposed mice granule cells. In both the MMC treated granule cells, mitochondrial calcium ion concentration was found to be high in comparison to the control granule cells.

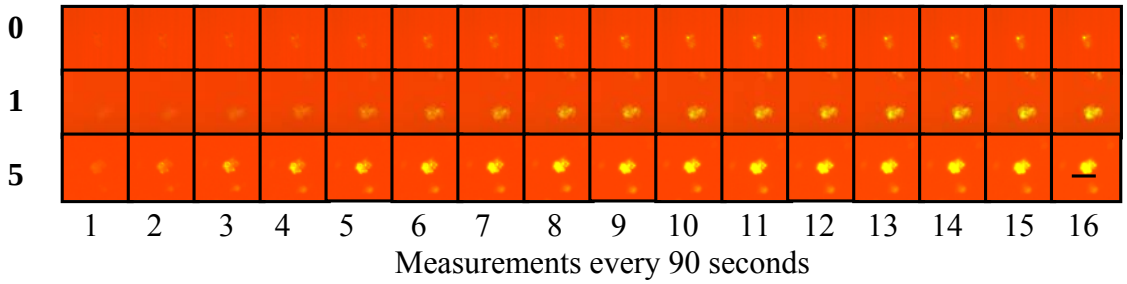

Figure IV-2A. Photomicrographs showing acutely isolated cerebellar granule cells loaded with CM-H_2DCFDA dye. Images of granule cells from control (0), 1.0 mg/kg (1) and 5.0 mg/kg (5) MMC treated mice loaded with CM-H_2DCFDA showing fluorescence (green) in proportion to the total cellular ROS generated. Scale bar in 16 = 10 microns

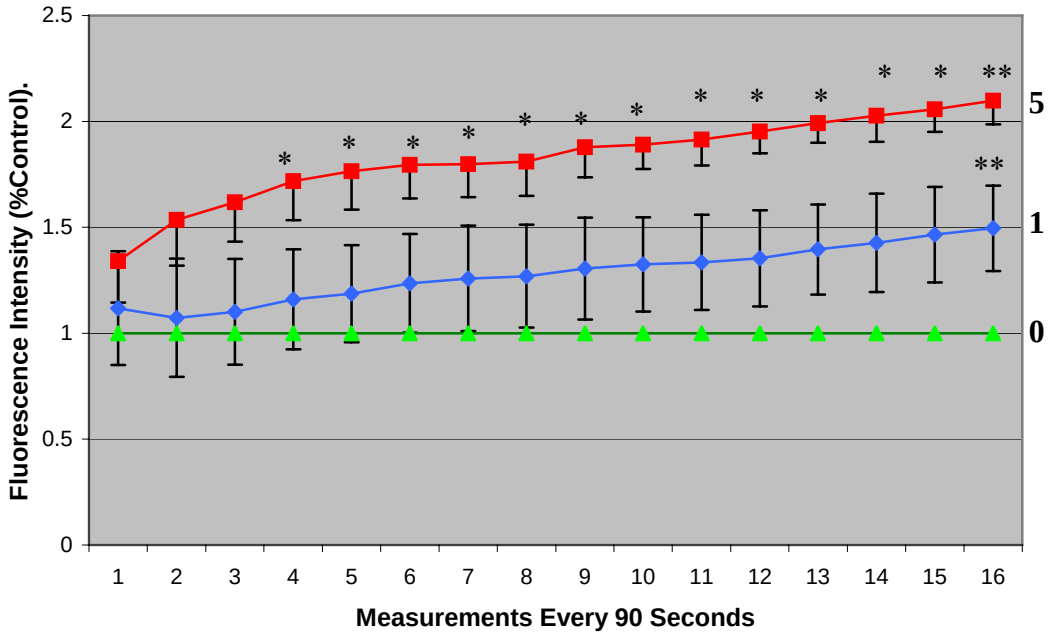

Figure IV-2B. Effects of MMC administration on total cellular ROS levels in granule cells. Graph revealing % control of the relative mean total cellular ROS of granule cells from control (0; n = 5), 1.0 mg/kg (1; n = 5) and 5.0 mg/kg (5; n = 5) MMC treated mice based on analysis of the intensity of fluorescence of CM-H_2DCFDA dye. GLM-Multivariate Analysis of Variance, GLM – repeated measure analysis and Tukey's post hoc test indicated a significant difference between control and 5.0 mg/kg MMC treatment groups at fourth measurement (*). All three-treatment groups differed statistically on the sixteenth measurement (**).

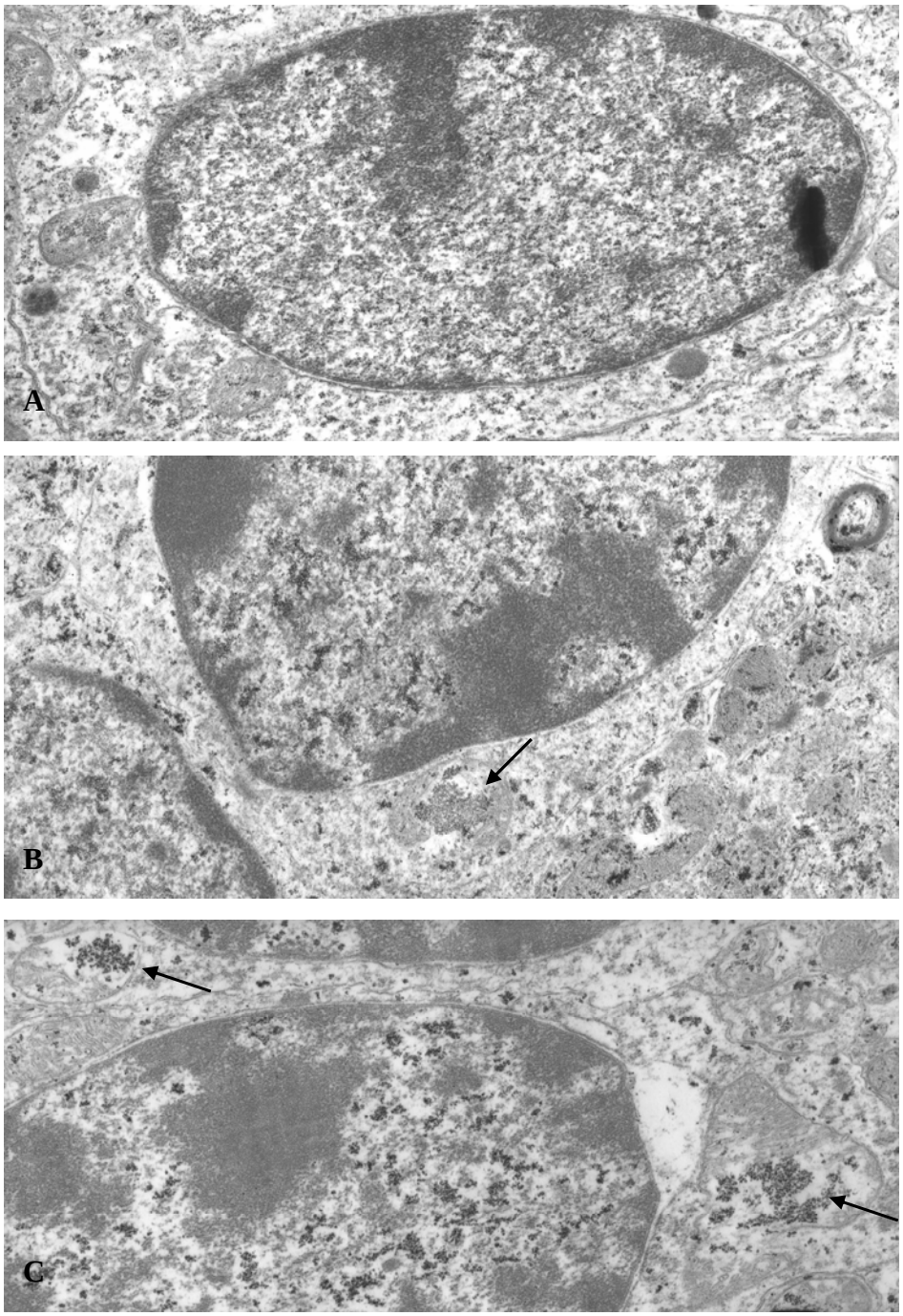

Figure IV-3. Electron photomicrographs of granule cells after oxalate-pyroantimonate fixation. A, B and C represent granule cell images from control, 1.0 mg/kg and 5.0 mg/kg MMC treated mice. Arrows represent calcium localization within the mitochondria in both the MMC treated mice granule cells.

Mitochondrial membrane potential

Figure IV-4A shows representative fluorescent photomicrographs of cerebellar granule cells from control, 1.0 mg/kg and 5.0 mg/kg MMC-treated mice. Fluorescent images of granule cells with clusters of mitochondria (red), that are TMRM dye-loaded in proportion to the membrane potential. Figure IV-4B summarizes the relative mean mitochondrial membrane potential of cerebellar granule cells from control, 1.0 mg/kg and 5.0 mg/kg MMC-treated mice based on analysis of fluorescence intensity of TMRM dye. GLM-Univariate Analysis of Variance and Tukey's HSD post hoc test indicated a significant difference between control and MMC-treated mice ($P < 0.001$). Significant differences were not observed between males and females ($P = 0.211$). There also was no significant interaction between treatment and gender ($P = 0.309$).

Activated caspase 3 immunohistochemistry

To determine the protein expression for activated caspase 3, 4-8 serial sagittal sections/mouse were immunostained with anti-activated caspase 3 antibody and immunopositive granule cells were counted. Immunohistochemical staining of cerebella from control and MMC treated mice showed few activated caspase 3 immunoreactive granule cells (Figure IV 5A and B).

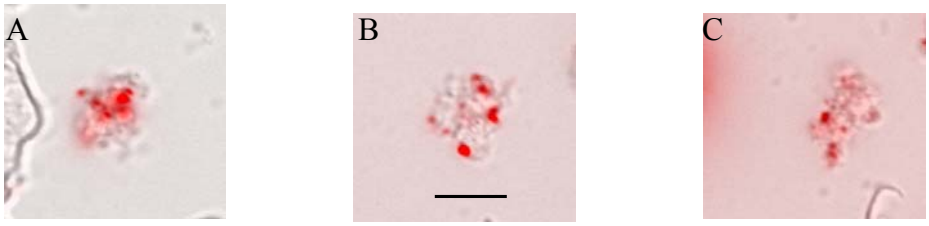

Figure IV-4A. Photomicrographs showing acutely isolated cerebellar granule cells loaded with TMRM dye. Fluorescent images of granule cells from control (A), 1.0 mg/kg (B) and 5.0 mg/kg (C) MMC treated mice with clusters of mitochondria (red), that are TMRM dye loaded in proportion to the membrane potential. Scale bar in B = 10 microns.

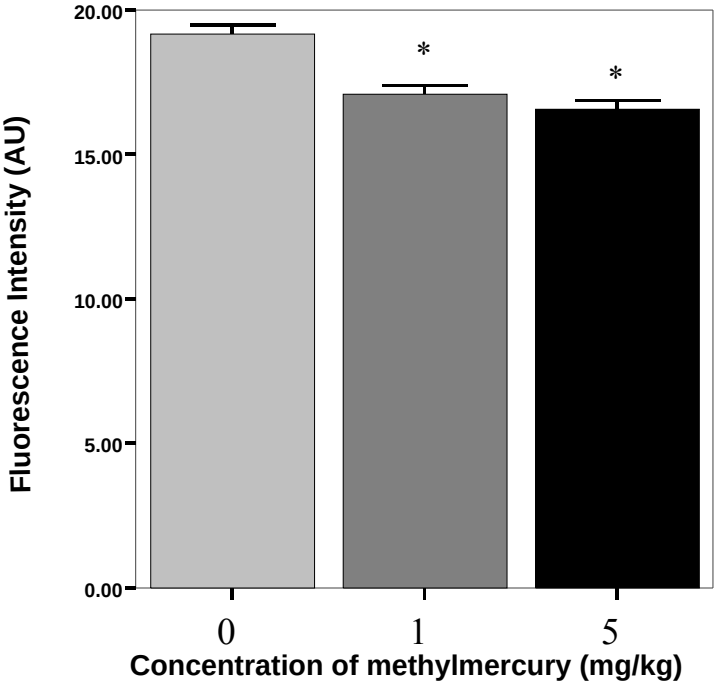

Figure IV-4B. Effects of mercury treatment on mitochondrial membrane potential of cerebellar granule cells. Graph revealing the relative mean mitochondrial membrane potential of granule cells from control (0; n = 5), 1.0 mg/kg (1; n = 5) and 5.0 mg/kg (5; n = 5) MMC treated mice based on analysis of the intensity of fluorescence of TMRM dye. GLM-Univariate Analysis of Variance and Tukey's HSD post hoc test indicated a significant ($P<0.001$) difference between control and MeHg treated mice. 1.0 mg/kg and 5.0 mg/kg MMC treated mice granule cells exhibited a significantly lower MMP (*).

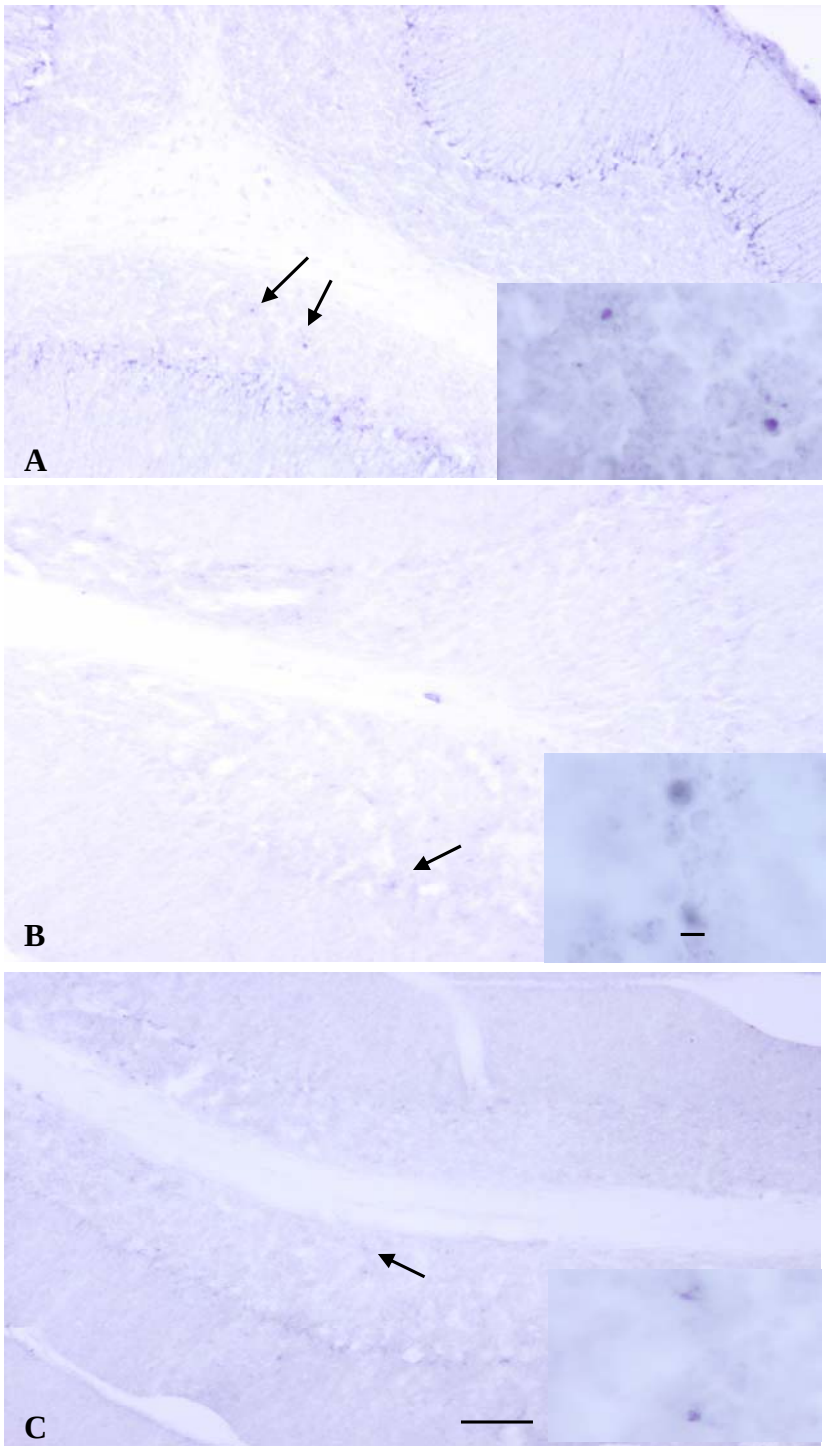

Figure IV-5A. Photomicrographs of activated caspase 3 immunohistochemical staining. Activated caspase 3 staining revealed few immunoreactive granule cells in control (A) and MMC exposed (B, C) granule cells (arrows). Scale bar in B = 10 microns; C = 100 microns.

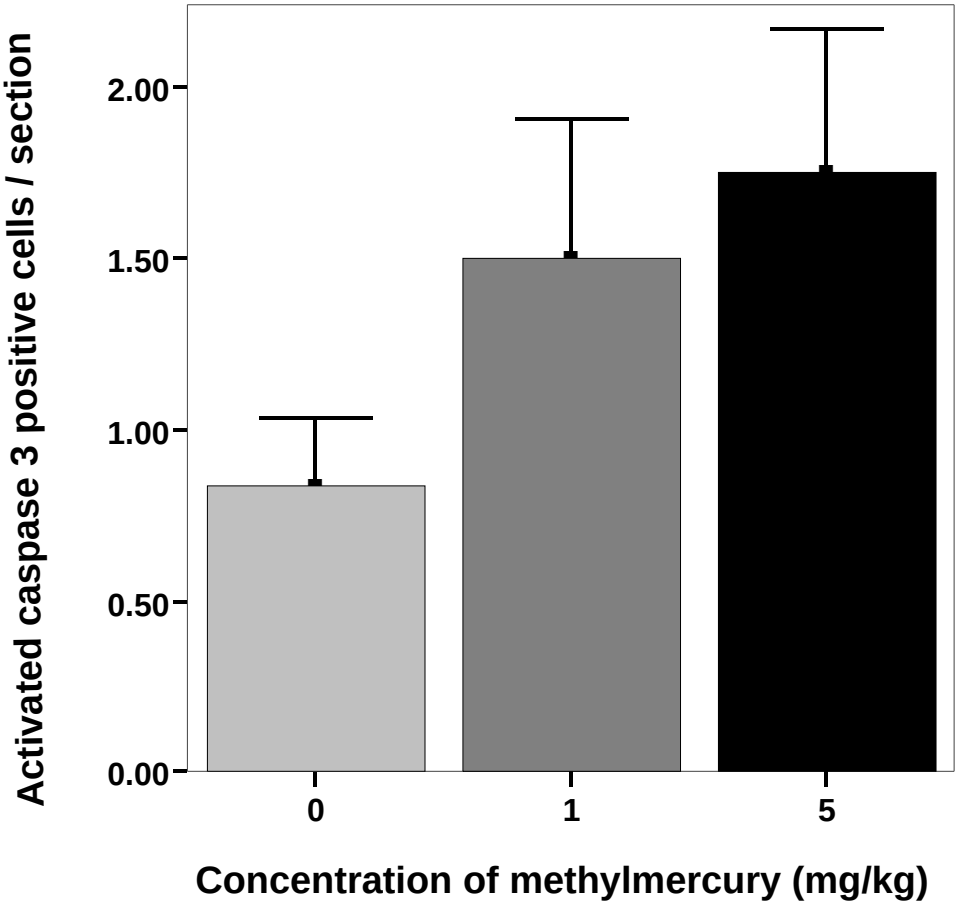

Figure IV-5B. Effects of MMC administration on activation of caspase 3 in mice granule cells. A GLM-Univariate Analysis of Variance indicated no significant difference in activated caspase 3 in granule cells from control (0; n = 6), 1.0 mg/kg (1; n = 6) and 5.0 mg/kg (5; n = 6) MMC treated mice (P = 0.121).

Fluoro-Jade labeling of dead cells

A comparison of Fluoro-Jade staining of cerebellar granule cells from control, 1.0 mg/kg and 5.0 mg/kg MMC treated mice is shown in photomicrographs found in Figure IV-6A. Fluoro-Jade is an anionic fluorescein derivative that selectively stains degenerating neurons irrespective of the mechanism of cell death (apoptosis or necrosis) (Schmued et al., 1997; Frank et al., 2003). Fluoro-Jade staining was performed to determine the extent of cell death and possibility of activation of other pathways of apoptosis (extrinsic via death receptors or intrinsic via release of mitochondrial associated proapoptotic proteins like AIF or Smac). Cells from 4-8 serial sagittal sections were counted from individual mice from each treatment group. A GLM – Univariate Analysis of Variance indicated no significant difference in Fluoro-Jade positive granule cells from control and MMC treated mice ($P = 0.397$) (Figure IV-6B). No significant difference was observed between males and females ($P = 0.145$), and interaction between gender and treatment was also not significant ($P = 0.269$).

DISCUSSION

The findings reported here demonstrate elevation of ROS levels, alteration in $[Ca^{2+}]i$ homeostasis and reduction in MMP in 1.0 mg/kg and 5.0 mg/kg MMC treated mouse granule cells when compared to control mouse granule cells. However, as shown by immunohistochemical staining for activated caspase 3, the most common pathway of apoptosis discussed in MeHg literature, was not activated at the concentrations of MMC used in this study and at the time point investigated.

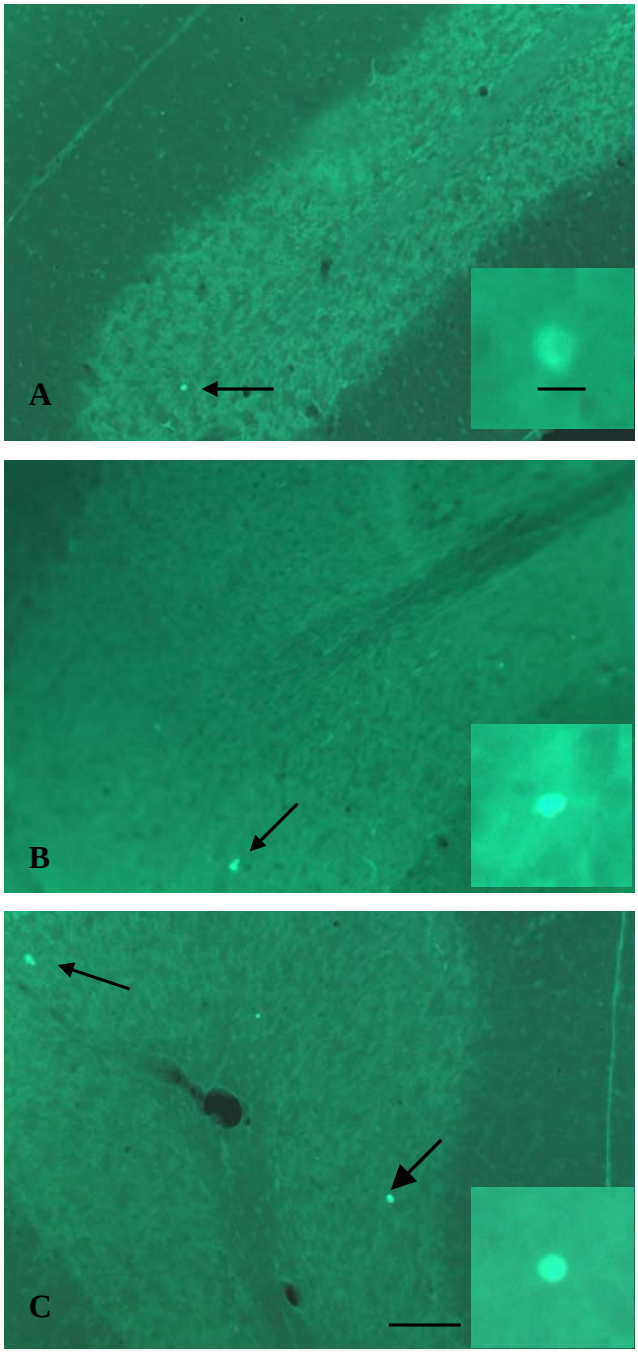

Figure IV-6A. Photomicrographs of Fluoro-Jade staining of control, 1.0 mg/kg and 5.0 mg/kg MMC exposed mice granule cells. The arrows indicate Fluoro-Jade positive cells. Inserts in A, B and C represent Fluoro-Jade positive cells at 40X. Scale bar in A = 10 microns; C = 100 microns.

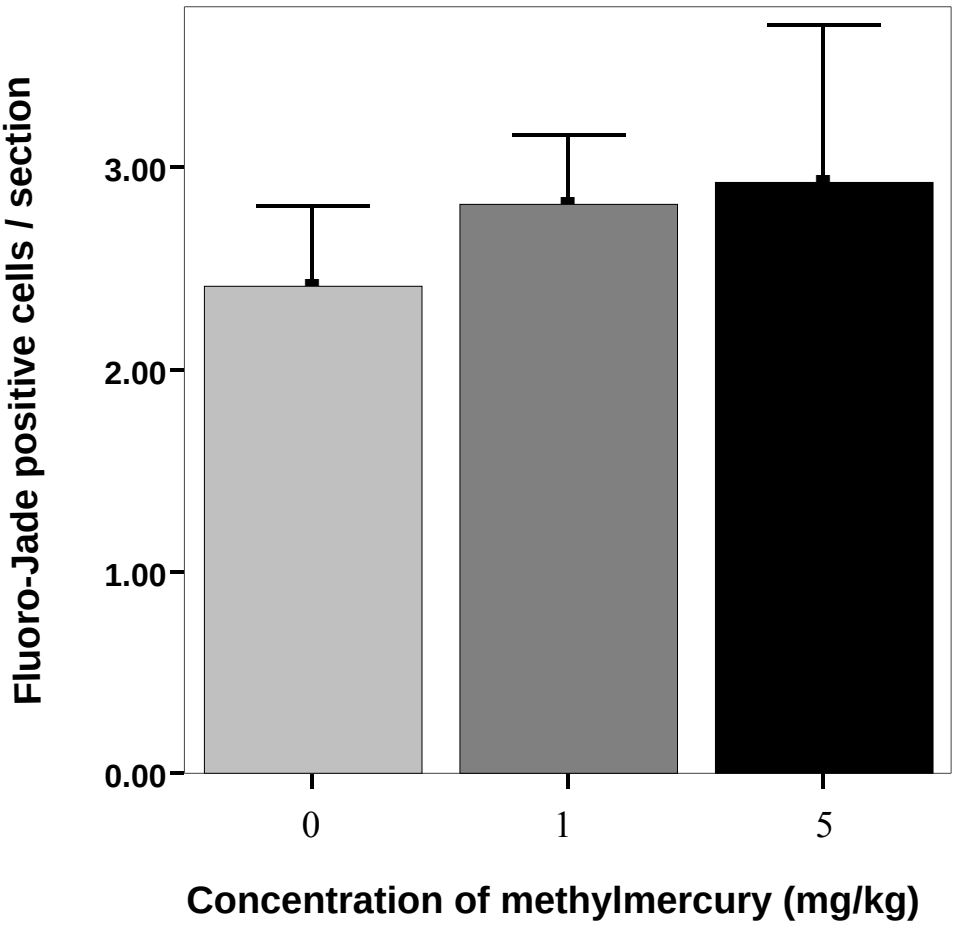

Figure IV-6B. Graph showing mean Fluoro-Jade positive cells from control, 1.0 mg/kg and 5.0 mg/kg MMC treated mice. A GLM-Univariate Analysis of Variance indicated no significant difference in Fluoro-Jade positive granule cells from control and MMC treated mice (P = 0.397).

Total cellular ROS levels were determined in control and MMC treated mice granule cells using CM-H_2DCFDA dye. CM-H_2DCFDA is a redox sensitive membrane permeant dye that gets trapped inside cells by binding of the chloromethyl (CM) group to cellular thiols. Subsequently CM-H_2DCFDA becomes fluorescent when activated by cellular ROS. Although there are no published data available to compare directly with the present results obtained by the technique used in this study (Figure IV-2A and B), results from several other laboratories demonstrated increased generation of ROS in MeHg induced neurotoxicity using cultured granule cells (Ishibashi et al., 2004; Limke and Atchison, 2002; Limke et al., 2003; Marty and Atchison, 1997; Marty and Atchison, 1998; Mundy and Freudenrich, 2000; Yee and Choi, 1996) or immortalized cell lines (Belletti et al., 2002; Gatti et al., 2004).

Oxidative stress as a result of MeHg toxicity was shown to interfere with the electron transport chain in mitochondria (Yee and Choi, 1996). Several studies reported alteration of $[Ca^{2+}]i$ homeostasis as a result of elevated ROS levels (Ishibashi et al., 2004; Marty and Atchison, 1997; Marty and Atchison, 1998). Qualitative analysis of transmission electron photomicrographs of oxalate-pyroantimonate perfused cerebella from control and MMC treated mice revealed excess calcium accumulation in mitochondria of granule cells from 1.0 mg/kg and 5.0 mg/kg MMC treated granule cells (Figure IV-3). These observations suggest that mitochondria are buffering the excess $[Ca^{2+}]i$ resulting in altered of $[Ca^{2+}]i$ homeostasis. Kamphuis et al., (1989) and Silklos et al., (2000) demonstrated $[Ca^{2+}]i$ distribution in rat hippocampus and spinal and oculomotor neurons of superoxide dismutase (SOD1) knockout mice, respectively, using

the oxalate-pyroantimonate technique. There are no published reports in the field of MeHg toxicity studies to demonstrate calcium ion distribution in the neurons using oxalate-pyroantimonate technique.

Cerebellar granule cells from 1.0 mg/kg and 5.0 mg/kg MMC exposed mice showed a marked decrease in MMP when compared to control mouse granule cells (Figure 4A and B). Intracellular factors like $[Ca^{2+}]i$ and ROS levels or even damage of mitochondria by MMC exposure could result in decreased MMP (Limke and Atchison, 2002). Elevated ROS levels and altered $[Ca^{2+}]i$ homeostasis demonstrated in this study could be the cause of loss of MMP in MMC exposed mouse granule cells. Bernardi et al., (1993) and Scorrano et al., (1997) demonstrated loss of MMP due to opening of a megapore called the mitochondrial permeability transition pore (MTP) as a result of direct binding of MeHg or in response to elevated ROS levels or altered $[Ca^{2+}]i$ homeostasis.

Apoptosis is a process of cell death that is controlled by the dying cell itself (Hengartner, 2000; Reed, 2000). A cell dying due to apoptosis shows characteristic signs like cell shrinkage, nuclear pyknosis and DNA fragmentation (Kroemer, 1997; Mattson, 2000). Loss of MMP is thought to occur in most mammalian cell types before apoptotic cell death (Kroemer, 2002). Loss of MMP is usually associated with the release of mediators of apoptosis such as cytochrome C. Cytochrome C associates with an adaptor molecule apaf-1 and caspase 9 resulting in activation of caspase 3. To determine caspase 3 activation we immunolabelled frozen serial sagittal sections of cerebella with anti-activated caspase 3 antibody (Figure V-5A and B). Our results showed that the most

discussed pathway of apoptosis i.e., activation of caspase 3 is not occurring at the concentrations of MMC used in this study. To rule out the possibility of activation of other pathways of apoptosis, frozen serial sections of cerebella from control and MMC treated mice were stained for neuronal degeneration using Fluoro-Jade. Very few Fluoro-Jade positive cells were observed per section in all treatment groups (Figure V-6A). Consistent with our results Fonfria et al., (2002) demonstrated absence of caspase 3 activation in cultured cerebellar granule cells with MeHg exposure but showed a significant increase in the translocation of apoptosis inducing factor (AIF) into the nucleus. AIF is a mediator of apoptosis also released from the mitochondria following loss of MMP. AIF acts independently of the caspase cascade pathway by translocating into the nucleus leading to DNA degradation and chromatin condensation (Castoldi et al., 2000; Fonfria et al., 2002). However, we do not expect to observe activation of this pathway, as we have found no difference in the granule cell death using Fluoro-Jade staining in control and MMC treated mice.

Nagashima et al., (1996) reported the process of apoptosis in cerebellar granule cells of rats exposed to a total MeHg dose of 40 mg/kg body weight using electron microscopy. In our study we did not find granule cells showing apoptotic changes in any of the treatment groups using electron microscopy. We believe that the concentrations of MeHg used in our study were not sufficient to kill granule neurons at the time we examined but enough to disturb cellular homeostasis.

In conclusion, these results show that short term, low to moderate concentrations of MeHg exposure through the most common route of exposure (oral) could result in

subcellular changes in terms of oxidative stress, altered $[Ca^{2+}]i$ homeostasis and loss of MMP in cerebellar granule cells. But these changes are not severe enough to induce apoptotic cell death.

CHAPTER V

NEUROBEHAVIORAL AND SUBCELLULAR CHANGES IN AGED MICE EXPOSED TO METHYLMERCURY

SUMMARY

Male and female C57BL/6J mice between 16-20 months age were exposed orally to five divided doses totaling 5.0 mg/kg of methylmercuric chloride (MMC) or sterile deionized water in moistened rodent chow. After a five-day waiting period, experimental mice were subjected to a standard battery of behavior testing for balance and motor coordination. Significant differences were observed between control and MMC treated mice in the total distance traveled in the open field, angle of foot placement in foot print analysis and total number of mice falling off in vertical pole test. Eleven days after the last dose of MMC or vehicle cerebellar granule cells were isolated. Total cellular reactive oxygen species (ROS) levels were elevated in granule cells from MMC treated mice when compared to controls. Basal intracellular calcium ion ($[Ca^{2+}]i$) concentrations were not altered after MMC treatment. Mitochondrial membrane potential analysis indicated a significant reduction in granule cells from MMC treated mice. These results indicate that short term; moderate dose of MMC in aged mice can be lead to disruption of cellular homeostasis and alter motor coordination and balance.

INTRODUCTION

Increases in oxidative stress and mitochondrial insufficiency play a central role in normal CNS senescence and age related neurodegenerative disorders including toxicant induced disorders. The phenomenon of aging is marked by progressive decline in the efficiency of physiological processes. The CNS is a critical organ for MeHg toxicity (Bakir et al., 1973). In adults, symptoms include weight loss, paresthesia, concentric constriction of visual fields and ataxia (Bakir et al., 1973). Human exposure (Kinjo et al., 1993) and animal studies (Rice, 1996; 1998) provide convincing evidence that developmental methylmercury exposure results in marked behavior effects during adulthood and aging. Harada (1995) reported a decline in simple activities of daily living such as getting dressed or washing in adult victims of Minamata disease, as they aged.

Most of the early studies (acute and chronic) using rodents examined neurobehavioral changes between 6-16 weeks of age following developmental exposure (Dore et al., 2001; Goulet et al., 2003; Inouye et al., 1985; Kakita et al., 2000; Kim et al., 2000; Newland and Rasmussen, 2000; Newland et al., 2004; Pereira et al., 1999; Rasmussen and Newland, 2001; Vicente et al., 2004; Watanabe et al., 1999; Yin et al., 1997). However little is known about the behavioral effects of MeHg exposure on aged individuals who could be potentially exposed to MeHg through the environment or by consumption of fish contaminated with MeHg.

MeHg is widely implicated as a cause of oxidative stress (Usuki et al., 2001; Gasso et al., 2001), alteration in $[Ca^{2+}]_i$ homeostasis (Atchison and Hare, 1994; Denny and Atchison, 1996; Castolidi et al., 2000) and opening of the MTP leading to apoptotic cell

death (Limke and Atchison, 2002; Limke et al, 2003). Most of these studies were either performed using immortalized cell lines or primary granule cell cultures. The aging nervous system is already subject to oxidative stress and mitochondrial insufficiency due to natural senescence processes. A potent neurotoxicant like MeHg also predominantly exerts its toxic effects through the same pathways as normal senescence resulting in deterioration the CNS. It would be interesting to examine the extent of toxic effects exerted by MeHg on the aging nervous system.

In the present study, male and female C57BL/6J mice at 16-20 months of age were exposed to MeHg via food using a total dose of 5.0 mg/kg body weight. They were compared with age matched control (given vehicle only) mice for behavior changes. In addition, the granule cells were acutely isolated to assess subcellular changes occurring due to normal aging process (controls) and compare those changes with MeHg treated mice.

MATERIALS AND METHODS

Subjects

C57BL/6J wild type (+/+) mice were originally obtained from The Jackson Laboratory (Bar Harbor, MA, USA) and a breeding colony was established at Texas A&M University in the laboratory of Dr. Louise C. Abbott. Male and female C57BL/6J: +/+ mice aged between 16-20 months were used in this study. A total of 45 mice, including 19 male and 26 female mice were used in the different experimental protocols. All mice were housed at the Laboratory Animal Research and Resource building, Texas

A&M University, in a constant temperature (21-22°C) and constant humidity (45-50%) room with a 12-hour light-dark cycle. All mice were housed individually for the duration of training, dosing and behavior testing. All procedures were carried out in accordance with the National Institutes of Health Guide for the Care and Use of Laboratory Animals (National Institutes of Health Publication No. 85-23, revised 1996).

Chemicals

Methylmercuric chloride (MMC; 95% purity) was obtained from Alfa Aesar (Ward Hill, MA, USA). A stock solution of 1.0 mg/ml MMC was prepared by dissolving in sterile deionized water and further diluted to 0.5 mg/ml with sterile, deionized water for addition to food. All MMC solutions were stored at 4ºC until used. Fluorescent dyes (TMRM, CM-H_2DCFDA and Fura-2AM) were obtained from Molecular Probes (Eugene, OR).

Dosing

The aged (16-20 months) mice were first trained to eat moistened rodent chow for five days as described earlier by Bellum et al (2005, in press). Briefly, starting on day one, all mice received 2.0 g moistened rodent chow daily for five consecutive days. Starting on day six the mice were divided into two treatment groups (control and 5.0 mg/kg MMC). The treated mice received 1.0 mg/kg MMC in 2.0 g of moistened rodent chow for five consecutive days to achieve a total dose of 5.0 mg/kg body weight. During this same five day period control mice received only vehicle (0.1 ml sterile

deionized water) in 2.0 g moistened rodent chow. The mice were given the moistened rodent chow with MMC or vehicle only during the dark phase of light:dark cycle and had access to dry rodent chow *ad libitum* only during the light phase of the light:dark cycle. All mice had access to water 24 hours every day.

Behavior testing

Behavioral assessments began on control (n=20) and 5.0 mg/kg MMC (n=25) treated mice six days after the final day of dosing. A series of behavior tests for coordination and exploration were used. First, the rota-rod was performed on days six, seven and eight after cessation of exposure to MMC or vehicle. Activity in the open field, which assessed horizontal and vertical exploration of a novel environment, was measured on days nine and 10. Foot placement and the vertical pole test were performed on day 11.

Rota-rod

The accelerating rota-rod, model 7650 (UGO Basile, Comerio, VA, Italy) was used to assess motor coordination in control and 5.0 mg/kg MMC treated mice. The rota-rod consisted of a knurled plastic rod (diameter = 3.0 cm; length = 30 cm) partitioned off with round plates into units of 4 cm in length in order to accommodate up to five mice simultaneously and to prevent escape from the sides. The rod was suspended at a height of 16 cm above five plastic levers attached to timers that stop as soon as the mice land on the levers. The rota-rod started rotating at 3 rpm and accelerated to 26 rpm over

duration of 3 min and then maintained a speed of 26 rpm. The mice were placed on the rod facing away from the experimenter. To avoid falling from the rod, mice had to walk in a forward direction as the rod turned. Starting on the sixth day after the mice received final dose of MMC or vehicle, the latency to falling from the rota-rod was measured for three consecutive days. Each mouse experienced four trials per day on the rota-rod with an intertrial interval of 10 minutes. The first 11 trials were considered training. The time each mouse spent before falling from the rota-rod on the fourth trial of third day was analyzed. Aged mice did not passively rotate with the rod as did the young adult mice and so the surface of the rod was not covered with smooth rubber tubing.

Activity in the open-field

The Versa Max system activity chamber (Accuscan Instruments, Inc., Columbus, OH) was used to assess horizontal and vertical exploration in control and 5.0 mg/kg MMC treated mice. The total distance traveled and rearing activity were recorded and analyzed as measures of horizontal and vertical exploration, respectively. Each activity chamber (42 X 42 cm) was made of Plexiglas (30 cm in height) and equipped with photocell beams that used x-, y- and z- coordinates to detect and digitally record horizontal and vertical movements. Each chamber was further divided into four equal compartments of (21 X 21 cm). Only two compartments (second of top row and first of bottom row) were used for testing in order to prevent overlap in beam pathways for mice being assessed simultaneously. The activity levels were recorded on consecutive days (nine and 10) after final day of dosing with either MMC or vehicle. Mice were always

placed in the same corner of the chamber in each trial and activity levels were recorded for 30 minutes on both days.

Foot print analysis

Foot print analysis was performed using a long (100 cm), narrow (width= 6.0 cm), plastic-coated walkway that was walled off at one end and on both sides. This test is useful in assessing subtle changes in motor coordination and balance. On day 11 after the final day of dosing with either MMC or vehicle, the hind paws of each experimental mouse were dipped in non-toxic glass paint and allowed to walk on a strip of paper placed on the floor of the walkway. The angle of foot placement (in degrees), stride length (in mm) and distance between the two hind feet (base stance, in mm) was measured.

Vertical pole test

The vertical pole test, which was modified from the method described in the literature, also was used to assess motor coordination and balance (Fernagut et al., 2003; Kurosaki et al., 2003; Matsuura et al., 1997). A 60 cm long 2.5 cm diameter plastic pipe with tape wound around it to provide adequate grip was used to perform the vertical pole test on control and 5.0 mg/kg MMC exposed mice. Initially, the pipe was held horizontally at a height of 50 cm above the surface of the counter that was padded with a soft cushion to prevent injuries from falling. Mice were placed approximately midway on the pole facing the end that was lifted up. Keeping one end of the pole stationary the

other end was lifted up to reach a 45-degree angle in 10 seconds. An additional 5 seconds was taken to shift the pole from 45 degrees to 90 degrees. Whether individual mice stayed on or fell off the pole during the 15 second testing period was recorded.

Acute isolation of cerebellar granule cells

Cerebellar granule cells were acutely isolated as described in Current Protocols in Toxicology (Oberdoerster, 2001). On the eleventh day after administration of the final dose of MMC, mice were anesthetized using isofluorane and killed by decapitation. The brain was removed from the cranial vault and the cerebellum separated from the rest of the brain. The meninges were gently teased away and the cerebellum was chopped in 6-8 pieces and transferred to a chilled 50ml falcon tube containing minimum essential medium with Earle's salts (MEM; Life Technologies inc., Rockville, MD) on ice. Cerebellar granule cells were isolated using dissociation medium containing MEM and 1.5U/ml protease (Sigma, St. Louis, MO) and plated onto cover slips coated with poly-D-lysine (Sigma, St. Louis, MO) or onto chambered slides.

Reactive oxygen species (ROS)

Cerebellar granule cells were acutely dissociated as described above, plated onto chambered slides and incubated in 95% O_2 and 5% CO_2 at 37°C for 25 minutes. The cells were loaded with an indicator dye, Chloromethyl-dihydrodichlorofluorescein diacetate (CM-H_2DCFDA) (Molecular Probes Inc., Eugene, OR) at a concentration of 500nmol and incubated in 95% O_2 and 5% CO_2 at 37°C for 8 minutes. CM-H_2DCFDA

is a redox-sensitive dye used to determine ROS levels. It is membrane permeable and gets trapped in cells by binding of the chloromethyl group to cellular thiols. Subsequently, the dye becomes fluorescent when oxidized by hydrogen peroxide and/or downstream free radical products of hydrogen peroxide. Sequential time course fluorescent image capturing was performed for 15 minutes using a 90 second interval with a 20X objective on an Olympus 1X-70 microscope and a Hamamatsu ORCA-ER cooled charge-coupled device camera at excitation and emission of 490nm and 520nm respectively. Image capturing and reactive oxygen species levels were analyzed using Simple PCI Version 5.0.0.1503 Compix Inc. and Imaging (Cranberry Township, PA).

Basal intracellular calcium ion levels

For basal intracellular calcium ion ($[Ca^{2+}]_i$) measurements, granule cells were acutely dissociated as described previously, plated onto chambered slides and incubated at 37°C for 20 minutes. The incubator was maintained at constant 95% oxygen and 5% carbon dioxide gas mixture. Cells were loaded with 5 μM Fura-2AM containing 20% pluronic acid and incubated at 37°C for 30 minutes. MEM media containing Fura-2AM was replaced by fresh MEM media and the cells were incubated at 37°C for an additional 30 minutes to allow complete de-esterification of the dye. The cells were exposed to dual excitation at 340 and 380 nm and fluorescence was monitored at 510 nm. Fluorescent images were acquired using 40X UV objective on an Olympus 1X-70 microscope and a Hamamatsu ORCA-ER cooled charge-coupled device camera. Image capturing and R-values were calculated using Simple PCI Version 5.0.0.1503 Compix

Inc. and Imaging System (Cranberry Township, PA). $[Ca^{2+}]_i$ was determined by the equation ($[Ca^{2+}]_i = K_D\ (F_{min}/F_{max})\ [(R - R_{min})/(R_{max} - R)]$, where R is the observed 340:380 fluorescence ratio and the dissociation constant (K_D) value used was 224. F_{min} and F_{max} 380 nm indicate fluorescence intensity at 380-wave length for minimum or 0 μmol and maximum calcium concentration respectively. R_{min} and R_{max} represent the ratio of F340/380 at minimum or 0 μmol and maximum calcium concentration respectively using a calibration kit (Molecular Probes Inc. Eugene, OR).

Mitochondrial membrane potential (MMP)

MMP was evaluated by using confocal fluorescence microscopy. Acutely dissociated cerebellar granule cells plated onto cover slips were incubated at 37°C in MEM for 25 minutes. Cells were loaded with an indicator dye, TMRM, at 150 nmol and further incubated in 95% O_2 and 5% CO_2 at 37°C for 15 minutes. TMRM is a lipophilic cation that accumulates in mitochondria in proportion to the mitochondrial membrane potential. Fluorescent images were acquired using a 40X oil objective on an Olympus 1X-70 microscope and a Hamamatsu ORCA-ER cooled charge-coupled device camera at excitation and emission of 555nm and 600nm respectively. Image capturing and membrane potential analysis were carried out using Simple PCI Version 5.0.0.1503 Compix Inc. and Imaging System (Cranberry Township PA).

Statistical analysis

A Chi-Square test was performed to analyze vertical pole test data. ROS data was analyzed using General Linear Model (GLM)-repeated measure analysis at $\alpha = 0.05$, using SPSS version 11.0 for Windows. Open field and foot print data were analyzed by GLM-Multivariate Analysis of Variance at $\alpha = 0.05$, using SPSS version 11.0 for Windows. Rota-rod, MMP and basal $[Ca^{2+}]i$ data were analyzed using GLM-Univariate Analysis of Variance at $\alpha = 0.05$, using SPSS version 11.0 for Windows. Significant differences among treatment and control groups were interpreted using the Tukey's honest significant difference (HSD) post hoc test.

RESULTS

Rota-rod performance

Figure V-1 shows the relative latency to falling exhibited by control and 5.0 mg/kg MMC exposed mice on the fourth trial of the third day of rota-rod testing. Overall, the ANOVA did not reveal any significant overall difference between control and MMC-treated mice, as the P value = 0.085. However, a significant treatment effect was observed (P = 0.012). No significant differences were observed between males and females (P = 0.134) and the interaction between treatment and gender (P = 0.243) also was not significant.

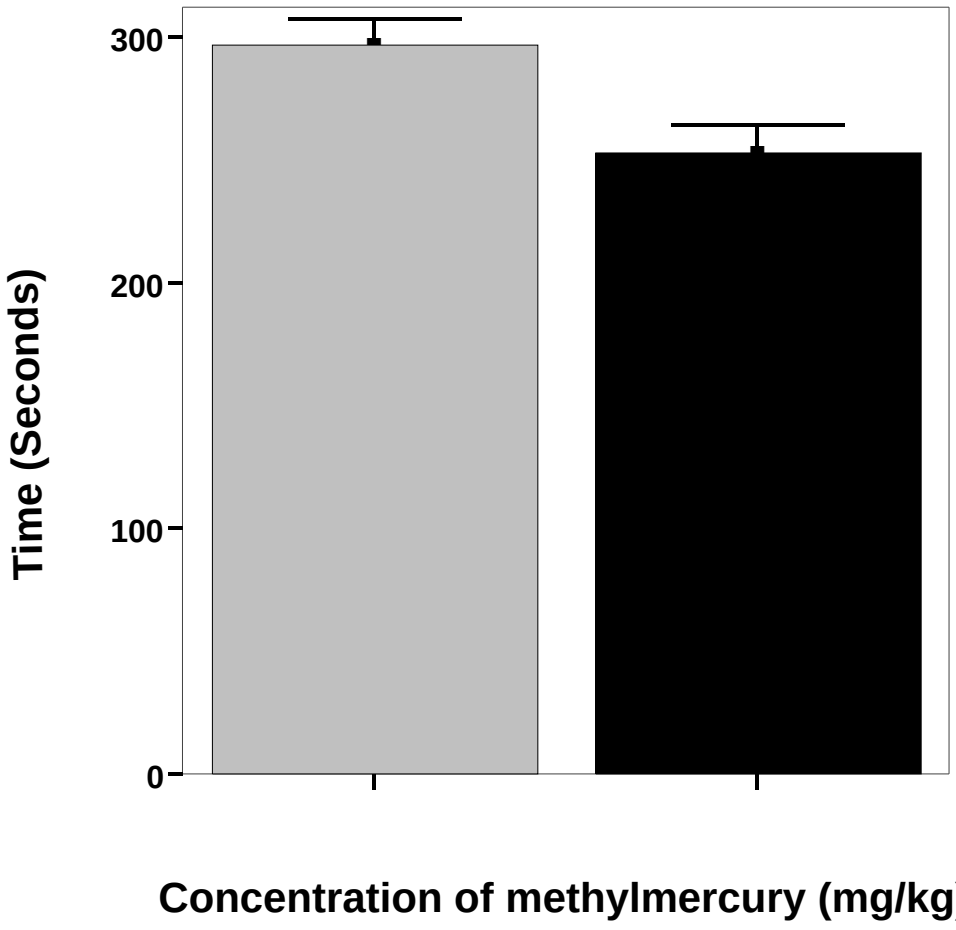

Figure V-1. Effects of MMC administration on cerebellar motor coordination in aged mice tested using accelerating rota-rod. Graph showing relative time spent on the accelerating rota-rod by control (n = 20) and 5.0 mg/kg MMC treated mice (n = 25) during trial four on the third day of testing. GLM-Univariate Analysis of Variance indicated no significant over all effect (P = 0.085) but showed a significant treatment effect (P = 0.012). Significant differences were not observed between males and females (P = 0.134) nor were there any significant interaction between treatment and gender (P = 0.243).

Open field activity

Preliminary assessment of motor activity or evaluation of gross abnormalities in locomotion can be identified during the first few minutes of test session in an open field (Crawley, 1999). We observed differences in the first five minutes of exploration when vehicle-treated mice were compared to 5.0 mg/kg MMC-treated mice. Figure V-2 shows total distance traveled and Figure V-3 shows rearing activity in the open field during the first five minutes of recording on day one for control, and MMC-treated mice. GLM Multivariate Analysis of Variance indicated a significant difference in total distance traveled ($P = 0.01$; Figure V-2), with the MMC-treated mice covering less total distance than control mice. There were no significant differences observed between males and females although there was a trend towards males covering more distance than females ($P = 0.057$). The interaction between MMC exposure and gender ($P = 0.125$) also did not reach significance. Rearing activity (Figure V-3) was not affected by MMC treatment ($P = 0.468$). Males and females did not differ in their responses ($P = 0.249$) nor were interaction effects observed during the first five-minute session on day one ($P = 0.404$).

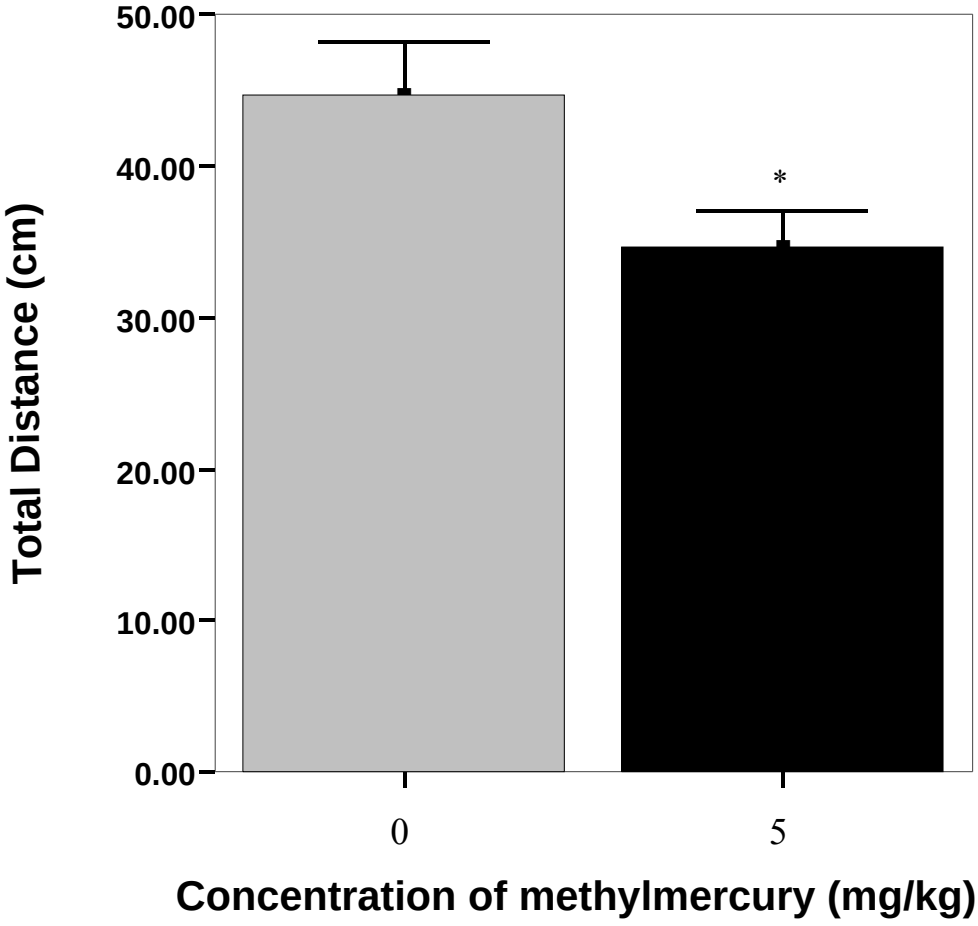

Figure V-2. Effect of MMC administration on horizontal activity level tested in aged mice in an open field chamber. Graphical representation of horizontal activity in the form of total distance traveled by control (n =20) and 5.0 mg/kg MMC treated mice (n = 25) observed during the first five minutes in the open field test. GLM-Multivariate Analysis of Variance indicated a significant difference in spontaneous locomotion (P = 0.01) between control and 5.0 mg/kg MMC treated mice (*).

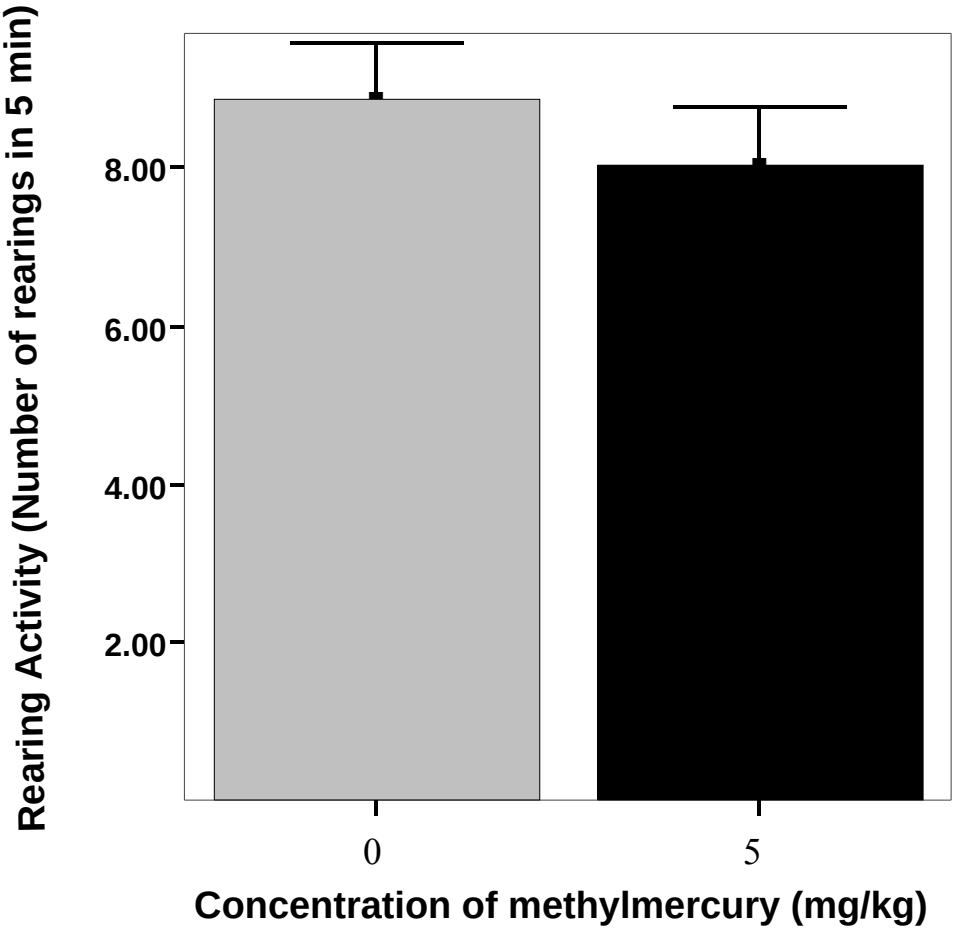

Figure V-3. Effect of MMC administration on vertical activity level tested in aged mice in an open field chamber. Graphical representation of rearing activity by control (n = 20) and 5.0 mg/kg MMC treated mice (n = 25) observed during the first five minutes in an open field test. GLM-Multivariate Analysis of Variance indicated no significant difference in rearing activity (P = 0.468) between the two groups of mice.

Foot print analysis

Figure V-4 summarizes the average angle of foot placement observed for control and 5.0 mg/kg MMC-treated mice. GLM-Multivariate Analysis of Variance indicated a significant difference between control and MMC-treated mice (P = 0.05), with the MMC-treated mice exhibiting a significantly larger angle of foot placement when compared to control mice. No gender effect was observed (P = 0.245) nor was any interaction effect between the MMC treatment and gender observed (P = 0.349). The stride length (P = 0.772) and base stance (i.e., distance between two hind paws (P = 0.568) also did not differ between control and MMC exposed mice (Figure V-5).

Vertical pole test

Table V-1 summarizes results from the vertical pole test between control and MMC exposed mice. A Chi-Square test indicated a significant difference existed between control and MeHg-treated mice at $\alpha = 0.05$ (Chi-Square calculated value = 6.51; Chi-Square table value = 5.991 at 4 degrees of freedom). The Chi-Square test performed with mice combined into male and female groups showed no significant difference (Chi-Square calculated value = 8.32; Chi-Square table value = 12.59 at $\alpha = 0.05$ and 6 degrees of freedom).

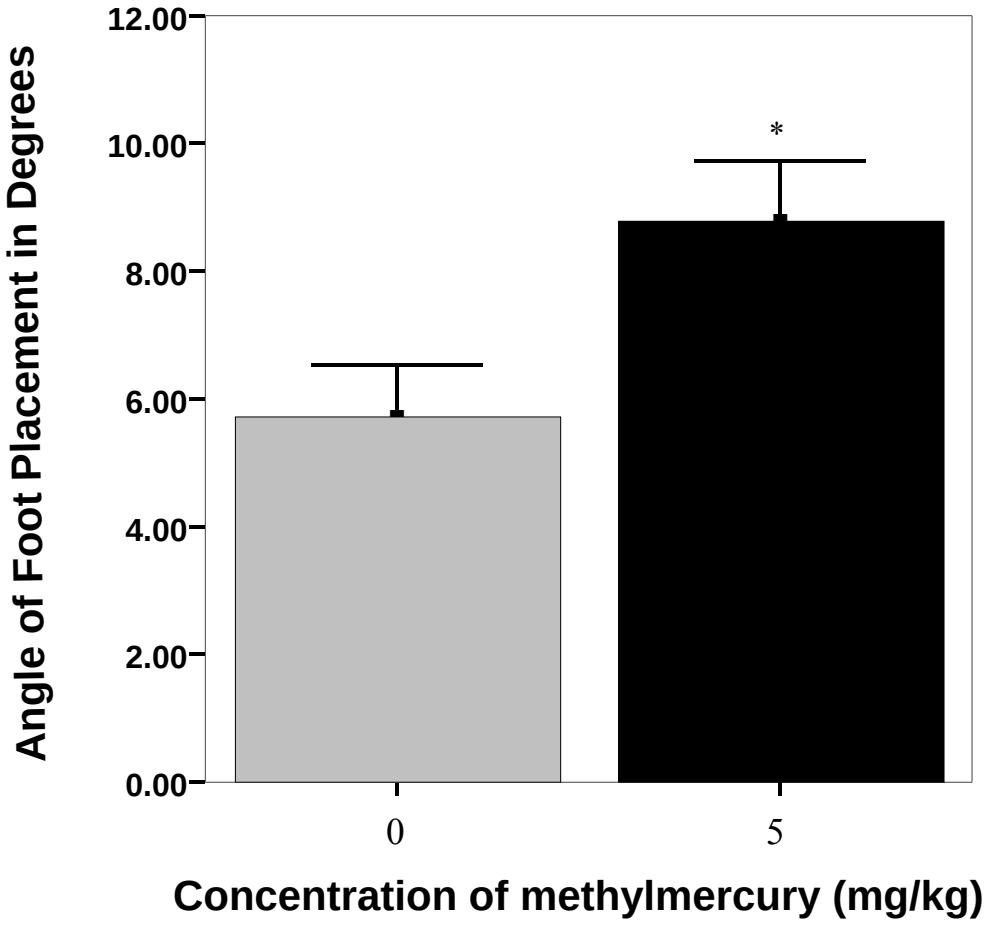

Figure V-4. Graph showing average angle of foot placement observed in the foot print analysis of control and MMC-treated aged mice. GLM-Multivariate Analysis of Variance indicated a significant difference between control and 5.0 mg/kg MMC treated mice (P= 0.05, *).

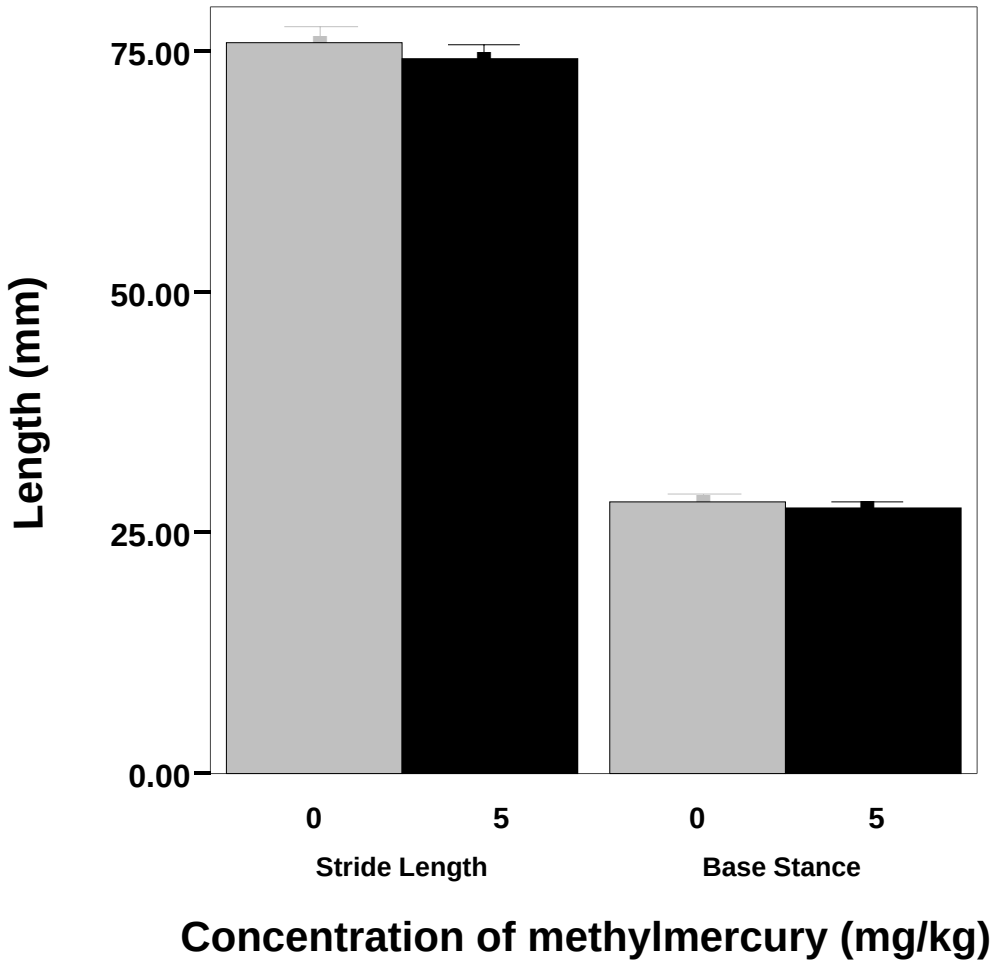

Figure V-5. Graph revealing average stride length and base stance observed in the foot print analysis of control and MMC treated aged mice. GLM-Multivariate Analysis of Variance indicated no significant difference in stride length (P = 0.772) and base stance (P = 0.568) between 0 mg/kg and 5.0 mg/kg MMC treated mice, between males and females (Stride length, P = 0.913; Base stance, P = 0.603) or interaction between gender and treatment (Stride length, P = 0.494; Base stance, P = 0.302).

Table V-1. Relative frequency of falling exhibited by 0 mg/kg and 5.0 mg/kg MMC treated aged mice subjected to vertical pole test. Chi-Square test indicated a significant difference between control and 5.0 mg/kg MMC treated mice at $\alpha = 0.05$ (Chi-Square calculated value = 6.51; Chi-Square table value at 2 degrees of freedom = 5.991).

Treatment MeHg (mg/kg)	Body wt. (gm)	Did not fall	Fell at/or before 45°	Fell between 45° and 90°	Total number of mice in each group
Control	37.96	12	0	2	14
5.0	39.04	7	1	9	17

Reactive oxygen species

Figure V-6A and B shows photomicrographs and graphical representation of the relative mean total cellular ROS levels of cerebellar granule cells from control and 5.0 mg/kg MMC-treated mice based on analysis of the intensity of fluorescence of CM-H_2DCFDA dye respectively. GLM-Multivariate Analysis of Variance (three-way ANOVA) indicated an overall significant difference between control and MMC-treated mice ($P<0.001$). The GLM-Repeated measure test also indicated a significant treatment effect ($P < 0.001$). Significant differences were not observed between males and females ($P = 0.120$), nor were there any significant interaction between treatment and gender ($P = 0.169$). GLM-Multivariate Analysis of Variance and the Tukey's HSD post hoc test indicated a significant difference ($P < 0.05$) starting with the fourth measurement (*) and the subsequent six consecutive measurements also were significantly different when control mice were compared to MMC-treated mice.

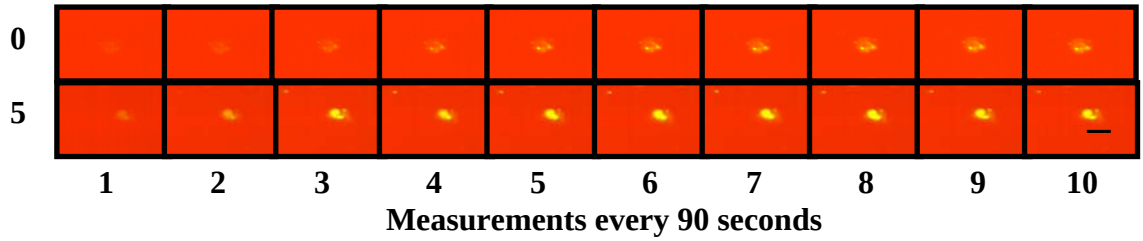

Figure V-6A. Photomicrographs showing acutely isolated cerebellar granule cells from aged mice loaded with CM-H_2DCFDA dye. Images of granule cells from control (0), and 5.0 mg/kg (5) MMC treated mice loaded with CM-H_2DCFDA showing fluorescence (green) in proportion to the total cellular ROS generated. Scale bar in 10 = 10 microns

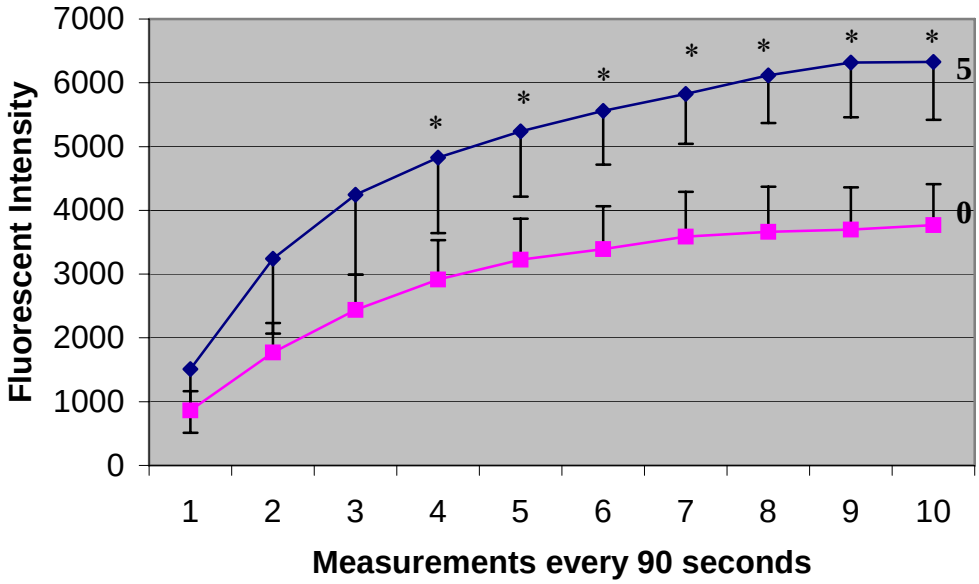

Figure V-6B. Effects of MMC administration on total cellular ROS levels in granule cells of aged control and MMC treated mice. Graph revealing relative mean total cellular ROS of granule cells from control (0; n = 6) and 5.0 mg/kg (5; n = 6) MMC treated mice based on analysis of the intensity of fluorescence of CM-H_2DCFDA dye. GLM-Multivariate Analysis of Variance (3-way ANOVA) and GLM-Repeated measure test indicated a significant difference ($P < 0.001$). GLM-Multivariate Analysis of Variance

and Tukey's HSD post hoc test indicated a significant difference ($P < 0.05$) from the fourth measurement (*).

Basal intracellular calcium

Figure V-7 summarizes the relative mean basal $[Ca^{2+}]i$ levels (in terms of the corrected "r" value) in cerebellar granule cells from control and 5.0 mg/kg MMC exposed mice based on the analysis of fluorescence intensity at 510 nm. In terms of nmol concentration average basal $[Ca^{2+}]i$ concentrations were found to be 99.9 and 105.32 nmols respectively for control and 5.0 mg/kg MMC exposed mice cerebellar granule cells. GLM-Univariate Analysis of Variance indicated no significant difference in basal $[Ca^{2+}]i$ levels between control and MMC treated granule cells ($P = 0.66$). There were no significant treatment ($P = 0.511$), gender ($P = 0.67$) or interaction ($P = 0.67$) effects with respect to basal $[Ca^{2+}]i$ levels.

Mitochondrial membrane potential

Photomicrographs in Figure V-8A show granule cells with clusters of mitochondria (in red) in proportion to the accumulation of TMRM dye. Figure V-8B summarizes the relative mean mitochondrial membrane potential of cerebellar granule cells from control and 5.0 mg/kg MMC-treated mice based on analysis of fluorescence intensity of TMRM dye. GLM-Univariate Analysis of Variance indicated an overall significant difference between control and 5.0 mg/kg MMC-treated mice ($P = 0.007$). A significant difference was observed with respect to treatment ($P = 0.002$) but not between males and females ($P = 0.589$). There also was no significant interaction between treatment and gender ($P = 0.07$).

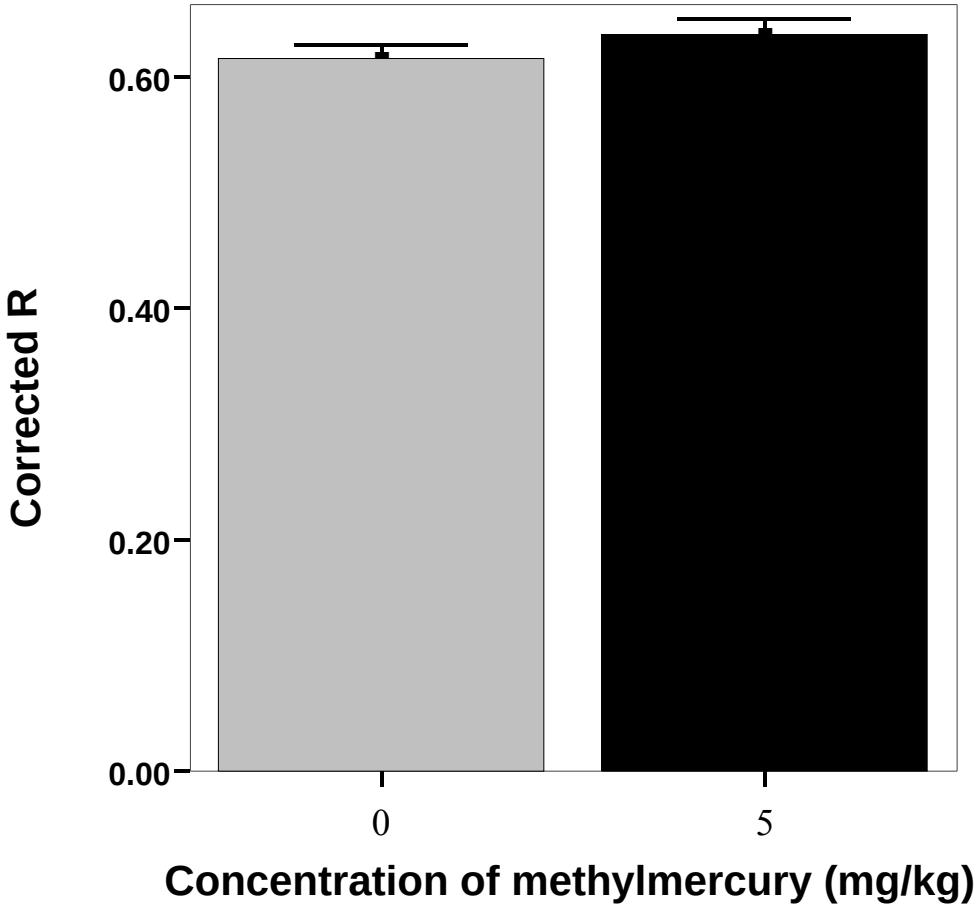

Figure V-7. The relative mean basal $[Ca^{2+}]i$ levels from granule cells in aged control and MMC treated mice. GLM-Univariate Analysis of Variance indicated no significant difference in the basal $[Ca^{2+}]i$ levels between control and MMC exposed mice granule cells (P = 0.66).

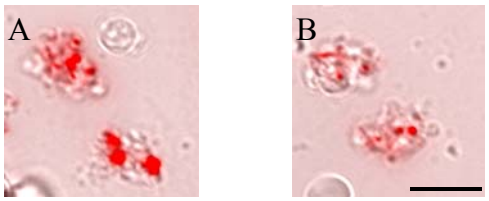

Figure V-8A. Photomicrographs showing acutely isolated cerebellar granule cells from aged mice loaded with TMRM dye. Fluorescent images of granule cells from control (A) and 5.0 mg/kg (B) MMC treated mice show clusters of mitochondria (red) that are TMRM dye loaded in proportion to the membrane potential. Scale bar in B = 10 microns.

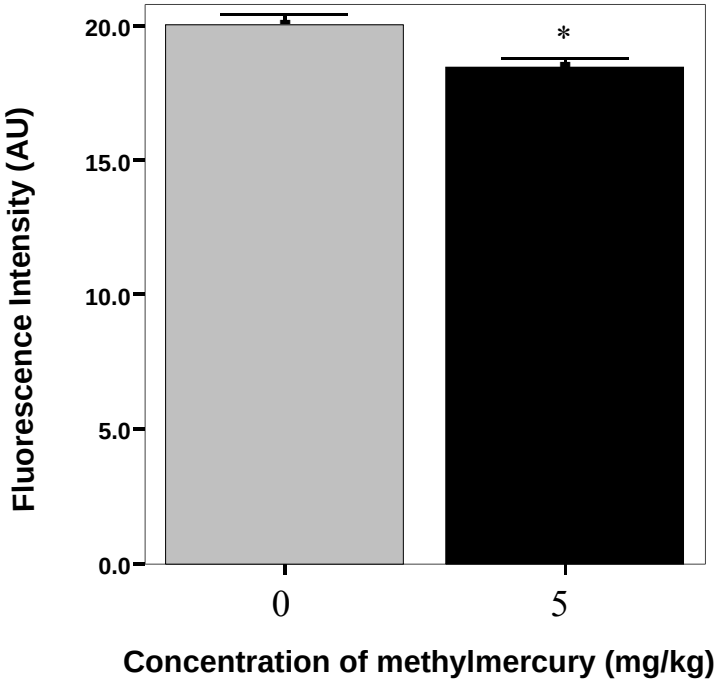

Figure V-8B. Effects of mercury treatment on mitochondrial membrane potential of cerebellar granule cells from aged mice. GLM-Univariate Analysis of Variance indicated a significant difference between control (n = 6) and 5.0 mg/kg MMC treated mice (n = 6) (P = 0.007). Significant differences were observed with respect to treatment (P = 0.002) but not between males and females (P = 0.589) or interaction between treatment and gender (P = 0.07).

DISCUSSION

The increased susceptibility of the aging nervous system to damage as a result of exposure to potent environmental toxicants like MeHg largely depends upon the reduced capacity of the CNS to withstand the toxic insult. Therefore, the objectives of this investigation were two fold. The first objective was to observe changes in behavior and/or motor coordination as a consequence of MMC exposure in aged mice. The second objective was to determine the subcellular changes in cerebellar granule cells associated with *in vivo* MMC exposure in the same mice.

We monitored behavior changes in aged mice exposed to 5.0 mg/kg MMC and compared these changes with age matched control mice. Performance on the rota-rod on the fourth trial of third day was not statistically significant (Figure V-1). However, the MMC exposed mice showed a tendency to fall from the accelerating rota-rod earlier than the control mice. Dore et al., (2001) tested the performance of mice prenatally exposed to 4.0 or 6.0 mg/kg MMC at 16 weeks of age at a constant speed of 20 rpm and found no differences in their performance when compared to control mice. In another experiment Goulet et al (2003) found no differences in the rota-rod performances of mice at 12 weeks of age that were chronically exposed to MMC in drinking water at 4, 6 and 8 ppm during fetal and early postnatal development. Both experiments compared the prenatal effects of MeHg exposure at 12 to 16 weeks of age but in our experiments we have exposed the mice at 16-20 weeks of age to test the acute effects of MeHg using an accelerating rota-rod. Activity in the open field was performed for 30 minutes on two consecutive days but first 5 minutes data was analyzed and compared. As described in

chapter III, we measured the locomotor activity of mice exposed to novel environment in terms of horizontal and vertical exploration. Mice that show deficits in motor movements might become restricted in terms of one or both exploratory movements and therefore, might show reduced activity. In our study, open field behavior testing revealed a statistically significant decrease in horizontal exploration in MeHg exposed mice (Figure V-2). The data are consistent with other rodent studies reported in the literature that examined horizontal exploration (Dore et al., 2001; Goulet et al., 2003; Kim et al., 2000; Lown et al., 1977; Pereira et al., 1999; Su and Okita, 1976). However, it is important to note that in our experiments, mice were exposed to acute doses of MMC between 16-20 months of age. Most of the behavior studies cited in the literature were performed on mice and/or rats exposed to MMC during gestation and early postnatal periods and tested between 6-16 weeks of age (Dore et al., 2001; Goulet et al., 2003; Kim et al., 2000). On the other hand consistent with some studies (Dore et al., 2001; Goulet et al., 2003) and contrary to others (Baraldi et al., 2002; Kim et al., 2000; Lown et al., 1977; Morganti et al., 1976; Salvaterra et al., 1973) we did not see any significant difference in rearing activity between control mice and mice exposed MMC (Figure V-3).

Of the three parameters analyzed using the foot print test, angle of foot placement was found to be significantly greater in MMC treated mice when compared to the controls (Figure V-4). An interesting difference in dose effect is observed in the performance of aged mice when compared to young adult mice. While the young adult mice showed a tendency towards increased angle of foot in 5.0 mg/kg MMC treatment,

aged mice showed a statistically significant difference in the angle of foot placement. Similar to young adult mice, the two treatment groups in aged mice did not differ statistically in stride length and base stance between the two hind paws (Figure V-5).

The vertical pole test as described in chapter III, was modified to assess motor coordination and balance deficits as a result of MMC toxicity. Mice without any motor deficits, when placed on the pole in a horizontal position facing towards the end that will be lifted (keeping the other end stationary), should be able to hold on and move up the pole as it is raised from a horizontal to a vertical position and maintain balance. In our experiments, 2 mice out of 14 control and 10 mice out of 17 mice treated with 5.0 mg/kg MMC were not able to maintain balance and fell off the pole before the pole reached 90 degrees (Table V-1). Most of the control mice moved up the pole while the MMC treated mice remained in one place or tried to move down the pole as it was being raised. When compared to the performance of young adult mice (37%), the percentage of mice falling from the pole was higher in MMC treated aged mice (58%).

Results from a number of laboratories using cultured cerebellar granule cells (Ishibashi et al, 2004; Limke and Atchison, 2002; Limke et al, 2002; Marty and Atchison, 1997; Marty and Atchison, 1998; Mundy and Freudenrich, 2000; Yee and Choi, 1996) or immortalized cell lines (Belletti et al, 2002; Gatti et al, 2004) provide convincing evidence that generation of ROS is a key event in MeHg induced neurotoxicity. However, these results have not been successfully replicated using *in vivo* models, at least in the case of aged rodent models. In our study we treated mice aged between 16 – 20 months with a total dose of 5.0 mg/kg MMC orally via food, isolated

cerebellar granule cells 11 days after the final dose of MeHg, then measured ROS levels. Results from the time course analysis performed using the fluorescent dye, CM-H_2DCFDA, indicated a significant increase in ROS levels in MMC exposed cerebellar granule cells compared to control granule cells (Figure V-6A and B). Control cerebellar granule cells also exhibited increased ROS levels over the time course used in this study, but the magnitude of increase in MMC-treated granule cells was greater and differed significantly from control granule cells starting from the fourth measurement (Figure V-6A and B).

Previously, it was reported that MeHg could induce oxidative stress by interfering with the electron transport chain (Yee and Choi, 1996) or by altering $[Ca^{2+}]i$ homeostasis (Ishibashi et al, 2004; Marty and Atchison, 1997; Marty and Atchison, 1998). However, basal $[Ca^{2+}]i$ levels were not significantly altered in cerebellar granule cells from MMC-treated mice when compared to control granule cells (Figure V-7). Within many cells including neurons, mitochondria are actively involved in the regulation of $[Ca^{2+}]i$ homeostasis (Duchen, 1999; Nicholls and Budd, 2000). In both the aged CNS and in the young CNS, mitochondria can buffer excess $[Ca^{2+}]i$ and sequester accumulated Ca^{2+} for long periods of time (Vergun et al, 1999).

Several studies that have assessed basal $[Ca^{2+}]i$ levels in neurons from the aged CNS have reported elevated basal $[Ca^{2+}]i$ levels (Martinez-Serrano et al, 1992; Kirischuk and Verkhratsky, 1996). But a few others reported no changes in basal $[Ca^{2+}]i$ levels (Hartmann et al, 1996; Murchison and Griffith, 1998). Xiong et al, (2002) in his experiments using brain slices obtained from aged mice under normal conditions

demonstrated that aged neurons exhibit mitochondrial dysfunction associated with alterations in $[Ca^{2+}]i$ homeostasis. This alteration could be manifested as a decreased capacity to maintain stable basal $[Ca^{2+}]i$ or recover the resting calcium values after stimulation. The granule cells in our experiments are from mice aged between 16-20 months. It is possible that basal $[Ca^{2+}]i$ measured with Fura2AM was elevated due to aging and so the difference between control and MMC exposed mice granule cells was not apparent.

Using TMRM dye to assess mitochondrial membrane potentials (MMP), we found that MMP was decreased in cerebellar granule cells from 5.0 mg/kg MMC-treated mice when compared to control granule cells (Figure V-8A and B). This decrease in membrane potential could be due to the action of MMC on intracellular factors like $[Ca^{2+}]i$ and ROS levels or could be due to damage to mitochondria caused by MMC directly (Limke and Atchison, 2002). MeHg is known to bind intracellular organelles such as mitochondria with high affinity (Chang and Hartmann, 1972) resulting in disruption cellular functions including respiration, regulation and transport of ions, and protein synthesis (Levesque and Atchison, 1991; Yee and Choi, 1996). Because of this high affinity binding, it is postulated that MeHg could bind to a site on the mitochondrial transition pore (MTP) and induce changes in permeability transition, an event characterized by a loss of membrane potential (Scorrano et al, 1997). MTP is a megapore formed on the inner mitochondrial membrane in response to a variety of insults including oxidative stress, anoxia or elevation of Ca^{2+} within the mitochondrial matrix (Bernardi et al, 1993). In the open configuration, the MTP not only allows

passage of molecules ≥ 1.5kDa but also dissipates the proton gradient across the inner mitochondrial membrane. Loss of the proton gradient is correlated with the decrease in mitochondrial membrane potential (White and Reynolds, 1996; Trost and Lemasters, 1997). In a study using cultured cerebellar granule cells, Limke and Atchison (2002) found that MeHg irreversibly bound to the MTP, which resulted in irreversible mitochondrial depolarization.

In this study we have demonstrated a significant effect of MeHg on neurobehavioral function of mice aged between 16-20 months. A treatment effect was seen on rota-rod performance. In the open field, horizontal exploration was reduced. In foot print test the angle of foot placement was increased and pole test results indicated a significant number of falls from the pole by MMC exposed mice. In comparison to the performance of young adult mice, the aged mice showed severe deficits in behavior at 5.0 mg/kg MMC exposure. We have also demonstrated a significant elevation of ROS levels and loss of MMP in MMC exposed mice granule cells. The basal $[Ca^{2+}]i$ levels however were not affected by MMC treatment. Using PC12 cells as a neuronal model, Kruman and Mattson (1999) demonstrated a two- to three fold increase in cytosolic calcium ($[Ca^{2+}]_C$) within minutes of exposure to an apoptosis inducer (starosporine). The cells however returned to basal levels within 4 hours after exposure. In PC12 cells they have demonstrated that this initial increase in the $[Ca^{2+}]_C$ is followed by a delayed increase in mitochondrial calcium ($[Ca^{2+}]_M$), accumulation ROS and loss of mitochondrial membrane potential. The granule cells in our study are isolated from mice 11 days after final dose of MMC. Results clearly indicate an elevation in ROS levels and

loss of membrane potential. Since the elevation of free $[Ca^{2+}]_C$ levels is an early event and is accompanied by a return to basal levels, we might have missed this change due to the 11 day wait period. We speculate that this early increases in $[Ca^{2+}]_C$ may have been missed due to a 11 day wait period.

The present findings suggest that *in vivo* methylmercury exposure in aged mice could lead to alteration in cellular homeostasis and this alteration could result in an alteration in behavior. The amount of methylmercury administered in the present study may not be sufficient to kill neurons but sufficient enough to disturb neuronal function and result in neurobehavioral changes.

CHAPTER VI

CONCLUSIONS

SUMMARY

Methylmercury (MeHg) is a highly neurotoxic and environmentally ubiquitous contaminant known to exert its toxic effects on both the developing and mature central nervous system. In two major epidemics of MeHg poisoning (Japan and Iraq), the primary route of exposure was through ingestion of contaminated food. In both of these incidences neurological dysfunction, characterized by cerebellar ataxia, was the primary sign of exposure. MeHg poisoning affects the central and peripheral nervous systems. The pattern of damage is very specific and correlates well with observed symptoms. Within the central nervous system, the cerebellum is primarily affected because MeHg accumulates in all cell layers of the cerebellum including Purkinje, Golgi, granule, stellate and basket cells. However, granule cells are the most affected neurons and cerebellar ataxia observed in MeHg poisoning is primarily attributed to the loss of these neurons. Specific subcellular changes associated with MeHg toxicity within CNS have been identified by *in vitro* assays. Mice of two different age groups were used as *in vivo* models, to evaluate subcellular and behavior changes associated with MeHg toxicity. These models provide an excellent opportunity to correlate the effects observed in these experiments to environmentally relevant exposure levels experienced by humans.

Behavior changes associated with cerebellar dysfunction were investigated using a standard battery of behavior tests for motor coordination and balance viz., rota-rod,

activity chamber, foot print analysis and the vertical pole test. To understand the specific subcellular changes leading to granule cell death or dysfunction in MeHg exposed mice, fluorescent confocal microscopy was used to investigate ROS levels. Fluorescent and electron microscopy were used to explore the possibilities of alteration in cellular calcium homeostasis. MMP changes were analyzed using fluorescent microscopy. Possibilities of a mitochondrial pathway of apoptosis were explored using immunohistochemistry for activation of caspase 3. Fluoro-Jade staining was used to screen for dying cells in MeHg treated mouse cerebella and compared with control mouse cerebella.

The present results indicated an increase in ROS levels in cerebellar granule cells from MeHg treated young adult and aged mice. Increase in ROS could affect calcium homeostasis and together could result in opening of the mitochondrial permeability transition pore (MTP). Electron microscopy revealed an alteration of calcium ion homeostasis, increased calcium sequestered in the mitochondria in MeHg treated young adult mice granule cells. When basal cytosolic calcium ion levels were measured using Fura-2AM significant differences were not observed between MeHg treated and control mice aged between 16-20 months. Loss of MMP was observed in MeHg treated granule cells of young adult and aged mice. Immunohistochemistry did not indicate activation of caspase 3, which is dependent on the release of cytochrome C from the mitochondria. Investigation of granule cell death using Fluoro-Jade did not reveal a significant difference between control and MeHg treated mice. Behavior tests indicated a significant reduction in motor coordination and balance in both young adult and aged mice.

The pathways leading to neuronal cell death following *in vivo* exposure of mice to MeHg are poorly understood. Several *in vitro* studies have demonstrated that alteration in calcium ion homeostasis could lead to apoptotic cell death *via* a mitochondrial pathway. Although we demonstrated elevated levels of ROS and loss of MMP in MeHg exposed mouse cerebellar granule cells, it was interesting to note that the most discussed pathway of apoptotic cell death i.e., through activation of caspase 3, did not occur in these cells. Also it is possible that the levels of MeHg used in our experiments might be high enough to disturb cellular homeostasis but might not be sufficient to trigger cell death as evidenced by Fluoro-Jade staining. However, MeHg at these levels could result in behavior changes as a result of disturbances in cellular homeostasis. The importance of the present investigation is that it provides new insights into the neurotoxic capabilities of *in vivo*, low dose oral MeHg exposure.

FUTURE STUDIES

At the concentrations of MeHg used in our study, there was clear evidence of subcellular changes in terms of elevated ROS and loss of MMP in both age groups of mice tested. These changes within cerebellar granule cells may not be sufficient to kill them at the time point tested, but certainly lead to behavior changes in terms of motor coordination and balance. It is possible that cell death as a result of MeHg toxicity has already occurred in the granule cells before the time point tested or there could be a delayed effect that would result in cell death at a later time point. To validate this hypothesis, cell death in granule cells at various time points after final dose of MeHg

should be tested. To address this hypothesis, mice can be killed at various time points starting from as early as 24 hours to 3-6 weeks after final dose. Immunohistochemical staining using anti-activated caspase 3 antibody and Fluoro-Jade staining can be performed on serial sagittal frozen sections of cerebella to determine possibility of early or delayed cell death due to MeHg toxicity.

On a broader perspective, apoptosis-related gene expression patterns in granule cells of mice exposed to the same doses of MeHg used in this study should be investigated using cDNA microarray analysis. Gene array technology can be used to carry out high throughput analysis to identify specific signaling pathways involved in MeHg-associated neuronal dysfunction and cell death. cDNA microarray analysis can be performed by extracting total RNA from cerebella of MeHg treated and control mice. Poly (A)+ mRNA can be isolated to generate ^{33}P-labeled cDNA and hybridized to the array. The array can then be exposed to film to perform autoradiography and generate quantitative information about gene expression patterns. The patterns of gene expression can be verified for mRNA expression using quantitative RT-PCR and western blotting or immunohistochemistry to verify changes in protein expression.

As was discussed in chapters IV and V, basal cytosolic calcium ion levels were not found to be elevated as evidenced by Fura-2AM analysis but alteration in calcium ion homeostasis was seen within the granule cells using electron microscopy. Mitochondria in the granule cells of mice exposed to the concentrations of MeHg used in this study may be buffering excess calcium ion in the cell and still carry out their functions relatively normal. It would be interesting to investigate the calcium ion

buffering capacity of the MeHg exposed granule cells in a depolarized state. To validate this hypothesis changes in free calcium ion concentrations upon depolarization of granule cells should be investigated. Intracellular calcium ion concentrations can be measured with Fura-2AM fluorescent dye as described in chapter V. In addition to the technique described in chapter V, after the dye-loading step granule cells should be exposed to a known depolarizing agent such as potassium chloride (KCl).

Loss of MMP is usually accompanied by depletion of intracellular ATP levels. To validate this hypothesis, ATP measurements can be performed in acutely isolated cerebellar granule cells (as described previously) using a bioluminescence assay kit HSII as described by Gatti et al., (2004).

REFERENCES

Abbott LC, Jacobowitz DM (1995) Development of calretinin-immunoreactive unipolar brush-like cells and an efferent pathway to the embryonic and early postnatal mouse cerebellum. Anat Embryol (Berl) 191:541-559.

Aberg B, Ekman L, Falk R, Greitz U, Persson G, Snihs JO (1969) Metabolism of methylmercury (203Hg) compounds in man. Arch Environ Health 19:478-484.

Adams JM, Cory S (1998) The bcl-2 protein family: arbiters of cell survival. Science 281:1322-1326.

Akshoomoff N, Courchesne E (1992) A new role for the cerebellum in cognitive operations. Behav Neurosci 106:731-738.

Ali SF, LeBel CP, Bondy SC, (1992) Reactive oxygen species formation as a biomarker of methylmercury and trimethyltin neurotoxicity. NeuroToxicology 13:637-648.

Allen JW, Shanker G, Aschner M (2001) Methylmercury inhibits the in vitro uptake of the glutathione precursor, cysteine, in astrocytes but not in neurons. Brain Res 891:148-157.

Allen JW, Shanker G, Tan KH, Aschner M (2002) The consequences of methylmercury exposure on interactive functions between astrocytes and neurons. NeuroToxicology 23:755-759.

Altman J (1972) Postnatal development of the cerebellar cortex in the rat. II. Phases in the maturation of Purkinje cells and of the molecular layer. J Comp Neurol 145:399-463.

Altman J, Bayer SA (1987) Development of the precerebellar nuclei in the rat: IV. The anterior precerebellar extramural migratory stream and the nucleus reticularis tegmenti pontis and the basal pontine gray. J Comp Neurol 257:529-552.

Altman J, Bayer SA (1997) Basic cellular organization and circuitry of the cerebellar cortex. In: Development of the cerebellar system (Altman J, Bayer SA, eds), pp 27-43, Boca Raton, Florida: CRC Press.

Amin-Zaki L, Elhassani S, Majeed MA, Clarkson TW, Doherty RA, Greenwood M (1974) Intra-uterine methylmercury poisoning in Iraq. Pediatrics 54:587-595.

Andressen C, Blumke I, Celio MR (1993) Calcium-binding proteins: selective markers of nerve cells. Cell Tissue Res 271: 281-208.

Arai N, Misugi K, Goshima Y (1990) Evaluation of a 1-metyl-4-phenyl-1,2,3,6-tetrahydropyridine (MPTP) - treated C57 black mouse model for parkinsonism. Brain Res 515:57-63.

Aschner M, Clarkson TW (1988) Uptake of methylmercury in the rat brain: effects of amino acids. Brain Res 462:31-39.

Aschner M, Eberle NB, Kimelberg HK (1991) Interactions of methylmercury with rat primary astrocyte cultures: methylmercury efflux. Brain Res 554:10-14.

Ashkenazi A, Dixit VM (1998) Death receptors: signaling and modulation. Science 281: 1305-1308.

Atchison WD (1986) Extracellular-dependent and independent effects of methylmercury on spontaneous and potassium evoked release of acetylcholine at the neuromuscular junction. J Pharmacol Exp Ther 237:672-680.

Atchison WD, Hare MF (1994) Mechanisms of methylmercury induced neurotoxicity. FASEB J 8:622-629.

ATSDR (1999) Toxicological profile for mercury. Atlanta, GA: Agency for Toxic Substances and Disease Registry.

Baimbridge KG, Celio MR, Rogers JH (1992) Calcium-binding proteins in the nervous system. Trends Neurosci 15:303-308.

Bakir F, Damulji SF, Amin-Zaki L, Murtadha M, Khalidi A, Clarkson TW, Smith JC (1973) Methylmercury poisoning in Iraq. Science 181:230-241.

Baraldi M, Zanoli P, Tascedda F, Blom JMC, Brunello N (2002) Cognitive deficits and changes in gene expression of NMDA receptors after prenatal methylmercury exposure. Environ. Health Perspect. 110:855 – 858 (Supplement).

Barja G (2002) Endogenous oxidative stress: relationship to ageing, longevity and caloric restriction. Ageing Res Rev 1:397-411.

Bearrs JJ, Limke TL, Atchison WD,(2001) Methylmercury (MeHg) causes calcium release from smooth endoplasmic reticulum (SER) inositol-1,4,5-triphosphate receptors in rat cerebellar granule neurons. The Toxicologist 60:184.

Belletti S, Orlandini G, Vettori MV, Mutti A, Uggeri J, Scandroglio R, Alinovi R, Gatti R (2002) Time course assessment of methylmercury effects on C6 Glioma cells: Submicromolar concentrations induce oxidative DNA damage and apoptosis. J Neurosci Res 70:703-711.

Bellum S, Thuett KA, Taylor RJ, Abbott LC (2005) Assessment of mercury concentrations in mouse brain using different routes of administration and different tissue preparations. Toxicol Mech Methods (In press).

Bennett MR, Farnell L, Gibson WG (2000) The probability of quantal secretion near a single calcium channel of an active zone. Biophys J 78:2201-2221.

Bernardi P, Veronese P, Petronilli V (1993) Modulation of the mitochondrial cyclosporine-A sensitive permeability transition pore. J Biol Chem 268:1005-1010.

Bernardi P, Colonna R, Costantini P, Eriksson O, Fontaine E, Ichas F, Massari S, Nicolli A, Petronilli V, Scorrano L (1998) The mitochondrial permeability transition. Biofactors 8:273-281.

Bernardi P, Scorrano L, Colonna R, Petronilli V, Di Lisa F (1999) Mitochondria and cell death. Mechanistic aspects and methodological issues. Eur J Biochem 264:687-701.

Berridge MJ (1998) Neuronal calcium signaling. Neuron 21:13-26

Berridge MJ, Lipp P, Bootman MD (2000) The versatility and universality of calcium signaling. Nat Rev Mol Cell Biol 1:11-21.

Boldin MP, Goncharov TM, Goltseve YV, Wallach D (1996) Involvement of MACH, a novel MORT1/FADD-interacting protease, in Fas/APO-1- and TNF receptor-induced cell death. Cell 85:803-815.

Brune D, Nordberg GF, Vesterberg O, Gerhardsson L, Wester PO (1991) A review of normal concentration of mercury in human blood. Sci Total Environ 100:235-282.

Carafoli E (2002) Calcium signaling: a tale for all seasons. Proc Natl Acad Sci USA 99:1115-1122.

Carter RJ, Llone LA, Humby T, Manglani L, Mahal A, Bates GP, Dunnett SB, Morton AJ (1999) Characterization of progressive motor deficits in mice transgenic for the human Huntington's disease mutation. J Neurosci 19:3248-3257.

Castoldi AF, Candura SM, Costa P, Manzo L, Costa LG (1996) Interaction of mercury compounds with muscarnic receptor subtypes in the rat brain. NeuroToxicology 17:735-741.

Castoldi AF, Barni S, Turin I, Gandini C, Manzo L (2000) Early acute necrosis, delayed apoptosis and cytoskeletal breakdown in cultured cerebellar granule neurons exposed to methylmercury. J Neurosci Res 59:775-787.

Catterall WA (2000) Structure and regulation of voltage-gated Ca2+ channels. Annu Rev Cell Dev Biol 16:521-555.

Celio MR (1990) Calbindin D-28k and parvalbumin in the rat nervous system. Neuroscience 35: 375-475.

Cernichiari E, Brewer R, Myers GJ, Marsh DO, Lapham LW, Cox C, Shamlaye CF, Berlin M, Davidson PW Clarkson TW (1995) Monitoring methylmercury during pregnancy: maternal hair predicts fetal brain exposure. Neurotoxicol 16:705-710.

Chan-Palay V, Palay SL, Brown JT, Van Itallie C (1977) Sagittal organization of olivocerebellar and reticulocerebellar projections: autoradiographic studies with 35S-methionine. Exp Brain Res 30:561-576.

Chang LW, Hartmann HA (1972) Electron microscopic and histochemical study on the localization and distribution of mercury in the nervous system after mercury intoxication. Exp Neurol 35:122-137.

Chang LW (1977) Neurotoxic effects of mercury. A review. Environ Res 14:329-373.

Chang LW (1997) Mercury related neurological syndromes and disorders. In: Mineral and metal neurotoxicology (Yasui M, Strong MJ, Ota K, Verity MA eds), pp 169-176, Boca Raton, Florida: CRC press.

Chang R (1991) Metallurgy and the chemistry of metals. In: Chemistry (Chang R ed), pp 853-856, New York: McGraw-Hill.

Charleston JS, Body RL, Bolender RP, Mottet NK, Vahter ME, Burbacher TM (1996) Changes in the number of astrocytes and microglia in the thalamus of the monkey Macaca fascicularis following long-term subclinical methylmercury exposure. NeuroToxicology 17:127-138.

Clarkson TW (2002) The three modern faces of mercury. Environ Health Perspect 110:11-23.

Coccini T, Randine G, Candura SM, Nappi RE, Prockop LD, Manzo L (2000) Low-level exposure to methylmercury modifies muscarnic cholinergic receptor binding characteristics in rat brain and lymphocytes: physiologic implications and new opportunities in biologic monitoring. Environ Health Perspect 108:29-33.

Cohen GM (1997) Caspases: the executioners of apoptosis. Biochem J 326:1-16.

Courchesne E, Townsend J, Saitoh O (1994) The brain in infantile autism: posterior fossa structures are abnormal. Neurology 44: 214-223.

Courtney MJ, Lambert JJ, Nicholls DG (1990) The interactions between plasma membrane depolarization and glutamate receptor activation in the regulation of cytoplasmic free calcium in cultured cerebellar granule cells. J Neurosci 10:3873-3879.

Crawley JN (1999) Behavioral phenotyping of transgenic and knockout mice. In: What's wrong with my mouse? (Crawley JN, ed) pp 48-49, New York: Wiley-Liss.

Crompton M, Costi A (1990) A heart mitochondrial pore with possible relevance to reperfusion injury. Biochem J 266:33-39.

Cryns V, Yuan J (1998) Proteases to die for. Genes Dev 12:1551-1570.

Daniel H, Levenes C, Crepel F (1998) Cellular mechanisms of cerebellar LTD. Trends Neurosci 21:401-407.

Davidson AM, Halestrap AP (1990) Partial inhibition by cyclosporine A of the swelling of liver mitochondria in vivo and in vitro induced by sub-micromolar [Ca^{2+}], but not by butyrate. Evidence for two distinct swelling mechanisms. Biochem J 268:147-152.

Davis LE, Kornfeld M, Mooney H, Fiedler KJ, Haaland KY, Orrison WW, Cernichiari E, Clarkson TW (1994) Methylmercury poisoning: long-term clinical, radiological, toxicological, and pathological studies of an affected family. Ann Neurol 35:680-688.

Denny MF, Hare MF, Atchison WD (1993) Methylmercury altars intrasynaptosomal concentrations of endogenous polyvalent cations. Toxicol Appl Pharmacol 122:222-232.

Denny MF, Atchison WD (1996) Mercurial-induced alteration in neuronal divalent cation homeostasis. NeuroToxicology 17:47-62.

Desclin JC (1974) Histological evidence supporting the inferior olive as the major source of cerebellar climbing fibers in the rat. Brain Res 77:365-384.

Dore FY, Goulet S, Gallager A, Harvey P-O, Cantin J-F, Aigle TD, Mirault M-E (2001) Neurobehavioral changes in mice treated with methylmercury at two different stages of fetal development. Neurotoxicol Teratol 23: 463-472.

Duchen MR, Biscoe TJ (1992) Mitochondrial function in type I cells isolated from the rabbit carotid body. J Physiol 450:13-31.

Duchen MR (1999) Contributions of mitochondria to animal physiology: from homeostatic sensor to calcium signaling and cell death. J Physiol 516:1-17.

Duchen MR (2004) Mitochondria in health and disease: perspectives on a new mitochondrial biology. Mol Asp Med 25:365-451.

Duguez S, Feasson L, Denis C, Freyssenet D (2002) Mitochondrial biogenesis during skeletal muscle regeneration. Am J Physiol Endocrinol Metab 282:E802-E809.

Eccles JC, Llinas R, Sasaki K (1964) Excitation of cerebellar Purkinje cells by the climbing fibers. Nature 203:245-246.

Eccles JC, Llinas R, Sasaki K (1966) The inhibitory interneurons within the cerebellar cortex. Exp Brain Res 1:1-16.

Eccles JC, Ito M, Szentagothai J (1967) The cerebellum as a neuronal machine. New York: Springer-Verlag.

Eisler R (2004) Mercury hazards from gold mining to humans, plants, and animals. Reviews of Environ Contamination and Toxicol 181:139-198.

Ekerot CF, Kano M (1985) Long-term depression of parallel fiber synapses following stimulation of climbing fibers. Brain Res 342:357-360.

Elsner J, Hodel B, Suter KE, Oelke D, Ulbrich B, Schreiner G, Cuomo V, Cagiano R, Rosengren LE, Karlsson JE, Haglid KG (1988) Detection limits of different approaches in behavioral teratology, and correlation of effects with neurochemical parameters. Neurotoxicol Teratol 10:155-167.

Ertel EA, Campbell KP, Harpold MM, Hofmann F, Mori Y, Perez-Reyes E, Schwartz A, Snutch TP, Tanabe T, Brinbaumer L, Tsien RW, Catterall WA (2000) Nomenclature of voltage-gated calcium channels. Neuron 25:533-535.

Feiz JA (1996) Cerebellar contributions to cognition. Neuron 16:13-15.

Fernagut P-O, Diguet E, Labattu B, Tlson F (2002) A simple method to measure stride length as an index of nigrostriatal dysfunction in mice. J Neurosci Methods 113:123-130.

Fernagut P-O, Chalon S, Diguet E, Guilloteau D, Tison F, Jaber M (2003) Motor behavior deficits and their histopathological and functional correlates in the nigrostriatal system of dopamine transporter knockout mice. Neuroscience 116:1123-1130.

Fitzgerald WF, Clarkson TW (1991) Mercury and monomethyl mercury: present and future concerns. Environ Health Perspect 96:159-166.

Floris A, Dino M, Jacobowitz DM, Mugnaini, E (1994) The unipolar brush cells of the rat cerebellar cortex and cochlear nucleus are calretinin-positive: a study by light and electron microscope immunocytochemistry. Anat Embryol 189:495-520.

Fonfria E, Dare E, Benelli M, Sunol C, Ceccatelli S (2002) Translocation of apoptosis-inducing factor in cerebellar granule cells exposed to neurotoxic agents inducing oxidative stress. Eur J Neurosci 16: 2013-2016.

Fox JH, Patel-Mandlik K, Cohen MM (1975) Comparative effects of organic and inorganic mercury on brain slice respiration and metabolism. J Neurochem 24:757-762.

Frank TC, Nunley MC, Sons HD, Ramon R, Abbott LC (2003) Fluoro-Jade identification of cerebellar granule cell and Purkinje cell death in the α_{1A} calcium ion channel mutant mouse, leaner. Neurosci 118:667-680.

Fridovich I (1978) The biology of oxygen radicals. Science 201:875-880.

Fujita S, Shimada M, Nakamura T (1966) H^3- thymidine autoradiographic studies on the cell proliferation and differentiation in the external and the internal granular layers of the mouse cerebellum. J Comp Neurol 128:191-208.

Fujita M, Takabatake E (1977) Mercury levels in human maternal and neonatal blood, hair and milk. Bull Environ Contam Toxicol 18:205-209.

Fujiyama J, Hirayama K, Yasutake A (1994) Mechanisms of methylmercury efflux from cultured astrocytes. Biochem Pharmacol 47:1525-1530.

Gaggi C, Zino F, Duccini M, Renzoni A (1996) Levels of mercury in scalp hair of fisherman and their families from Camara de Lobos-Madeira (Portugal): a preliminary study. Bull Environ Contam Toxicol 56:860-865.

Gasso S, Sunol C, Sanfeliu C, Rodriguez-Farre E, Cristofol RM (2000) Pharmacological characterization of the effects of methylmercury and mercuric chloride on spontaneous noradrenaline release from rat Hippocampal slices. Life Sci 67:1219-1231.

Gasso S, Cristofol RM, Selema G, Rosa R, Rodriguez-Farre E, Sanfeliu C (2001) Antioxidant compounds and Ca2+ pathway blockers differentially protect against methylmercury and mercuric chloride neurotoxicity. J Neurosci Res 66:135-145.

Gatti R, Belletti S, Uggeri J, Vettori MV, Mutti A, Scandroglio R, Orlandini G (2004) Methylmercury cytotoxicity in PC12 cells is mediated by primary glutathione depletion independent of excess reactive oxygen species generation. Toxicology 204:175-185.

Gerschenson LE, Rotello RJ (1992) Apoptosis: a different type of cell death. FASEB J 6:2450-2455.

Ghez C, Thach WT (2000) The cerebellum. In: Principles of neural science (Kandel ER, Schwartz JH, Jessell TM, eds), pp 823-852, New York: McGraw-Hill.

Gilbert PF (2001) An outline of brain function. Brain Res Cogn Brain Res 12:61-74.

Girard M, Dumont C (1995) Exposure of James Bay Cree to methylmercury during pregnancy for years 1983-91. Water Air Soil Pollut 80:13-19.

Glickstein M (1994) Cerebellar agenesis. Brain 117:1209-1212.

Golden TR, Hinerfeld DA, Melov S (2002) Oxidative stress and ageing: beyond correlation. Ageing Cell 1:117-123.

Goulet S, Dore FY, Mirault M-E (2003) Neurobehavioral changes in mice chronically exposed to methylmercury during fetal and early postnatal development. Neurotoxicol Teratol 25:335-347.

Grandjean P, Weihe PJ, Jorgensen RF, Clarkson T, Cernichiari E, Videro T (1992) Impact of maternal seafood diet on fetal exposure to mercury, selenium, and lead. Arch Environ Health 47:185-195.

Grandjean P, Weihe PJ (1998) A new era of mercury hazards. Environ Res 77:67.

Gray EG (1961) The granule cells, mossy synapses and Purkinje spine synapses of the cerebellum: light and electron microscopic observations. J Anat 95:345-356.

Green DR, Reed JC (1998) Mitochondria and apoptosis. Science 281:1309-1312.

Gunter TE, Buntinas L, Sparagna G, Eliseev R, Gunter K (2000) Mitochondrial calcium transport: mechanisms and functions. Cell Calcium 28:285-296.

Hammers FPT, Lankhorst AJ, Laar TLV, Veldhuis WB, Gisper WH (2001) Automated quantitative gait analysis during over ground locomotion in the rat: its application to spinal cord contusion and transaction injuries. J Neurotrauma 18:187-201.

Hamori J and Szentagothai J (1966) Identification under electron microscope of climbing fibers and their synaptic contacts. Exp Brain Res 1:65-81.

Harada M (1977) Congenital Minamata disease. Intrauterine methylmercury poisoning. Teratol 18:285.

Harada M (1995) Minamata disease: Methylmercury poisoning in Japan caused by environmental pollution. Crit Rev Toxicol 10:1 – 24.

Hare MF, McGinnis KM, Atchison WD (1993) Methylmercury increases intracellular concentrations of Ca2+ and heavy metals in NG108-15 cells. J Pharmacol Exp Ther 266:1626-1635.

Hare MF, Atchison WD (1995a) Methylmercury mobilizes Ca2+ from intracellular stores sensitive to inositol 1,4,5-trophosphate in NG108-15 cells. J Pharmacol Exp Ther 272:1016-1023.

Hare MF, Atchison WD (1995b) Methylmercury increases Ca2+ influx through nifedipine- and tetrodotoxin-sensitive pathways in NG108-15 cells. Toxicol Appl Pharmacol 135:299-307.

Harman D (1956) Ageing: a theory based on free radical and radiation chemistry. J Gerontol 11:298-300.

Hartmann H, Eckert A, Velbinger K, Rewsin M, Muller WE (1996) Down-regulation of free intracellular calcium in dissociated brain cells of aged mice and rats. Life Sci 59:435-449

Hasel K.W, Sutcliffe JG (1990) Nucleotide sequence of a cDNA coding for mouse cyclophilin. Nucleic Acids Res 18:4019.

He L, Poblenz AT, Medrano CJ, Fox DA (2000) Lead and calcium produce rod photoreceptor transition pore. J Biol Chem 275:12175-12184.

Hecker LH, Allen HE, Dinman BD (1974) Heavy metals in acculturated and unacculturated population. Arch Environ Health 29:181-185.

Hedlund B, Bartfai T (1979) The importance of thiol- and disulfide groups in agonist and antagonist binding to the muscarnic receptor. Mol Pharmacol 15:531-544.

Hengartner MO (2000) The biochemistry of apoptosis. Nature 407:770-776.

Hirayama A, Yasutake A (1986) Sex and age differences in mercury distribution and excretion in methylmercury administered mice. J Toxicol Environ Health 18:49-60.

Horn R (2000) A new twist in the saga of charge movement in voltage-dependent ion channels. Neuron 25: 511-514.

Ichas F, Jouaville LS, Sidash SS, Mazat J-P, Holmuhamedov EL (1994) Mitochondrial calcium spiking: a transduction mechanism based on calcium-induced permeability transition involved in cell calcium signaling. FEBS Letters 348(2): 211-215.

Ichas F, Mazat J-P (1998) From calcium signaling to cell death: two conformations for the mitochondrial permeability transition pore. Switching from low- to high-conductance state. Biochim Biophys Acta 1366:33-50.

Imura N, Miura K, Inokawa M, Nakada S (1980) Mechanism of methylmercury cytotoxicity: by biochemical and morphological experiments using cultured cells. Toxicology 17:767-771.

Inouye M, Murao K, Kajiwara Y (1985) Behavioral and neuropathological effects of prenatal methylmercury exposure in mice. Neurobehav Toxicol Teratol 7:227-232.

InSug O, Datar S, Koch CJ, Shapiro IM, Shenker BJ (1997) Mercuric compounds inhibit human monocyte function by inducing apoptosis: evidence for formation of reactive oxygen species, development of mitochondrial membrane permeability transition and loss of reductive reserve. Toxicology 124:211-224.

Ishibashi TU, Oyama Y, Nakao h, Umebayashi C, Nishizaki Y, Tatsuishi T, Iwase K, Murao K, Seo H (2004) Effect of thimerosal, a preservative in vaccines, on intracellular Ca^{2+} concentration of rat cerebellar neurons. Toxicology 195:77-84.

Ito M (1984a) General introduction. In: The cerebellum and neural control (Ito M, ed), pp 1-10, New York: Raven Press.

Ito M (1984b) Purkinje cells: morphology and development. In: The cerebellum and neural control (Ito M, ed), pp 21-39, New York: Raven Press.

Ito M (1984c) Granule cells. In: The cerebellum and neural control (Ito M, ed), pp 74-85, New York: Raven Press.

Ito M (2000) Mechanisms of motor learning in the cerebellum. Brain Res 886:237-245.

Izquierdo I, Medina JH (1998) On brain lesions, the milkman and Sigmunda. Trends Neurosci 21:423-426.

Juang MS (1976) Depression of frog muscle contraction by methylmercuric chloride and mercuric chloride. Toxicol Appl Pharmacol 35:183-185.

Kakita K, Wakabayashi M, Su Y, Yoneoka M, Sakamoto F, Ikuta H, Takahashi (2000) Intrauterine methylmercury intoxication consequence of the inherent brain lesions and cognitive dysfunction in maturity. Brain Res 877:322-330.

Kamphuis W, Huisman E, Wadman WJ, Bergkamp FJ, Lopes Da Silva FH (1989) Transient increase of cytoplasmic calcium concentration in the rat hippocampus after kindling-induced seizures. An ultrastructural study with the oxalate-pyroantimonate technique. Neurosci 29:667-674.

Kass GE, Orrenius S (1999) Calcium signaling and cytotoxicity. Environ Health Perspect 107 (Suppl 1): 25-35.

Kawamata O, Kasama H, Omata S, Sugano H (1987) Decrease in protein phosphorylation in central and peripheral nervous tissues of methylmercury-treated rat. Arch Toxicol 59:346-352.

Kerper LE, Ballatori N, Clarkson TW (1992) Methylmercury transport across the blood brain barrier by an amino acid carrier. Am J Physiol 262: R761-R765.

Kerr FJR (1971) Shrinkage necrosis: a distinct mode of cellular death. J Pathol 97:557-562.

Kerr FJR, Wyllie AH, Currie AR (1972) Apoptosis: a basic biological phenomenon with wide-ranging implications in tissue kinetics. Br J Cancer 26:239-257.

Kershaw TG, Clarkson TW, Dhahir PH (1980) The relationship between blood brain levels and dose of methylmercury in man. Arch Environ Health 35:28-36.

Kidd VJ, Lahti JM, Teitz T (2000) Proteolytic regulation of apoptosis. Semin Cell Dev Biol 11:191-201.

Kim C-Y, Nakai K, Kasanuma Y, Satoh H (2000) Comparison of neurobehavioral changes in three inbred strains of mice prenatally exposed to methylmercury. Neurotoxicol Teratol 22:297-403.

Kinjo Y, Higashi H, Nakano A, Sakamoto M, Sakai R (1993) Profile of subjective complaints and activities of daily living among current patients with Minamata disease after 3 decades. Environ Res 63:241-251.

Kirischuk S, Verkhrasky A (1996) Calcium homeostasis in aged neurons. Life Sci 59:451-459.

Kluck RM, Bossy-Wetzel E, Green DR, Newmeyer DD (1997) The release of cytochrome c from mitochondria: a primary site for bcl-2 regulation of apoptosis. Science 275:1132-1136.

Komulainen H, Bondy SC (1987) Increased free intrasynaptosomal Ca^{2+} by neurotoxic organometals: distinctive mechanisms. Toxicol Appl Pharmacol 88:77-86.

Kosta L, Byrne AR, Zelenko V (1975) Correlation between selenium and mercury in man following exposure to inorganic mercury. Nature 254:238-239.

Kroemer G (1997) Mitochondrial implication in apoptosis. Towards an endosymbiont hypothesis of apoptosis evolution. Cell Death Differ 4:443-456.

Kroemer G (2002) Introduction: mitochondrial control of apoptosis. Biochim 84:103-104.

Kruman II, Mattson MP (1999) Pivotal role of mitochondrial calcium uptake in neural cell apoptosis and necrosis. J Neurochem 72:529-540.

Kuhnert PM, Kuhnert RM, Erhard P (1981) Comparison of mercury levels in maternal blood, fetal cord blood, and placental tissues. Am J Obstet Gynecol 139:209-213.

Kulkarni SK (1977) Open field test: its status in psychopharmacology. Ind J Pharmac 9: 241-246.

Kuntz WD, Pitkin RM, Bostrom AW, Hughes MS (1982) Maternal and cord blood background mercury levels. A longitudinal surveillance. Am J Obstet Gynecol 143:440-443.

Kurosaki R, Akasaka M, Michimata M, Matsubara M, Imai Y, Araki T (2003) Effects of Ca^{2+} antagonists on motor activity and the dopaminergic system in aged mice. Neurobiol Aging 24:315-319.

Kuznetsov DA, Zavijalov NV, Govorkov AV, Sibileva TM (1987) Methylmercury-induced nonselective blocking of phosphorylation processes as a possible cause of protein synthesis inhibition *in vitro* and *in vivo*. Toxicol Lett 36:153-160.

Lange W (1975) Cell number and cell density in the cerebellar cortex of man and some other mammals. Cell tissue Res 157: 115-124.

Larramendi EM, Victor T (1967) Programmed cell death: its possible contribution to neurotoxicity mediated by calcium channel antagonists. Brain Res 587:233-240.

Larsen WJ (1997) Development of the brain and cranial nerves. In: Human embryology (Larsen WJ, ed) pp 411-454, New York: Churchill Livingston.

LeBel CP, Ali SF, McKee M, Bondy SC (1990) Organometal-induced increases in oxygen reactive species: the potential of 2',7'-dichlorofluorescin diacetate as an index of neurotoxic damage. Toxicol Appl Pharmacol 104:17-24.

LeBel CP, Ali SF, Bondy SC (1992) Deferoxamine inhibits methylmercury-induced increases in reactive oxygen species formation in rat brain. Toxicol Appl Pharmacol 61:460-468.

Leiner H, Leiner A, Dow R (1991) The human cerebro-cerebellar system: its computing, cognitive and language skills. Behav Brain Res 44:113-128.

Levesque PC, Atchison WD (1988) Effect of alteration of nerve terminal Ca^{2+} regulation on increased spontaneous quantal release of acetylcholine by methylmercury. Toxicol Appl Pharmacol 94:55-65.

Levesque PC, Atchison WD (1991) Disruption of brain mitochondrial calcium sequestration by methylmercury. J Pharmacol Exp Ther 256:236-242.

Lewandowski TA, Ponce RA, Charleston JS. Hong S, Faustman EM (2003) Effect of methylmercury on midbrain cell proliferation during organogenesis: potential cross-species differences and implications for risk assessment. Toxicol Sci 75:124-133.

Lewit-Bentley A, Rety S (2000) EF- hand calcium-binding proteins. Curr Opin Struct Biol 10:637-643.

Leyson K, Morgan AJ (1991) An integrated study of the morphological and gross-elemental consequences of methylmercury intoxication in rats, with particular attention on the cerebellum. Scanning Microscopy 5:895-904.

Li P, Nijhawan D, Budihardjo I, Srinivasula SM, Ahmad M, Alnemri ES, Wang X (1997) Cytochrome C and dATP-dependent formation of Apaf-1/caspase-9 complex initiates an apoptotic protease cascade. Cell 91:479-489.

Limke TL, Atchison WD (2002) Acute exposure to methylmercury opens the mitochondrial permeability transition pore in rat cerebellar granule cells. Toxicol Appl Pharmacol 178:52-61.

Limke TL, Otero-Montanez JK, Atchison WD (2003) Evidence for interactions between intracellular calcium stores during methylmercury-induced intracellular calcium dysregulation in rat cerebellar granule neurons. J Pharmacol Exp Ther 304:949-958.

Limke TL, Heidemann SR, Atchison WD (2004) Disruption of intraneuronal divalent cation regulation by methylmercury: are specific targets involved in altered neuronal

development and cytotoxicity in methylmercury poisoning? NeuroToxicology 25:741-760.

Linnane AW, Zhang C, Baumer A, Nagley P (1992) Mitochondrial DNA mutation and the ageing process: bioenergy and pharmacological intervention. Mutat Res 275:195-208.

Lithgow T, van Driel R, Bertram JF, Strasser A (1994) The protein product of the oncogene bcl-2 is a component of the nuclear envelope, the endoplasmic reticulum and the outer mitochondrial membrane. Cell Growth Differ 5:411-417.

Liu X, Kim CN, Yang J, Jemmerson R, Wang X (1996) Induction of apoptotic program in cell-free extracts: requirement for DATP and cytochrome c. Cell 86:147-157.

Llinas R, Sugimori M, Silver RB (1995) The concept of calcium concentration microdomains in synaptic transmission. Neuropharmacol 34:1443-1451.

Lopez-Artiguez M, Grilo A, Martinez D, Soria ML, Nunez L, Ruano A, Moreno E, Gracia-Fuente F, Repetto M (1994) Mercury and methylmercury in population risk groups on the Atlantic coast of southern Spain. Arch Environ Contam Toxicol 27:415-419.

Lown BA, Morganti JB, Stineman CH, Massaro EJ (1977) Differential effects of acute methylmercury poisoning in the mouse arising from route of administration: LD50, tissue distribution and behavior. Gen Pharmac 8:97-101.

MacIntosh DL, Williams PL, Hunter DJ, Sampson LA, Morris SC, Willet WC, Rimm EB (1997) Evaluation of a food frequency questionnaire-food composition approach for estimating dietary intake of arsenic and methylmercury. Cancer Epidemiol Biomarkers Prev 6:1043-1050.

Magistretti PJ, Pellerin L, Rothman DL, Shulman RG (1999) Energy on demand. Science 283:496-497.

Mahaffey KR, Mergler D (1998) Blood levels of total and organic mercury of residents of the upper St. Lawrence River basin, Quebec: association with age, gender, and fish consumption. Environ Res 77:104-114.

Marani E, Voogd J (1979) The morphology of the mouse cerebellum. Acta Morphol Neerl Scand 17:33-52.

Marini AM, Strauss KI, Jacobowitz DM (1997) Calretinin-containing neurons in rat cerebellar granule cell cultures. Brain Res Bull 42:279-288.

Martin JH (1996) The cerebellum, In: Neuroanatomy (Martin, JH, ed), pp 291-322. Stamford, CT: Appleton & Lange.

Martinez-Serrano A, Blanco P, Satrustegui J (1992) Calcium binding to the cytosol and calcium extrusion mechanisms in intact synaptosomes and their alterations with aging. J Biol Chem 267:4672-2679.

Marty MS and Atchison WD (1997) Pathways mediating Ca2+ entry in rat cerebellar granule cells following in vitro exposure to methylmercury. Toxicol Appl Pharmacol 147:319-330.

Marty MS and Atchison WD (1998) Elevations in intracellular Ca2+ as a probable contributor to decreased viability in cerebellar granule cells following acute exposure to methylmercury. Toxicol Appl Pharmacol 150:98-105.

Massaro, EJ (1996) The developmental cytotoxicity of mercurials. In: Toxicology of metals (Chang, LW ed), pp1047-1082, Boca Raton, FL: CRC Press.

Matsumoto H, Takeuchi T (1965) Fetal Minamata disease: a neurological study of two cases of intrauterine intoxication by a methylmercury compound. J Neuropathol Exp Neurol 24:563-564.

Matsuura K, Kabuto H, Makino H, Ogawa N (1997) Pole test is a useful method for evaluating the mouse movement disorder caused by striatal dopamine depletion, J Nourosci Methods 73:45-48.

Mattson MP (2000) Apoptosis in neurodegenerative disorders. Nat Rev Mol Cell Biol 1: 120-129.

McCrea RA, Bishop GA, Kitai ST (1976) Intracellular staining of Purkinje cells and their axons with horse-radish peroxidase. Brain Res 118:132-136.

Meldolesi J, Pozzan T (1998) The endoplasmic reticulum Ca2+ store: a view from the lumen. Trends Biochem Sci 23:10-14.

Meldolesi J (2000) Rapidly exchanging Ca2+ stores in neurons: molecular, structural and functional properties. Prog Neurobiol 65:309-338.

Merry DE, Korsmeyer SJ (1997) Bcl-2 gene family in the nervous system. Ann Rev Neurosci 20:245-267.

Miale IL, Sidman RL (1961) An autoradiographic analysis of histogenesis in the mouse cerebellum. Exp Neurol 4:277-296.

Middleton FA, Strick PL (1998) The cerebellum: an overview. Trends Neurosci 21: 367-369.

Miura K, Suzuki K, Imura N (1978) Effects of methylmercury on mitotic mouse glioma cells. Environ Res 17:453-471.

Miura K, Inokawa M, Imura N (1984) Effects of methylmercury and some metal ions on microtubule networks in mouse glioma cells and in vitro tubulin polymerization. Toxicol Appl Pharmacol 73:218-231.

Miura K, Koide N, Himeno S, Nakagawa I, Imura N (1999) The involvement of microtubular disruption in methylmercury-induced apoptosis in neuronal and nonneuronal cell lines. Toxicol Appl Pharmacol 160:279-288.

Morganti JB, Lown BA, Salvaterra P, Massaro EJ (1976) Effects on open-field behavior of mice exposed to multiple doses of methylmercury. Gen Pharmac 7:41-44.

Mugnaini E, Floris A (1994) The unipolar brush cell: a neglected neuron of the mammalian cerebellar cortex. J Comp Neurol 339:174-180.

Mundy WR, Freudenrich TM (2000) Sensitivity of immature neurons in culture to metal-induced changes in reactive oxygen species and intracellular free calcium. NeuroToxicology 21:1135-1144.

Murchison D, Griffith WH (1998) Increased calcium buffering in basal forebrain neurons during aging. J Neurophysiol 80:350-364.

Muzio M, Chinnaiyan AM, Kischkel FC, O'Rourke K, Shevchenko A, Ni J, Scaffidi C, Bertz JD, Zhang M, Gentz R, Mann M, Krammer PH, Peter ME, Dixit VM (1996) Flice, a novel FADD-Homologous ICE/CED-3-like protease, is recruited to the CD95 (Fas/APO-1) death-inducing signaling complex. Cell 85:817-827.

Nagashima K, Fujii Y, Tsukamoto T, Nukuzuma S, Satoh M, Fujita M, Fujioka Y, Akagi H (1996) Apoptotic process of cerebellar degeneration in experimental methylmercury intoxication of rats. Acta Neuropathol 91:72-77.

Nakagawa T, Zhu H, Morishima N, Li E, Xu J, Yankner BA, Yuan J (2000) Caspase-12 mediates endoplasmic-reticulum-specific apoptosis and cytotoxicity by amyloid-beta. Nature 403:98-103.

Neustadt DG, Frostholm A, Rotter A (1988) Topographical distribution of muscarnic cholinergic receptors in the cerebellar cortex of the mouse, rat, guinea pig, and rabbit: a species comparison. J Comp Neurol 272:317-330.

Newland MC, Reile AP (1999) Blood and brain mercury levels after chronic gestational exposure to methylmercury in rats. Toxicol Sci 50:106-116.

Newland MC, Rasmussen EB (2000) Aging unmasks adverse effects of gestation exposure to methylmercury in rats. Neurotoxicol Teratol 22:819-828.

Newland MC, Reile PA, Langston JL (2004) Gestational exposure to methylmercury retards choice in transition in aging rats. Neurotoxicol Teratol 26:179-94.

Nicholls DG, Scott ID (1980) The regulation of brain mitochondrial calcium-ion transport. The role of ATP in the discrimination between kinetic and membrane-potential-dependent calcium-ion efflux mechanisms. Biochem J 186:833-839.

Nicholls DG, Budd SL (2000) Mitochondria and neuronal survival. Physiol Rev 80:315-360

Nielsen JB (1992) Toxicokinetics of mercuric chloride and methylmercuric chloride in mice. J Toxicol Environ Health 37:85-22.

Nierenberg DW, Nordgren RE, Chang MB, Siegler W, Blayney MG, Hochberg F, Toribara TY, Cernichiari E (1998) Delayed cerebellar disease and death after accidental exposure to dimethylmercury. N Eng J Med 338:1672-1675.

Norseth T, Clarkson TW (1970) Studies on the biotransformation of ^{203}Hg-labeled methylmercury chloride in rats. Arch. Environ. Health 21:717-727.

Oberdoerster J (2001) Isolation of cerebellar granule cells from Neonatal rats: In: Current protocols in toxicology (Maines MD, Costa LG, Hodgson E, Reed DJ, Sipes IG., eds) Unit 12.7, Hoboken, NJ: John Wiley and Sons.

Oertel WH (1993) Neurotransmitters in the cerebellum. Scientific aspects and clinical relevance. Adv Neurol 61: 33-75.

Ohno Y, Ishida K, Ikeda K, Ishibashi T, Okada K, Nakamura M (1994) Evaluation of bradykinesia induction by SM-9018, a novel 5-HT2 and D2 receptor antagonist, using the mouse pole test. Pharmacol Biochem. Behav 49:19-23.

O'Kusky J (1983) Methylmercury poisoning of the developing nervous system: Morphological changes in neuronal mitochondria. Acta Neuropathol (Berl) 61:116-122. 15.

O'Leary JL, Smith JM, Inukai J, O'Leary M (1970) The inferior olive as a store of climbing fibers in the rat. Bibl Psychiatr 143:128-137.

O'Leary JL, Inukai J, Smith JM (1971) Histogenesis of the cerebellar climbing fiber in the rat. J Comp Neurol 142:377-391.

Oppenheim RW (1991) Cell death during development of the nervous system. Ann Rev Neurosci 14:453-501.

Oskarsson A, Schutz A, Skerfving S, Hallen, IP, Ohlin B, Lagerkvist BJ (1996) Total and inorganic mercury in breast milk and blood in relation to fish consumption and amalgam fillings in lactating women. Arch Environ Health 51:234-241.

Ottersen OP, Storm-Mathisen J (1984) Glutamate- and GABA-containing neurons in the mouse and rat brain, as demonstrated with a new immunocytochemical technique. L Comp Neurol 229:374-392.

Ottersen OP, Zhang N, Walberg F (1992) Metabolic compartmentation of glutamate and glutamine: morphological evidence obtained by quantitative immunocytochemistry in rat cerebellum. Neurosci 46:519-534.

Palkovits M, Magyar P, Szentagothai J (1971) Quantitative histological analysis of the cerebellar cortex in the cat. 3. Structural organization of the molecular layer. Brain Res 34:1-18.

Papa S, Skulachev VP (1997) Reactive oxygen species, mitochondria, apoptosis and aging. Moll Cell Biochem 174:305-319.

Parent A (1996) Cerebellum. In: Human neuroanatomy (Parent A, ed) pp 583-604. Philadelphia, PA: Williams and Wilkins Inc.

Pastorino JG, Tafani M, Rothman RJ, Marcinkeviciute A, Hoek JB, Farber JL (1999) Functional consequences of the sustained or transient activation by Bax of the mitochondrial permeability transition pore. J Biol Chem 274:31734-31739.

Paulin M (1993) The role of the cerebellum in motor control and perception. Brain Behav Evol 41:39-50.

Payne JN (1983) Axonal branching in the projections from precerebellar nuclei to the lobulus simplex of the rat's cerebellum investigated by retrograde fluorescent double labeling. J Comp Neurol 213:233-240.

Pearson HA, Sutton KG, Scott RH, Dolphin AC (1995) Calcium binding in the pore of L-type calcium channels modulates high affinity dihydropyridine binding. J Biol Chem 270: 18201-18204.

Pereira ME, Morsch VM, Christofari RS, Rocha JBT (1999) Methylmercury exposure during postnatal brain growth alters behavioral response to SCH 23390 in young rats. Bull Environ Contam Toxicol 63:256 – 262.

Perkins GA, Renken CW, Frey TG, Ellisman MH (2001) Membrane architecture of mitochondria in neurons of the central nervous system. J Neurosci Res 66:857-865.

Petronilli V, Nicolli A, Costantini P, Colonna R, Bernardi P (1994) Regulation of permeability transition pore, a voltage-dependent mitochondrial channel inhibited by cyclosporine A. Biochim Biophys Acta 1187:255-259.

Petronilli V, Penzo D, Scorrano L, Bernardi P, Di Lisa F (2001) The mitochondrial permeability transition, release of cytochrome c and cell death. Correlation with the duration of pore openings in situ. J Biol Chem 276: 12030-12034.

Portera-Cailliau C, Price DL, Martin LJ (1997a) Excitotoxic neuronal death in the immature brain is an apoptosis-necrosis morphological continuum. J Comp Neurol 378:70-87.

Portera-Cailliau C, Price DL, Martin LJ (1997b) Non-NMDA and NMDA receptor-mediated excitotoxic neuronal deaths in adult brain are morphologically distinct: further evidence for an apoptosis-necrosis continuum. J Comp Neurol 378:88-104.

Raff M (1998) Cell suicide for beginners. Nature 396:119-122.

Randall A, Tsien RW (1995) Pharmacological dissection of multiple types of Ca^{2+} channel currents in rat cerebellar granule neurons. Neurosci 15:2995-3012.

Randall A, Benham CD (1999) Recent advances in molecular understanding of voltage gated Ca^{2+} channels. Mol Cell Neurosci 14:255-272.

Rasmussen EB, Newland MC (2001) Developmental exposure to methylmercury alters behavioral sensitivity to d-amphetamine and pentobarbital in adult rats. Neurotoxicol Teratol 23:45-55.

Reed JC (2000) Mechanisms of apoptosis. Am J Pathol 157:1415-1430.

Renken C, Siragusa G, Parkins G, Washington L, Nulton J, Salamon P, Frey TG (2002) A thermodynamic model describing the nature of the crista junction: a structural motif in the mitochondrion. J Struct Biol 138:137-144.

Rhyu IJ, Abbott LC, Walker DB, Sotelo C (1999) An ultrastructural study of granule cell/Purkinje cell synapses in tottering (tg/tg), Leaner (tg^{la}/tg^{la}) and compound heterozygous tottering/leaner (tg/tg^{la}) mice. Neurosci 90:717-728.

Rice DC (1995) Neurotoxicity of lead, methylmercury and PCBs in relation to the Great Lakes. Environ Health Perspect 103:71-87.

Rice DC (1996) Sensory and cognitive effects of developmental methylmercury exposure in monkeys, and a comparison to effects in rodents. Neurotoxicology 17:139-154.

Rice DC (1998) Age related increase in auditory impairment in monkeys exposed in utero plus postnatally to methylmercury. Toxicol Sci 44:191-196.

Rikuzo H, Mitsuhiro O (1996) Minamata disease and other mercury syndromes. In: Toxicology of Metals (Chang LW, ed), Boca Raton, FL: CRC Press.

Risher JF, Murray HE, Prince GR (2002) Organic mercury compounds: human exposure and its relevance to public health. Toxicology & Industrial Health 18:109-160.

Rodier PM, Aschner M, Sager PR (1984) Mitotic arrest in the developing CNS after prenatal exposure to methylmercury. Neurobehav Toxicol Teratol 6:379-385.

Rogers JH (1989) Immunoreactivity for calretinin and other calcium-binding proteins in cerebellum. Neurosci 31:711-721.

Rossi AD, E. Ahlbom E, S-O. Ogren S-O, P. Nicotera P (1997) Prenatal exposure to methylmercury alters locomotor activity of male but not female rats. Exp Brain Res 117: 428-436.

Rotonda J, Nicholson DW, Fails KM, Gallant M, Gareau Y, Labella M, Peterson EP, Rasper DM, Rail R, Vaillancourt JP, Thornberry NA, Becker JW (1996) The three-dimensional structure of apopain/CPP32, a key mediator of apoptosis. Nat Struct Biol 3:619-625.

Rowe IC, Treherne JM, Ashford ML (1996) Activation by intracellular ATP of a potassium channel in neurons of rat basomedial hypothalamus. J Physiol 490:97-113.

Rowland IR, Davis MJ, Evans JG (1980) Tissue content of mercury in rats given methylmercuric chloride orally: influence of intestinal flora. Arch Environ Health 35:155-160.

Rustam H, Von Burg R, Amin-Zaki L, El Hassani S (1975) Evidence for a neuromuscular disorder in methylmercury poisoning. Arch Environ Health 30:190-195.

Rustay NR, Wahlsten D, Crabbe JC (2003) Influence of task parameters on rota-rod performance and sensitivity to ethanol in mice. Behav Brain Res 141:237-249.

Sager PR, Doherty RA, Olmsted JB (1983) Interaction of methylmercury with microtubules in cultures cells and in vitro. Exp Cell Res 146:127-137.

Sager PR, Aschner M, Rodier PM (1984) Persistent, differential alteration in developing cerebellar cortex of male and female mice after methylmercury exposure. Dev Brain Res 12:1-11.

Sager PR (1988) Selectivity of methylmercury effects on cytoskeleton and mitotic progression in cultured cells. Toxicol Appl Pharmacol 94:474-486.

Sakamoto M, Nakano A, Kajiwara Y, Naruse I, Fujisaki T (1993) Effects of methylmercury in postnatal developing rats. Environ Res 61:43-50.

Sakamoto M, Kakita A, Wakabayashi K, Takahashi H, Nakano A, Akagi H (2002) Evaluation of changes in methylmercury accumulation in the developing rat brain and its effects: a study with consecutive and moderate dose exposure throughout gestation and lactation periods. Brain Res 949:51-59.

Salvata N, Pirola C (1994) Analysis of mercury traces by means of solid sample atomic-absorption spectrometry. Industrie Alimentari 33 (332):1229-1238.

Salvaterra P, Lown B, Morganti J, Massaro EJ (1973) Alterations in neurochemical and behavioral parameters in the mouse induced by low doses of methylmercury. Acta Pharmacol Toxicol 33:177-190.

Samson FE, Nelson SR (2000) The ageing brain, metals and oxygen free radicals. Cell Mol Biol 46:499-707.

Sanfeliu C, Sebastia J, Ki SU (2001) Methylmercury neurotoxicity in cultures of human neurons, astrocytes, neuroblastoma cells. Neurotoxicology 22:317-327.

Santella L, Bolsover S (1999) Calcium in the nucleus. In: Calcium as a cellular regulator (Carafoli E, Klee C, eds), pp 487-511, New York: Oxford University Press.

Sarafian T, Verity MA (1990) Altered patterns of protein phosphorylation and synthesis caused by methylmercury in cerebellar granule cell culture. J Neurochem 55:922-929.

Sarafian TA, Verity MA (1991) Oxidative mechanisms underlying methylmercury neurotoxicity. Int J Dev Neurosci 9:149-155.

Sarafian TA, Vartavarian L, Kane DJ, Bredesen DE, Verity MA (1994) Bcl-2 expression decreases methylmercury-induced free radical generation and cell killing in a neural cell line. Toxicol Lett 74:149-155.

Sastry PS and Rao KS (2000) Apoptosis and nervous system. J Neurochem 74:1-20.

Savill L, Fadok V, Henson P, Haslett C (1993) Phagocyte recognition of cells undergoing apoptosis. Immunol Today 14:131-136.

Savitz SI, Rosenbaum DM (1998) Apoptosis in neurological disease. Neurosurgery 45:555-572.

Scarlett JL, Murphy MP (1997) release of apoptogenic proteins from the mitochondrial intermembrane space during the mitochondrial permeability transition. FEBS Letters 418(3):282-286.

Scorrano L, Petronilli V, Bernardi P (1997) On the voltage dependence of the mitochondrial transition pore. J Biol Chem 272:12295-12299.

Schmued LC, Albertson C, Slikker Jr W (1997) Fluoro-Jade: a novel fluorochrome for the sensitive and reliable histochemical localization of neuronal degeneration. Brain Res 751:37-46.

Shamoo AE, Maclennan DH, Eldefrawi ME (1976) Differential effects of mercurial compounds on excitable tissues. Chem Biol Interact 12:41-52.

Shanker G, Aschner M (2003) Methylmercury-induced reactive oxygen species formation in neonatal cerebral astrocyte cultures is attenuated by antioxidants. Mol Brain Res 110:85-91.

Shanker G, Aschner JL, Syversen T, Aschner M (2004) Free radical formation in cerebral cortical astrocytes in culture induced by methylmercury. Mol Brain Res 128:48-57.

Shenker BJ, Berthold P, Decker S, Mayro S, Rooney C, Vitale L (1992) Immunotoxic effects of mercuric compounds on human lymphocytes and monocytes. II. Alterations in cell viability. Immunopharmacol Immunotoxicol 14:555-577.

Shenker BJ, Berthold P, Rooney C, Vitale L, DeBolt K, Shapiro IM (1993) Immunotoxic effects of mercuric compounds on human lymphocytes and monocytes. III. Alterations in B-cell function and viability. Immunopharmacol Immunotoxicol 15:87-112

Shenker BJ, Guo TL, Shapiro IM (1998) Low-level methylmercury exposure causes human T-cells to undergo apoptosis: evidence of mitochondrial dysfunction. Environ Res 77:149-159.

Shenker BJ, Guo TL, Shapiro IM (2000) Mercury-induced apoptosis in human lymphoid cells: evidence that the apoptotic pathway is mercurial species dependent. Environ Res 84:89-99.

Shiji Y, Uedono Y, Ishikura H, Takeyama N, Tanaka T (1995) DNA damage induced by tumor necrosis factor-alpha in L929 cells is mediated by mitochondrial oxygen radical formation. Immunol 84:543-548.

Siciliano SD, Sangster A, Daughney CJ, Loseto L, Germida JJ, Rencz AN, O'Driscoll NJ, Lean DR (2003) Are methylmercury concentrations in the wetlands of Kejimkujik National Park, Nova Scotia, Canada, dependent on geology? J Environ Quality 32:2085-2094.

Silklos L, Engelhardt JI, Reaume AG, Scott RW, Adalbert R, Obal I, Appel SH (2000) Altered calcium homeostasis in spinal motoneurons but not in oculomotor neurons of SOD-1 knockout mice. Acta Neuropathol 99:517-524.

Siveri M, Leggio M, Molinari M (1994) The cerebellum contributes to linguistic production: a case of agrammatic speech following a right cerebellar lesion. Neurology 44 2047-2050.

Slupsky CM, Skyes BD (1999) The structural basis of regulation by calcium-binding EF-hand proteins. In: Calcium as a regulator (Carafoli E, Klee C, eds) pp 73-99, New York: Oxford University Press.

Smeitink J, Van Del Heuvel L, DiMauro S (2001) The genetics and pathology of oxidative phosphorylation. Nat Rev Genet 64:1505-1510.

Smith JC, Allen PV, Von Burg R (1997) Hair methylmercury levels in US women. Arch Environ Health 52:476-480.

Snider WD (1994) Functions of neurotrophins during nervous system development: what the knockouts are teaching us. Cell 77:627-638.

Somjen GG, Herman SP, Klein R (1973) Electrophysiology of methylmercury poisoning. J Pharmacol Exp Ther 186:579-592.

Somlyo AP, Bond M, Somlyo AV (1985) Calcium content of mitochondria and endoplasmic reticulum in liver frozen rapidly in vivo. Nature 314:622-525.

Sparagna GC, Gunter KK, Sheu SS, Gunter TE (1995) Mitochondrial calcium uptake from physiological-type pulses of calcium. A description of the rapid uptake mode. J Biol Chem 270:27510-27515.

Spyker JM, Smithberg M (1972) Effects of methylmercury on prenatal development in mice. Teratology 5:181-190.

Spyker JM, Sparber SB, Goldberg AM (1972) Subtle consequences of methylmercury exposure: behavioral deviations in offspring of treated mothers. Science 177:621-623.

Stern AH, Gochfeld M, Weisel C, Burger J (2001) Mercury and methylmercury exposure in the New Jersey pregnant population. Arch Environ Health 56:4-10.

Su MQ, Okita GT (1976) Behavioral effects on the progeny of mice treated with methylmercury. Toxicol Appl Pharmacol 38:195-205.

Takeuchi T, Morikawa N, Matsumoto H, Shiraishi Y (1962) A pathological study of Minamata disease in Japan. Acta Neuropathol 2:40.

Takeuchi T, Eto K, Eto N (1979) Neuropathology of childhood cases of methylmercury poisoning with prolonged symptoms, with particular reference to the decortication syndrome. Neurotoxicology 1:1.

Thornberry NA, Bull HG, Calaycay JR, Chapman KT, Howard AD, Kostura MJ, Miller DK, Molineaux SM, Weidner JR, Aunins J, Elliston KO, Ayala JM, Casano FJ, Chin J, Ding G, Egger LA, Gaffney EP, Limjuco G, Palyha OC, Raju SM, Rolando AM, Salley JP, Yamin TT, Lee TD, Shively JE, MacCross M, Mumford RA, Schmidt JA, Tocci MJ (1992) A novel heterodimeric cysteine protease is required for interleukin-1β processing in monocytes. Nature 356:768-774.

Thornberry NA, Lazebnik Y (1998) Caspase enemies with. Science 281:1312-1316.

Trost LC, Lemasters JJ (1997) Role of mitochondrial permeability transition in salicylate toxicity to cultured rat hepatocytes: implications for the pathogenesis of Reye's syndrome. Toxicol Appl Pharmacol 147:431-441.

U.S. EPA (1997) Mercury study report to Congress. Vol. IV: An assessment of exposure to mercury in the United States. EPA-452/R-97-006. Washington, DC: U.S. Environmental Protection Agency, Office of Air Quality Planning and Standards and Office of Research and Development.

U.S. EPA (2001) Water quality criterion for the protection of human health: methylmercury. EPA 0823-R-01-001. Washington, DC: U.S. Environmental Protection Agency.

Usuki F, Yasutake A, Umehara F, Tokunaga H, Matsumoto M, Ito K, Ishiura S, Higuchi I (2001) *In vivo* protection of a water soluble derivative of vitamin E, Trolox, against methylmercury-intoxication in the rat. Neurosci Lett 304:199-203.

Uzman L (1960) The histogenesis of the mouse cerebellum as studied by its tritiated thymidine uptake. J Comp Neurol 114:137-159.

Vergun O, Keelan J, Khodorov BI, Duchen MR (1999) Glutamate-induced mitochondrial depolarization and perturbation of calcium homeostasis in cultured rat Hippocampal neurons. J Physiol 519:451-466.

Verity MA, Brown WJ, Cheung M (1975) Organic mercurial encephalopathy: *in vivo* and *in vitro* effects of methylmercury on synaptosomal respiration. J Neurochem 25: 759-766.

Verity MA, Brown WJ, Cheung M, Czer G (1977) Methylmercury inhibition of synaptosome and brain slice protein synthesis: *in vivo* and *in vitro* studies. J Neurochem 29:673-679.

Vicente E, Boer M, Netto C, Fochesatto C, Dalmaz C, Siqueira IR, Goncalves C-A (2004) Hippocampal antioxidant system in neonates from methylmercury intoxicated rats. Neurotoxicol Teratol 26 817 – 823.

Voogd J, Glickstein M (1998) The anatomy of the cerebellum. Trends Neurosci 21:370-375.

Walberg F, Jansen J (1961) Cerebellar corticulovestibular fibers in the cat. Exp Neurol 3:32-52.

Watanabe C, Yin K, Kasanuma Y, Satoh H (1999) *In utero* exposure to methylmercury and Se deficiency converge on the neurobehavioral outcome in mice. Neurotoxicol Teratol 21:83-88.

Wigdal SS, Rebecca AK, Franklin JL, Haak-Frendscho M (2002) Cytochrome C release precedes mitochondrial membrane potential in cerebellar granule neuron apoptosis: lack of mitochondrial swelling. J Neurochem 82: 1029-1038.

White RJ, Reynolds IJ (1996) Mitochondrial depolarization in glutamate-stimulated neurons: an early signal specific to excitotoxin exposure. J Neurosci 16:5688-5697.

Xiong J, Verkhratsky A, Toescu EC (2002) Changes in mitochondrial status associated with altered Ca^{2+} homeostasis in aged cerebellar granule neurons in brain slices. J Neurosci 22:10761-10771.

Yang J, Liu X, Bhaila K, Kim CN, Ibrado AM, Cai J (1997) Prevention of apoptosis by bcl-2: release of cytochrome c from mitochondria blocked. Science 275:1129-1131.

Yasutake, A, Hirayama K (1986) Strain difference in mercury excretion in methylmercury-treated mice. Arch Toxicol 59:99-102.

Yasutake A, Hirayama K (1988) Sex and strain differences of susceptibility to methylmercury toxicity in mice. Toxicology 51:47-55.

Yee S, Choi BH (1994) Methylmercury poisoning induces oxidative stress in the mouse brain. Exp Mol Pathol 60:188-196.

Yee S, Choi BH (1996) Oxidative stress in neurotoxic effects of methylmercury poisoning. Neurotoxicology 17:17-26.

Yin K, Watanabe C, Inaba H, Satoh H (1997) Growth and behavioral changes in mice prenatally exposed to methylmercury and heat. Neurotoxicol Teratol 19:65-71.

Yoshino Y, Mozai T, Nakao K (1966) Biochemical changes in the brain in rats poisoned with an alkylmercury compound, with special reference to the inhibition of protein synthesis in brain cortex slices. J Neurochem 13:1223-1230.

Yuan Y, Atchison WD (1999) Comparative effects of methylmercury on parallel-fiber and climbing-fiber responses of rat cerebellar slices. J Pharmacol Exp Ther 288:1015-1025.

Zamzami N, Susin SA, Marchetti P, Hirsch T, Gomez-Monterrey I, Castedo M, Kroemer A (1996) A mitochondrial control of nuclear apoptosis. J Exptl Med 183(4):1533-1544.

Zeng FY, Soldner A, Schoneberg T, Wess J (1999) Conserved extracellular cysteine pair in the M3 muscarnic acetylcholine receptor is essential for proper receptor cell surface localization but not for G protein coupling. J Neurochem 72:2404-2414.

Zoratti M, Szabo I (1995) The mitochondrial permeability transition. Biochim Biophys Acta 1241(2):139-176.

Zou H, Henzel WJ, Liu X, Lutschg A, Wang X (1997) Apaf-1, a human protein homologous to C. elegans CED-4, participates in cytochrome c-dependent activation of caspase-3. Cell 90:405-413.

VITA

Name:

Sairam Bellum

Address:

Department of Veterinary Integrative Biosciences
College of Veterinary Medicine and Biomedical Sciences
Texas A&M University
VMA Building Room 107, 4458 TAMU, College Station, TX 77843-4458

Email Address:

bsr1972@yahoo.com

Education:

Ph.D., Toxicology, Texas A&M University, 2005

M.V.Sc., Veterinary Pathology, Acharya NG Ranga Agricultural University, India, 1999

B.V.Sc & A.H., Veterinary Science and Animal Husbandry, Acharya NG Ranga Agricultural University, India, 1995

Publications:

Bellum S, Thuett KA, Taylor RJ, Abbott LC (2005) Assessment of mercury concentrations in mouse brain using different routes of administration and different tissue preparations. Toxicol Mech Methods (In press).